Zebrafish Larvae as a Model Organism to Study Biotransformation

Master thesis in Pharmacy

Anette Sivertsen

Centre for Pharmacy,
Department of Clinical Science
University of Bergen

2022/2023

Abstract

The zebrafish larva is an increasingly used model organism in many fields of research, including drug development. Due to traits like their small size, rapid development, and high degree of genetic similarity with humans, they could likely represent a valuable model for investigating pharmacokinetic properties such as biotransformation in preclinical research.

In this study, zebrafish larvae were used as a model system to investigate biotransformation of simvastatin, fluvastatin, and captopril using LC-MS/MS (ESI QQQ) for analysis. Zebrafish larvae were exposed to the drugs through aquatic exposure, and both the embryo water and the zebrafish larvae were analyzed for contents of drugs and selected metabolites. Procedures for sample preparation were established, and suitable LC-MS/MS methods were developed for the selected analytes.

This study highlights that differences in developmental stages of the zebrafish larvae need to be considered when investigating biotransformation of drugs with this model system, since the maturation of several organs might affect the accumulation and elimination rates of the administered drugs. We encountered issues related to signal suppression and matrix effects when embryo water and homogenized zebrafish larvae were present in the samples. We also established that adsorption issues of hydrophobic drugs, like simvastatin, can contribute to poor signals or lack of detection when using plastic-based equipment for sample preparation. These considerations should be investigated further when using the zebrafish larva model.

Despite these analytical reservations, metabolites of the administered drugs were detected in samples collected from zebrafish larvae, showing the value of zebrafish larvae as a model system in biotransformation studies. However, before the zebrafish larva can be appropriately validated as a model system to study biotransformation, further research is thus needed.

Acknowledgements

First of all, I would like to thank my supervisors Prof. Lars Herfindal and Prof. Silje Skrede for all their guidance and valuable inputs throughout the work with this master project.

Further, I would like to thank PhD-candidates Ingeborg Nerbø Reiten and Jan-Lukas Førde for your guidance with zebrafish handling and care, and for collecting zebrafish embryos for me almost every week throughout the year. And to everyone else in the Herfindal research group: Thank you for welcoming and including me into your group. You have all contributed to making this year a positive, exciting, and educational experience.

Special thanks to Torunn Eide for teaching me how to operate and maintaining the LC-MS/MS instrument, interpreting results, and guidance with sample preparations. You have motivated me to continue exploring, even when things seemed unmanageable. I really appreciate all our conversations, both personal and professional, and I will miss spending time with you in the laboratory.

To my fellow master students – We have endured ups and downs, many days filled with frustration, but also many victories and achievements throughout this degree. The last five years together at UiB have been absolutely fantastic and I am left with many happy memories.

Finally, thank you Harry for your encouraging words and continuous support throughout this year. You have been busy writing your own thesis this year, but you always took your time to listen.

Anette

Abbreviations

2OH-FLV	2-hydroxy-fluvastatin
ACN	Acetonitrile
CAPT	Captopril
CAPT-pBPB	Captopril derivatized with 2,4'-dibromoacetophenone (pBPB)
CYP	Cytochrome P450 (a group of metabolizing enzymes)
DC	Direct current
DICAPT	Disulfide captopril
Dpf	Days post fertilization
E3	Embryo water
ENA	Enalapril
ESI	Electro Spray Ionization
EtOH	Ethanol
FLV	Fluvastatin
Hpf	Hours post fertilization
ISTD	Internal standard
LC	Liquid chromatography
LC-MS/MS	Liquid chromatography-Tandem Mass Spectrometry
LC_{50}	Lethal Concentration for 50% of the population
MeOH	Methanol
MQ	Milli-Q water
MRM	Multiple Reaction Monitoring
MS	Mass spectrometry
MTC	Maximum tolerated concentration
OH-FLV	Hydroxy-fluvastatin
p-BPB	2,4'-dibromoacetophenone
QQQ	Triple Quadrupole instrument
RF	Radio frequency
SIM	Single Ion Monitoring
SMV	Simvastatin
SMV-A	Simvastatin acid

Table of contents

1 Introduction

1.1 Drug discovery and development

The discovery and development of new drugs is a long and time-consuming process that requires a lot of resources, both economically and materially. The average time from drug discovery until a drug reaches the market is 12-15 years (2), and the estimated price tag ranges from 324 million to 2,8 billion USD according to data from 2009 to 2018 (3). Drug development is a multidisciplinary research process, and the involvement of several professional fields contributes to its complexity. For every 10 000 potential chemical structures identified and synthesized, roughly 500 will be tested in animals, 10 will reach phase I of clinical trials and only one final candidate will attain regulatory approval (4, p.284). Even though some of the drug candidates succeed and gains a regulatory approval, most of the lead compounds involved in a drug development process fail due to unacceptable unwanted and adverse effects, or because of a lack of therapeutical effect (5). The road from identification and selection of promising drug candidates to a marketed drug is both long and uncertain, but essential in order to improve the treatment of several severe diseases.

1.1.1 The four stages of drug development

The drug development process is typically divided into four stages: Discovery and development, Preclinical research, Clinical trials and finally, Regulatory Approval (6), as illustrated in Figure 1.1.

Drug development stage	**Discovery and development**	**Preclinical research**	**Clinical trials**	**Regulatory Approval**
Estimated time spent	4.5 years	1 year	6.5 years	1.5 years
*% of the cost per new molecular entity**	26 %	7 %	62 %	5 %

* A new molecular entity is a novel compound that has not previously been approved for human use (7).

Figure 1.1*: The four stages of drug development, the estimated time spent for each stage, and the % of the cost per new molecular entity. The figure is adapted from (8).*

Before the search for promising drug candidates can start, researchers must identify and validate a relevant drug target for the therapeutic area or disease of interest (4, p. 197). It is important

that the target is druggable, meaning that upon binding of drug-like molecules, it has the potential to be modulated and give a therapeutic effect (9). Next, an extensive search for possible small molecular compounds that can bind to the selected target can be carried out. High throughput screenings (HTS) of entire compound libraries can be performed to evaluate drug candidates' effect on the target using digital screenings or more complex cell-based assays (2). Knowledge-based screenings are also widely used, where compounds are selected from libraries based on their chemical properties and previous knowledge of their affinity to similar drug targets (2). The most promising drug candidates can progress to preclinical studies, where properties like toxicity, pharmacokinetic and pharmacodynamic profiles, as well as physicochemical properties and formulation possibilities, are assessed (2). Methods and model systems for collecting data on these properties will be further discussed in section 1.1.2.

In clinical trials, lead compounds are tested in humans for the first time. In phase I, a small group of individuals will be exposed to the lead compound (20-80 participants), and in phase II and III larger groups of participants are included; a few hundred, and several hundred to a few thousand, respectively (10). After clinical trials, the lead compounds can be reviewed by a governmental authority, like the Food and Drug Administration (FDA) in USA or the European Medicinal Agency (EMA) in Europe, and eventually gain regulatory approval as a marketed drug (11). Both safety and efficacy are assessed throughout the drug development process, but post-market surveillance and safety monitoring continues long after the drug is marketed to reveal potential uncovered and harmful effects or revise indications or dosages (12).

The decision to stop – an economical point of view

As mentioned, drug discovery and development are very expensive processes, and sponsors and investors are often involved with funding (13). Clinical trials are by far the most resource demanding stage of the development process (2), consuming around 63% of the total costs according to data from 2010 (14). Nevertheless, preclinical animal studies also account for a significant share of the resource requirements. Each individual animal, whether it is a mouse, a dog, or a monkey, requires expenses related to housing, research facilities and trained personnel, in addition to the cost of the animal itself. The high attrition rate seen in drug development is caused by two main problems; the drug candidates are not safe, or not providing a desired therapeutic effect (2). To reduce the economic risk for the investors, early characterization of a representative pharmacokinetic and toxicological profile of the lead compounds in preclinical research can help in allocating resources to the drug candidates that

are most likely to succeed (15). From an economic point of view, every decision to proceed is a commitment to large investments. Thus, sound data supporting the decision to proceed to animal tests is equally important to data supporting the initiation of clinical trials. The decision to stop, on the other hand, comes with no costs and should always be considered, especially when the data basis of the lead compound is deficient.

1.1.2 Preclinical drug development

In the preclinical drug development phase, researchers work to collect data on the lead compounds' pharmacokinetic and pharmacodynamic profile, their toxicity, formulation options and possibilities for large-scale production (16, p. 752). This involves several scientific specialties, creating a complex and multidisciplinary field of research (17). Ideally, the characteristics of the lead compounds determined in preclinical research should as accurately as possible reflect the behavior of the drug when administered to humans. This can be difficult to achieve in practice, but by involving an array of different assays, the predictions are steadily improving. The main approaches employed today are presented below.

In silico modelling

Experiments that are conducted through computer modelling or simulations, are called *in silico* assays (18). In *silico* approaches are especially useful in the earliest stages of the drug development process when it comes to identifying drug targets and optimizing lead compounds, even before chemical synthesis (19). *In silico* methods are also widely used for making predictions on the pharmacokinetic profile of lead compounds based on their structure-property relationships, and moreover assisting in the selection and prioritization of lead compounds with the most favorable profiles for further *in vitro* assays (20). Although these assays have many beneficial applications in early drug development, they only provide predictions.

In vitro experiments

In vitro means "in glass", and refers to experiments conducted outside of an organism, typically in cell cultures and other biological tissues (21). There are many advantages to *in vitro* assays in preclinical drug development. For one, they provide controlled testing environments with a high degree of standardization potential and low experimental variability (22). As many different cell lines are available, *in vitro* assays can be used for obtaining a variety of information on cytotoxicity and toxicity on different cell types (22), as well as predictions of

pharmacokinetic properties such as biotransformation and clearance (15). *In vitro* experiments contribute to reducing the number of experimental animals required, since many drug candidates are ruled unfit in these types of assays. However, cell-based assays are a very isolated model systems, and do not allow for detection of potential drug-interactions that may occur within a complete organism.

In vivo experiments

To represent the complex nature of a whole organism, it is essential to include *in vivo* model systems in preclinical drug development. Biological responses that might occur once a drug-like compound is administered to whole organisms, such as the involvement of the immune system, adverse effects, and drug interactions, needs to be addressed as thoroughly as possible before lead compounds are administered to human participants. To obtain data on these kinds of interactions, several different animal models are available, such as zebrafish, mice, rats, rabbits (23), dogs and non-human primates (monkeys) (24).

However, it is challenging to use non-human models to predict every potential effect, outcome, or interaction that can occur in humans once a drug is administered. No matter how similar the model is, the translational power of a non-human model system will never be 100% (5). Differences in target proteins, cellular defense-mechanisms, and immune cells and -responses between the model system and humans can have a significant impact on how the organism tolerates the drug. An example where adverse toxicity was observed in humans, but not in either human blood cells, mice, or monkeys during preclinical studies, was the use of TGN1412 (theralizumab) for the treatment of B-cell chronic lymphocytic leukemia and rheumatoid arthritis. Cytokine release syndrome and multi-organ failure was observed in several healthy human individuals, but not in the selected preclinical model systems (5). Small differences in the distribution, reactivity, and quantity of the drug targets across these model systems, masked this serious and unacceptable effect (5), illustrating that it is very difficult to accurately portray the biological complexity of humans.

1.2 Research on animals and the "Three Rs"

Nonetheless, to identify potential toxicity and adverse reactions of drug candidates and their metabolites, it is essential to perform studies on animals as they represent the biological complexity and physiology that is present in humans to a higher degree than *in vitro* models do

(5). However, with the inclusion and use of experimental animals in preclinical research, methods contributing to reduced and refined use of experimental animals is a priority. In recent years, the "three Rs" have become accepted as important principles in this regard.

The Three Rs are comprised of "Replacement, Reduction and Refinement", and represent an internationally accepted ethical framework for the use of animals for research purposes (25). Animal models should be *Replaced* with non-animal models when possible, the number of animals included in research should always be *Reduced* to a minimum and the laboratory practice should be *Refined* to minimize the stress inflicted on the animals and to facilitate for animal welfare (26). Even though a reduction in the number of animals being used is a goal, it is still necessary to use enough animals so that the results of the experiments provide statistically significant data.

Toxicological studies on mammals are expensive, time-consuming and raises major ethical questions (27). Because of this, and in order to comply with the "three Rs", there is a need for developing and establishing alternative *in vivo* models for toxicological screenings, that both represent the required biological complexity and holds a high translational power to humans (27).

When is an animal not an animal?

According to European Legislation (28), larval stages of living organisms that feed independently, are defined as experimental animals. Zebrafish larvae feed independently from the age of 120 hours post fertilization (hpf) at the earliest (27) and can therefore be excluded from these regulations until they reach this stage of development. The use of fish embryos, like those of zebrafish, are considered as methods of replacement or refinement, because these life-forms are less likely to experience pain, suffering, distress, or lasting harm compared to other mammalian research animals (27). In addition, they offer a much less costly model for systematic testing of toxic effects of drug candidates, than mammals (27). Zebrafish larvae are complex, and harbor central physiological processes needed to study important properties of drug candidates, such as pharmacokinetics. More on these central processes and traits will be elaborated in section 1.4.

1.3 Pharmacokinetics

Pharmacokinetics is the study of how the body interacts with a drug, from the point of administration until it is completely eliminated from the body (29). There are generally four main focuses to be considered when describing the pharmacokinetic profile of a drug: administration, distribution, metabolism, and elimination (ADME). The method of administration must allow for sufficient absorption, the drug must be distributed to relevant parts of the body, it must be processed in a way that retains the activity and does not produce toxic bi-products, and eventually it must be eliminated from the body at an appropriate rate (30). Next, the subject of metabolism, also known as biotransformation, will be further discussed as this is the most important ADME feature for this master project.

1.3.1 Biotransformation

Biotransformation, also referred to as metabolism, is an important detoxification process in which foreign (xenobiotics) and endogenous substances are chemically modified (31). Biotransformation can be separated into two main stages: phase I reactions and phase II reactions. In phase I, the metabolizing enzymes perform oxidation, reduction, or hydrolysis reactions, to make the compounds more hydrophilic (32). An important group of metabolizing enzymes involved in oxidative phase I reactions, is the family of cytochrome P450 enzymes, often referred to as 'CYPs' (33). Next, these products can be further modified via phase II reactions, also known as conjugation-reactions. In this step, endogenous compounds such as glucuronic acid or sulphate are added to the metabolite, making it even larger and more polar, facilitating excretion from the kidneys (32). Some important groups of enzymes involved in these phase II reactions are UDP-glucuronosyltransferases (UGTs), sulfonyltransferases (SULTs), and glutathione S-transferases (GSTs) (34). The liver is the main site for biotransformation (16, p. 133), although metabolizing enzymes located in extrahepatic tissues, such as the intestine, also contributes to these metabolic reactions (32).

Several different outcomes are possible when drugs are metabolized by these enzymatic reactions. Some drugs are inactivated, and others sustain their pharmacological activity. In addition, some drugs are inactive when administered, and require metabolic modifications for them to become pharmacologically active substances. Drugs like these are called prodrugs (35). Prodrugs are useful for tackling several physicochemical challenges related to the structural backbones of drugs, such as issues related to acid sensitivity in the stomach, chemical stability,

poor membrane permeability, toxicity, and short durations of action (4, p. 266). Moreover, some biotransformation reactions generate metabolites that can cause adverse reactions and toxicity (5). Paracetamol for instance, which is a commonly used analgetic, is normally inactivated in the liver via several conjugation reactions with glucuronic acid and sulphate. In addition, paracetamol can be oxidized to the reactive metabolite *N*-acetyl-*p*-benzoquinonimine (NAPQI), which in turn is inactivated (and detoxified) through glutathione-conjugation. In the case of a paracetamol overdose, or if the storage of glutathione is exhausted, these NAPQI-metabolites will not be inactivated, and can potentially cause hepatotoxicity and acute hepatic failure (36). Since metabolic products can cause toxicities and adverse effects, it is important to include and perform safety testing in the presence of relevant drug-metabolizing enzymes during preclinical drug development, as the absence of these enzymes could mask potential toxic effects of the compound being tested (5).

1.3.2 Biotransformation of the compounds included in this thesis

In this thesis, three drugs with known metabolic profiles will be subject for testing in zebrafish larvae: simvastatin, fluvastatin and captopril. In the following sections, the mechanisms of action and the metabolic profiles of these compounds will be presented.

1.3.2.1 Statins

Simvastatin and fluvastatin belong to a group of cholesterol-lowering agents called statins, commonly used to treat hypercholesterolemia and different types of hyperlipidemias (37). They act as competitive inhibitors of 3-hydroxy-3-methylglutaryl-coenzyme A reductase (HMG-CoA-reductase) – an enzyme that catalyzes the rate limiting step in the biosynthesis of cholesterol (37). When this enzyme is inhibited, the intrahepatic cholesterol levels will *de*crease, and as a response to this, the body will *in*crease the number of low-density lipoprotein (LDL) receptors. This will again decrease the LDL levels in circulation (38). The overall effects of statins are a decrease in the total cholesterol and LDL-cholesterol levels, but they also contribute to a slight increase in HDL-lipoproteins and reduce triglyceride levels in plasma (38).

Simvastatin

Simvastatin is a prodrug that need to metabolized into its active form before it can exhibit a clinical effect (39). The inactive lactone ring of simvastatin must be converted to its carboxylic acid form (Simvastatin-hydroxy-acid) for the compound to become active, as shown in Figure

1.2 (4, p. 190). This hydrolysis reaction occurs both spontaneously and by carboxylesterases located in the intestine, liver, and plasma (40). Simvastatin is mainly metabolized via CYP3A4 to 6-hydroxy, 6-hydroxymethyl and 6-exomethylene derivatives, and given that the lactone ring has been hydrolyzed, all these metabolites are pharmacologically active (40).

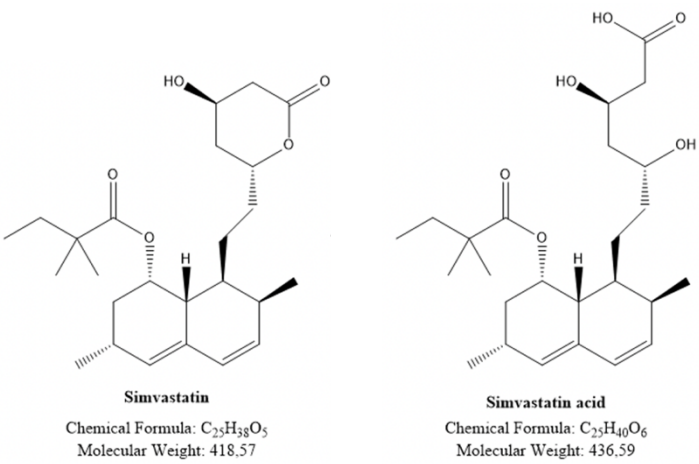

Figure 1.2: *Simvastatin and its active, hydroxylated metabolite simvastatin acid.*

Fluvastatin

Fluvastatin is not a prodrug, but it is still subject for hepatic biotransformation. It is relatively hydrophilic compared to other statins, because of its carboxylic group (41). Fluvastatin is a substrate to several CYP-enzymes. It is predominantly metabolized to 6-hydroxy fluvastatin and N-desisopropyl fluvastatin, exclusively via CYP2C9. Another hydroxylated metabolite 5-hydroxy fluvastatin, is produced by both CYP2C9 and CYP2C8, in addition to CYP3A4 and CYP2D6 (41). In addition to these metabolites, other metabolic pathways of fluvastatin include β-oxidation, lactone formation, and finally, phase II reactions making conjugates with either glucuronic acid or sulfate (42). A selection of these metabolites was monitored in the experiments conducted in this thesis. These selected metabolites chosen for analysis are illustrated in Figure 1.3. The hydroxylated metabolites of fluvastatin are to some extent pharmacologically active, but as they are substrates for glucuronidation they are rapidly eliminated into feces via bile.

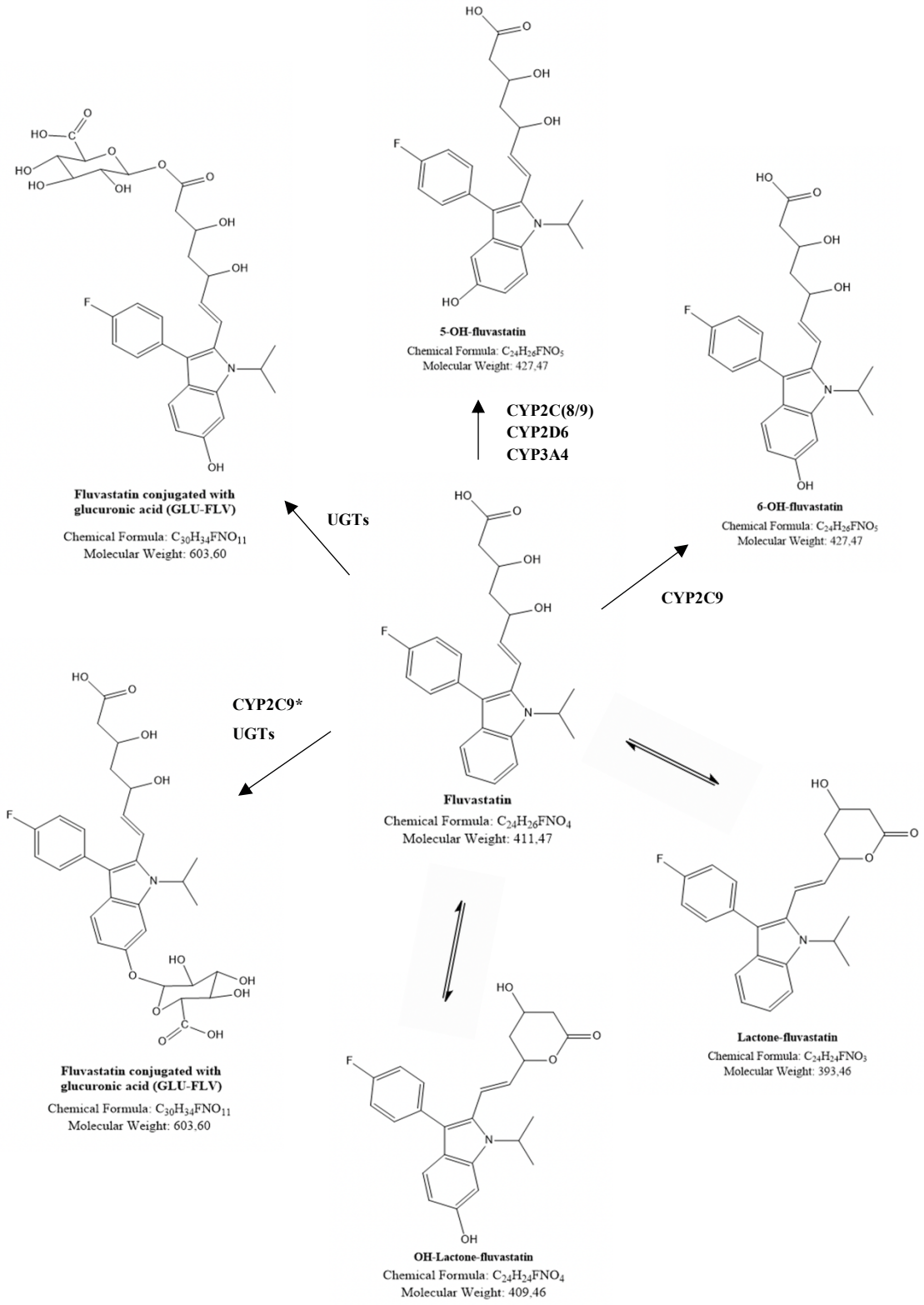

Figure 1.3: *The selection of metabolites of fluvastatin that were subject for analysis in this master project. Their molecular structures, chemical formulae and molecular weights are illustrated. In addition, relevant metabolizing enzymes and chemical reactions are listed.*

**With the formation of GLU-FLV, the glucuronic acid moiety can be added to either a 5-OH- or 6-OH-FLV molecule (the addition at the 6-position is illustrated here). As the main CYP-enzyme involved in the formation of both 5- and 6-OH-FLV is CYP2C9, only this is CYP-enzyme is listed for this metabolite as a simplification.*

1.3.2.2 Angiotensin Converting Enzyme Inhibitors (ACE-inhibitors)

Captopril is an angiotensin converting enzyme (ACE) inhibitor; a group of blood-pressure-lowering drugs that have an important clinical use in the treatment of hypertension and heart failure (43). ACE is an enzyme that converts angiotensin I to angiotensin II, the latter being a potent vasoconstrictor and a key component of the renin-angiotensin-aldosterone system (RAAS) (44). RAAS contributes to the regulation of hemodynamics and the water- and electrolyte balance, and it provides an important mechanism for maintaining homeostasis. ACE also catalyzes the breakdown of bradykinin – a protein with vaso*dilating* properties – and thus, by inhibiting ACE, more bradykinins will be available. The main blood-pressure-lowering effect is caused by the reduction of angiotensin II levels, but an increase in bradykinin may also contribute to some extent (43).

Captopril

Captopril is a pharmacologically active substance in its own capacity and does not require metabolic modification to be pharmacologically active. However, the chemical structure of captopril includes a sulfhydryl group that is readily available for oxidation reactions (44). Hepatic biotransformation can produce different inactive conjugates with the sulfhydryl-containing amino acid cysteine, resulting in disulfide bridge-containing metabolites (44). In addition, two captopril molecules can also form a disulfide bridge, yielding the metabolite disulfide captopril (see Figure 1.4). Captopril can also bind covalently, but reversibly to plasma proteins (45). The biotransformation of captopril can be catalyzed enzymatically and non-enzymatically, probably involving enzymes such as glutathione reductase, thiol-disulfide transhydrogenase, and thiol-reductase (45).

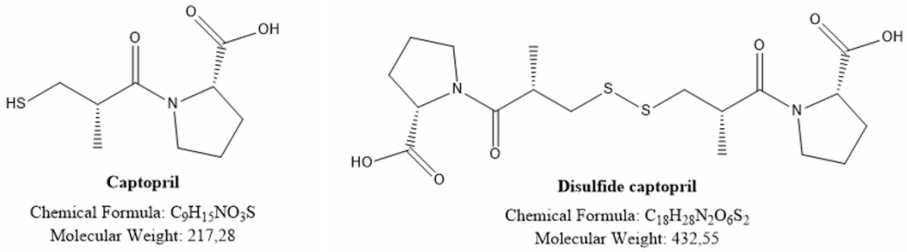

Figure 1.4: *Chemical structures of captopril and its metabolite disulfide captopril, their chemical formulae, and molecular weights.*

1.4 Zebrafish larvae as research models

1.4.1 Zebrafish larvae as model organisms in drug development

Bridging the gap between in vitro and in vivo models

The use of zebrafish in early drug development is already well-established. From a researcher's perspective, early life stages of zebrafish offer many favorable traits that contribute to their increasing popularity. For one, since they are not categorized as experimental animals until 120 hpf, there are less regulations regarding the laboratory facilities, personnel and applications associated with performing experiments on them – saving both time and money. Zebrafish larvae are small and can be kept in multi-well plates (46). This is ideal for testing of several drug candidates simultaneously in high-throughput screenings and contributes to a high statistical confidence (47). Adult female zebrafish can produce several hundred eggs weekly, and the embryos and larvae develop rapidly. Compared to different rodent *in vivo* models, this contributes to a shorter experimental time. Taken together, zebrafish larvae hold a unique position, as they offer the complexity of an *in vivo* model, as well as the scale and high throughput screening possibilities of an *in vitro* model (1).

A prerequisite that needs to be met when using non-human *in vivo* models in drug development research, is that both the genetics and the biology of the model system must have a certain degree of similarity to humans. Genome sequencing has shown that approximately 70% of the human genome has zebrafish orthologues (1). Furthermore, the anatomy of several tissues in the zebrafish, such as the heart, bone, blood, liver, pancreas, and intestine show structural similarities with higher vertebrates (48, p. 4).

The embryos of zebrafish are optically transparent, which allows for direct visualization of several developmental processes *in vivo*. Due to this characteristic, these model organisms have had a considerable value in understanding complex biological processes in higher vertebrates, such as vascular and lymphatic development (49, 50). Another benefit of the zebrafish larvae is that they are closer to a juvenile than a fetal stage in terms of biological development. Their vital organs are functioning, and their nervous system is mature (46); traits that are advantageous when the goal is to translate the obtained results to developed vertebrates.

1.4.2 Pharmacokinetics in zebrafish and zebrafish larvae

Drug administration to zebrafish larvae

Zebrafish larvae can absorb small-molecular drugs via their gills and through their skin (48, p. 109). Therefore, a widely used method for administering drugs to zebrafish larvae is by dissolving the compound directly in their aquatic environment (47). This administration method is advantageous in that the procedure is relatively easy to perform, and only milligrams of the test compounds are required. Some compounds are poorly water soluble and must be dissolved in an organic solvent that is miscible with water, before further dilution. Dimethyl sulfoxide (DMSO) and methanol (MeOH) are often used for this purpose (51). It is also important to keep in mind that ionizable compounds are dependent on pH for being in the uncharged state, which is necessary for crossing of biological membranes (52, 53).

Absorption-dependent administration limits dosage control (48, p. 112), because there is no way of ensuring that each larva absorbs the exact same amount of drug. The internal exposure of drug in the zebrafish larvae is often not quantified, and this can possibly lead to false positive or negative results (54). In addition, drugs can be administered via microinjection into different organs and tissues of the zebrafish larvae (55). While this allows for more reliable dosage control, microinjections are more invasive, and require more advanced equipment and training of the laboratory personnel.

Drug metabolism in zebrafish larvae

The liver in zebrafish has the same functions as the liver in humans, including xenobiotic biotransformation (56). At 5 dpf, the liver of zebrafish is fully functional, making young zebrafish larvae promising and interesting models for investigation of biotransformation (56).

The full array of CYP-genes in zebrafish, their expression during different developmental stages as well as their relation to the human CYPs, have been identified and mapped by Goldstone et al. (57). This research showed that the CYP-genes relevant for xenobiotic metabolism (CYP families 1-3) in zebrafish have a clear evolutionary relationship with their human orthologs through shared synteny (57). Table 1.1 shows a summary of the synteny comparison of CYP-enzymes involved in biotransformation of xenobiotics, adapted from the work done by Goldstone et al. (57). Since many of the CYP-genes in zebrafish have direct

orthologs to humans, the metabolic potential is likely to be similar as well (1). Several studies have established that zebrafish have the potential to perform both phase I and phase II reactions through the discovery of such metabolites (54, 58-60).

Table 1.1: *Synteny comparison of the major CYP-enzymes involved in biotransformation of xenobiotics in zebrafish and humans. This table is retrieved from (1).*

Zebrafish	Human
CYP1A	CYP1A1/1A2
CYP1B1	CYP1B1
CYP1C1,2	–
CYP1D1	CYP1D1P
CYP2Ks	CYP2W1
CYP2N13	CYP2J2
CYP2Ps	CYP2J2
CYP2R1	CYP2R1
CYP2U1	CYP2U1
CYP2V1	CYP2J2
CYP2X1-10	–
CYP2Y3,4	CYP2A/B/F/S
CYP2AA1-12	–
–	CYP2D
–	CYP2C
CYP2AD2,3,6	CYP2J2
CYP2AE1,2	–
CYP3A65	CYP3A-se1,-se2[a]
CYP3C1-4	CYP3A3,4,7
CYP4F43	CYP4F
CYP4V7,8	CYP4V2
CYP4T8	–
CYP5A1	CYP5A1
CYP7A1	CYP7A1
CYP7B1	CYP7B1
CYP7C1	–

It is important to note that the activity of a protein does not necessarily correlate to the expression of its gene. Both similarities and differences have been found when it comes to the metabolic profiles and the metabolizing enzymes in zebrafish compared to humans. In a translational context, ortholog genes would ideally encode CYP-enzymes producing the same kind of metabolites, but when using non-human model system this scenario is not always observed. For instance, ibuprofen is metabolized to hydroxy-ibuprofen in humans mainly via CYP2C enzymes (CYP2C8/9/19) (61). Jones et al. (62), observed the formation of hydroxy-ibuprofen in zebrafish larvae (72-96 hpf), even though no CYP2C ortholog genes or enzymes have been identified in zebrafish (57). In another study, performed by Saad et al. (59), the metabolism of several CYP-prone drugs in zebrafish were studied. One of these, midazolam, is a substrate CYP3A4-induced metabolism in humans (63). Even though zebrafish have an ortholog gene to human CYP3A4, no metabolism was seen for midazolam in zebrafish (*in vitro* assay, zebrafish liver microsomes and embryo microsomes compared to human liver microsomes) (59). There are also cases where both ortholog genes *and* equal metabolites are conserved in adult zebrafish (sibutramine and stanozolol (64)), and zebrafish larvae (clofibric acid, 4-100 hpf (60), paracetamol, 5 dpf (54)) compared to humans.

The maturation of the zebrafish needs to be taken into consideration when reviewing the results from biotransformation studies on zebrafish larvae (54). In a study on zebrafish larvae (5 dpf) using paracetamol as the study compound, the metabolite paracetamol-sulfate was more abundant than paracetamol-glucuronide. This ratio matches with that seen in human infants and newborns but does not match that seen mature individuals (54). By comparing the liver microsomes of adult zebrafish to microsomes of zebrafish larvae (5-120 hpf), researchers found

that the metabolic activity of CYP-enzymes were considerably lower in zebrafish embryos than in adult fish (59). The overall expression of CYP-enzymes increases in zebrafish larvae post hatching (> 72 hpf), illustrating the importance of considering the maturity level of zebrafish in a study design, especially if the data is to be interpreted and translated to mature individuals of higher vertebrates (54).

Elimination routes

There are several biological considerations to be discussed surrounding elimination routes in zebrafish larvae. The skin and the gills of the zebrafish larvae are important organs that maintain homeostasis through electrolyte balance and oxygen uptake (65), and once compounds of low molecular weights are dissolved in the embryo water, they can be absorbed *and* eliminated via passage through the skin (46). The kidneys and digestive tract can also possibly contribute to the elimination of drugs and their metabolites. In zebrafish larvae, the glomerular filtration starts at around 48 hpf, but the kidneys are not fully mature and size-selective until 4 dpf (66). By 96 hpf, there is a continuous passage throughout the digestive tract of the zebrafish larvae (67), possibly including this as an elimination route as well.

1.4.3 Zebrafish in biotransformation studies

Anselmo et al. published a review article in 2018 called *Zebrafish (*Danio rerio*): A valuable tool for prediction the metabolism of xenobiotics in humans?* where they present and compare published articles containing the words “zebrafish” and “metabolism” or “metabolite” in the title, abstract or keywords. This article showed that the interest in using zebrafish and zebrafish larvae as models for biotransformation has increased considerably since the beginning of the 21st century (1), and many findings and results point towards a promising and positive direction.

However, there is a lack of standardization regarding the experimental conditions in the published studies on biotransformation in zebrafish larvae. Factors such as the age of the fish (embryos to adults), different administration routes (exposure in water, spiked food, and injections), husbandry facilities (experimental temperature, light/dark cycles), exposure time (minutes to days) and different organic solvents in varying concentrations (DMSO and MeOH), differ between the published data that make up the knowledge basis on this subject (1). In addition, the use of *in vivo* models always come with a degree of biological variability. Taken

together, there are many aspects regarding the experimental conditions that should be more standardized before zebrafish and their larval life-stages can be adequately validated as model systems to study biotransformation.

1.5 Aims

There is a continuous need for developing new *in vivo* model systems for predicting and mapping biotransformation pathways and products of novel drug candidates as early as possible in the drug development process. Ethical challenges surrounding research conducted on animals makes non-animal model systems an attractive approach, and zebrafish embryo and larvae may provide a unique model system for this purpose. These larval life-forms could be of great value in preclinical drug development, possibly contributing to a greater pharmacokinetic knowledge basis for the selection on lead compounds that are most likely to succeed and attain regulatory approval. Zebrafish larvae have a well-established place in several research fields, such as developmental biology, drug development and toxicology (1) but their place in studying biotransformation is yet to be further investigated.

The main aim of this master project was to explore zebrafish larvae as a model system for biotransformation with simvastatin, fluvastatin, and captopril as test compounds. To explore this, the aforementioned drugs were administered to zebrafish larvae through aquatic exposure, and both the embryo water and zebrafish larvae were analyzed for contents of precursor drugs and selected metabolites. To analyze these samples, LC-MS/MS was used, because of the high sensitivity and selectivity of this instrumentation, and procedures for sample preparation and suitable LC-MS/MS methods were developed and optimized.

2 Experimental theory

2.1 Chromatography

Chromatography is a separation method that allows for physical separation of different compounds in a mixture by distributing them across two different phases (68). A common nominator for all types of chromatography is that separation happens as a mobile phase transports the mixture of compounds over a still-standing stationary phase. The mobile phase travels across the stationary phase with a specific flow rate, whilst carrying analytes from the mixture. Compounds with a high affinity to the stationary phase will be more retained than the mobile phase, and thus be slowed down. The time it takes for a compound to elute over the stationary phase is called *retention time*, and if compounds in a mixture have different retention times, they will be separated from each other. The properties and combination of mobile and stationary phase, as well as the chemical properties of the analytes, will affect the basis for the separation. Ion exchange, partition, adsorption, and size exclusion are all techniques which allow for separation based on the compounds' molecular properties (68).

2.1.1 Reversed Phase Liquid Chromatography

In reversed phase liquid chromatography (RPLC), compounds are separated based on their hydrophobic characters; the most hydrophobic compounds will have the strongest retention, and more hydrophilic compounds will have weaker retention (Figure 2.1). The stationary phase is typically made up of silica with hydrophobic side chains that is packed in a column. Commonly used hydrophobic side chains are octadecyl (C18), octyl (C8) and Phenylpropyl (Phenyl, $(CH_2)_3$-C_5H_6), here listed from most to least hydrophobic (69, p. 162). Van der Waals forces between these hydrophobic surfaces and the analytes are the most important interactions for retention (69, p. 164).

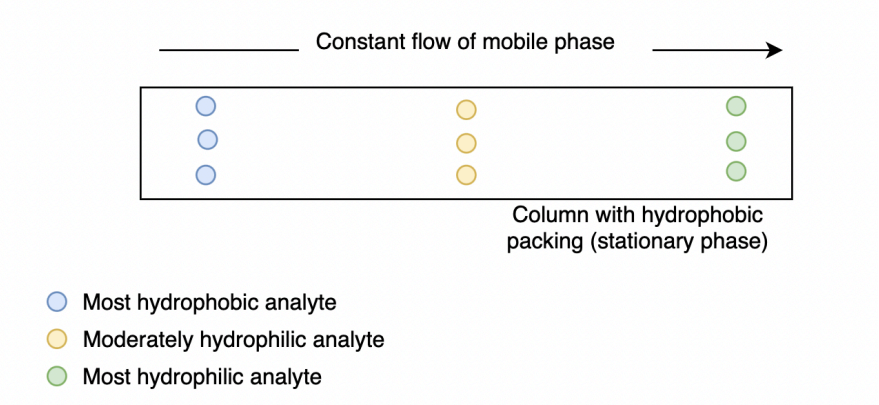

Figure 2.1: *Principle of reversed phase chromatography. Adapted from (69, p. 140).*

These stationary packings all have different applications and advantages. C18 is a popular option as a stationary phase in RPLC, as it is applicable to most pharmaceutical formulations (70, p. 319). When working with aromatic compounds, phenyl packings can provide a slightly more selective analysis, as pi-pi-interactions between phenyl and the aromatic rings of the analytes can contribute to greater retention (70, p. 319). Silica-based packing materials tolerate mobile phases in the pH range of 2-8 (69, p. 168, 70, p. 309). If the pH is too high (basic) the silica can dissolve, and if too low (acidic), the hydrophobic side chains may be cleaved of from the silica, thus ruining the stationary phase (69, p. 168).

The mobile phase is aqueous, and most often consist of water mixed with an organic solvent. The strength of the mobile phase depends on the composition of water and organic solvent, as well as the organic solvent itself. Methanol (MeOH), Acetonitrile (ACN) and Tetrahydrofuran (THF) are examples of organic solvents used in reversed phase chromatography, and out of these, MeOH is the weakest and THF the strongest solvent (69, pp. 166-168). A high grade of organic solvent increases the strength of the mobile phase, and with a strong mobile phase, the retention of the analytes will decrease (70, p. 313). Analytes that can be ionized are sensitive to the pH of the mobile phase. To modify the pH, buffers such as phosphate, acetic acid, or formic acid, can be added to the mobile phase. Ions are hydrophilic and will therefore be poorly retained on the stationary phase (69, pp. 166-168).

2.1.2 High Performance Liquid Chromatography (HPLC)

The principles described in above can be applied to high performance liquid chromatography (HPLC), which is a LC-setup where the chromatographic separation occurs under high pressure (71). The column used in HPLC is tightly packed to allow for a better separation, and because of this tight packing, an applied high pressure is required for the eluent to be able to pass through. In preclinical drug development and pharmaceutical analysis, HPLC is a commonly used method for ensuring separation of the analytes in a sample prior to detection (70, p. 302). A typical setup for HPLC involves a reservoir for the mobile phase(s), a high-pressure pump, an injector (often automated), and a column packed with stationary phase. This system is then coupled to a detector, for example a mass spectrometer, which translates the generated signals to interpretable chromatograms for data-analysis on a computer. A typical HPLC-setup is illustrated in Figure 2.2

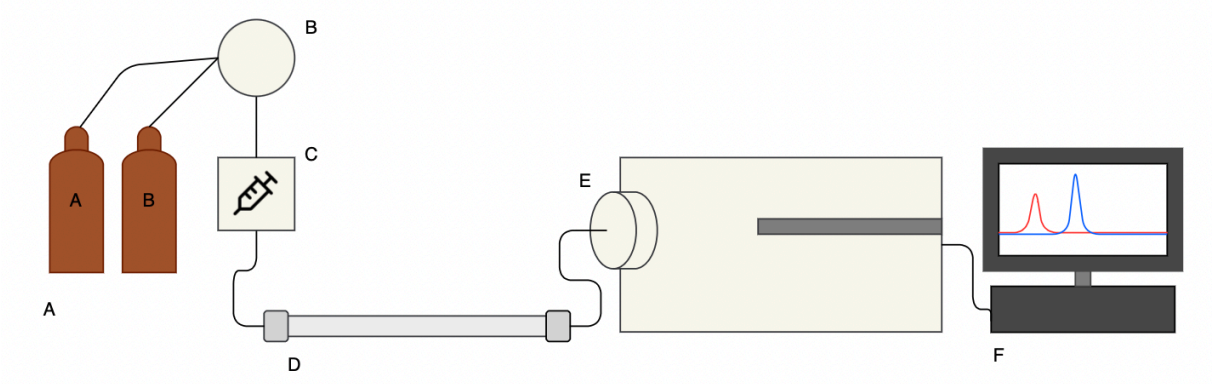

Figure 2.2: *HPLC setup.* ***A****: Reservoir with mobile phases (here, two flasks contain two different mobile phases (mobile phase A and B).* ***B****: Binary pump.* ***C****: Autosampler with injector.* ***D****: Column (stationary phase).* ***E****: Detector. Here, a mass spectrometer is illustrated, with tubing from the column leading inn to the ion source to the MS.* ***F****: Computer for analysis. Adapted from (69, p. 174).*

2.2 Mass spectrometry detection

Mass spectrometry (MS) is the preferred detection method for quantitating drugs in biological samples because of its high selectivity and sensitivity (70, p. 205). MS is also suitable for providing qualitative data on metabolite detection and identification (72), making it a superior analysis method for screenings related to the selection and characterization of lead compounds and their pharmacokinetic properties in drug discovery and development. Compared to other detectors used in pharmaceutical analysis, MS is quite expensive, and it requires regular service and support by highly trained personnel (70, p. 205).

When analytes from a sample enter a mass spectrometer, they will undergo three main processes. First, the analytes are ionized and enter gas phase in the ion source. Next, these generated ions are filtered in a mass analyzer based on their mass to charge (*m*/z) ratio. Filtered ions that have a stable trajectory through the mass analyzer, will reach a detector that produces signals. These signals are amplified before they are translated to mass spectra or chromatograms (if coupled with HPLC) which can be interpreted on a computer. These processes will now be more elaborated.

2.2.1 Electrospray ionization

In the LC-MS/MS instrument used in this thesis, electrospray ionization (ESI) is used to generate ions. ESI is readily compatible with HPLC since the ionization happens under atmospheric pressure (70, p. 205). Moreover, ESI is a soft ionization technique, as the degree

of fragmentation in the ion source is poor (70, p. 207). ESI can be operated in positive of negative mode, generating positive or negative ions for detection, respectively.

After compound separation with LC, the flow of mobile phase containing the sample (eluent) is transferred from the LC-column to the MS through a narrow peek tube. Next, the eluent passes through a needle to which a high electrical potential is applied (70, p. 205). If this electrical potential is positive, repulsive electrostatic forces will ensure that the positive ions will pass through the needle. Conversely, the negative ions will be attracted to the needle, and be kept from proceeding further into the MS. Next, droplets containing analytes and positive charges will exit the needle, and under the influence of a constant flow of nitrogen gas holding a high temperature, the eluent will start to evaporate (70, pp. 205-206). The positive charges ions will come closer and closer as the droplets' size is reduced. Eventually the surface tension of the droplet can no longer withstand the charge-charge repulsions (Coulomb force), resulting in an "explosion" of the droplet ("Coulomb explosion"). This creates several smaller, yet still charged droplets. These processes (evaporation and Coulomb explosion) are repeated several times, and eventually charged analytes (molecule ions) exist in gas phase (73). A negative charge (opposite charge than the ions generated) is applied to the heated capillary inlet into the mass analyzer to attract the ions. See Figure 2.3 for details. This capillary is very narrow in diameter, minimizes the leak of atmospheric pressure from the ion source to the mass analyzer. This is important, since the mass analyzer requires vacuum conditions (70, pp. 205-206).

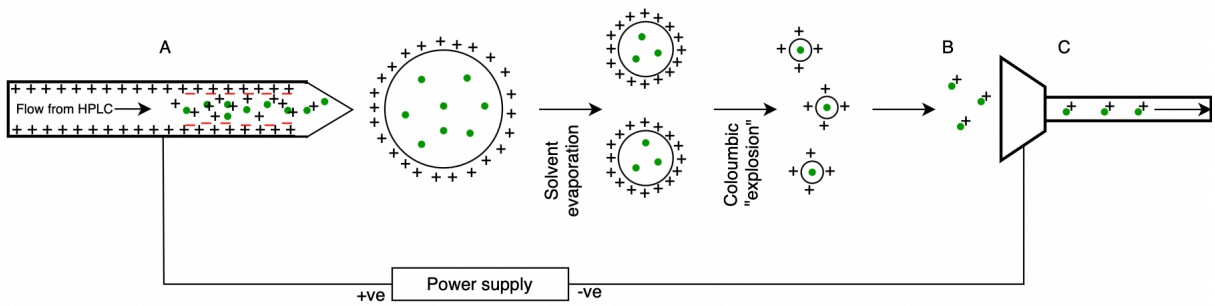

Figure 2.3*: Electrospray ionization, positive mode. The green dots represent analytes from the sample, the black '+' represent positively charged ions, the red '–' represent negatively charged ions. Droplets containing mobile phase and analytes from a sample are shot out from the needle and evaporate under the influence of a constant flow of nitrogen gas. Once they get smaller and smaller, they explode because of charge-charge repulsions (Coloumbic explosion). Eventually the analytes have gained charged and exist in gas phase. They are then attracted to the heated capillary inlet, leading into the MS.* ***A****: Charged needle leading into the ion source. The needle is positively charged, which attracts the negative ions and lets the positive ions pass through.* ***B****: Charged analyte ions.* ***C****: Capillary inlet into the MS/MS. The cone is negatively charged, attracting the analyte ions. Next, they travel through a thin capillary into the MS/MS. The figure is adapted from (73).*

In positive mode using ESI, ionization of the analytes is typically obtained by protonation $[M+H]^+$, and in negative mode deprotonation contribute to much of the ionization $[M-H]^-$. However, addition of adduct ions from the mobile phase can also contribute to ionization. Examples of typical adduct ions for positive mode are $NH4^+$ if the mobile phase contains ammonium, and Na^+ or K^+ if traces of these ions are present. Common adduct ions for negative mode are Cl^-, $HCOO^-$ and CH_3COO^- (70, p. 208).

2.2.2 Mass Analyzers

In short, mass analyzers work as ion filter. Selected ions are able to pass through this filter, and unwanted ions will not. The instrument used in this thesis is equipped with mass analyzers called quadrupoles, which are coupled in tandem and separated by a collision cell. This type of setup is often called a "Triple Quadrupole", or "QQQ", and is illustrated in Figure 2.4. The inner workings of the quadrupoles will be explained below. All types of mass analyzers operate under vacuum conditions. This is important, as it keeps the analyte ions from colliding with other air-borne molecules during analysis (69, pp. 267-268).

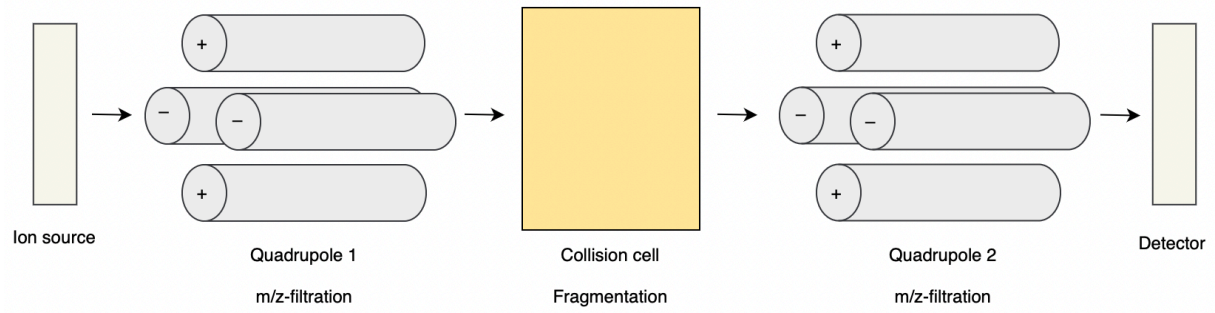

Figure 2.4: *Inner workings of a triple quadrupole (QQQ) mass analyzer. Ions generated in the ion source enter the first quadrupole, where ions are filtered based on selected m/z-ratios. In the collision cell (often referred to as the 'second quadrupole'), the precursor ions filtered out in the first quadrupole are fragmented into product ions. These product ions are then filtered in the second quadrupole, and selected product ions finally reach the detector. Adapted from (74, p. 99).*

Quadrupoles

The charged ions generated from the ion source are filtered in the mass analyzer based on their mass to charge ratio (*m/z*-ratio). A quadrupole consists of four parallel rods positioned orthogonally around a central axis. Electric fields of radio frequencies (RF) and direct currents (DC) are applied to the opposite pairs of rods to make a fluctuating voltage. One pair has the opposite voltage polarity than the other pair. When the charged ions are moving through the quadrupole, the voltage applied will influence the ions to move in an oscillating way. Ions with

a *m/z*-ratio that resonate with the DC and RF applied, will have a stable trajectory through the quadrupole and be available for detection. The ions that do not have a resonating *m/z*-ratio will have an unstable flight path through the quadrupoles, colliding with the rods and thus be trapped (Figure 2.5). In this way, only ions with a selected *m/z*-ratios will be detected (70, p. 216).

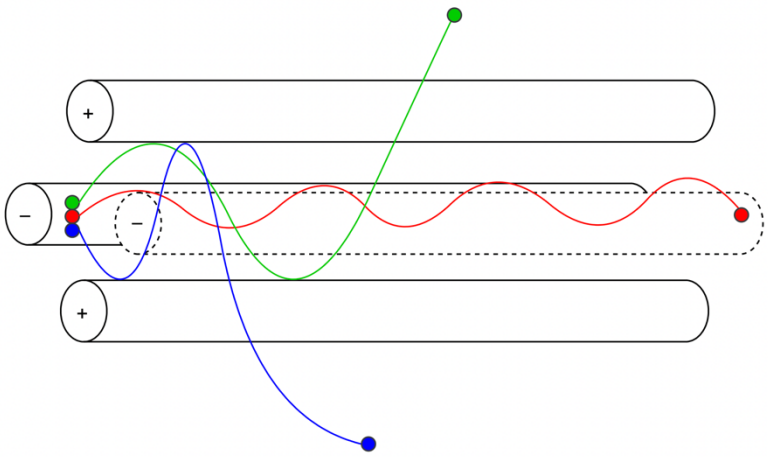

Figure 2.5*: Inner workings of a quadrupole. Four parallel rods are positioned orthogonally around a central axis, with two and two rods having opposite voltage polarity of the applied DC and RF. The green, red, and blue dots represent ions and their flight paths through the quadrupole. The m/z of the red ion resonate with the applied DC and RF, and has a stable trajectory through the quadrupole. The green and blue ions do not resonate with the applied DC and RF and will therefore be trapped. Adapted from (69, p. 269)*

Static and Scanning mode

If the DC and RF in a quadrupole are set to specific voltages during the whole scan time, the mode is called "static mode". Consequently, only ions with selected *m/z*-ratios will have a stable trajectory through the quadrupole, and all other ions will be filtered out. This mode is also known as Selected Ion Monitoring (SIM), and it is the most sensitive mode for MS analysis as the whole dwell time is spent filtering only selected *m/z*-ratios. If the DC and RF are ramped during the scan, a continuous range within an interval of *m/z*-ratios will be included in the filtration. This mode is called "scanning mode". Scanning mode is less sensitive than SIM, but it is very useful for qualitative detection and studying fragmentation pattern of unknown substances (75, pp. 14-18).

Multiple Reaction Monitoring (MRM)

Multiple Reaction Monitoring (MRM) is a mode available for triple-quadrupole instruments. As mentioned, a triple-quadrupole contains two quadrupoles placed in tandem separated by a collision cell. When operating in MRM mode, both quadrupoles are set to static mode (75, pp.

14-18). The first quadrupole is programmed to filter out only selected precursor ions. Next, these filtered precursor ions enter a collision cell, where they are fragmented to product ions by collision with an inert gas, such as nitrogen (70, p. 238). The second quadrupole is then programmed to filter out only certain fragment ions. By filtering for both specific precursors *and* product ions, this makes an especially valuable method for both quantitative and qualitative analysis, as it increases both the selectivity and the sensitivity of the instrument.

2.2.3 Electron multipliers

An efficient ion detector is important to the overall sensitivity of a MS. The number of ions that are filtered out through the mass analyzers are generally quite small, and therefore a significant amplification is needed to produce detectable signals for obtaining mass spectra or chromatograms (74, p. 176). Electron multipliers (EM) are widely used for ion detection in MS (74, p. 177), and an illustration of how they work is shown in Figure 2.6. Once the charged ions exiting the mass analyzer strike the surface of a high-potential electrode, secondary charged particles, such as electrons, will emit from the surface layer (74, p. 177). Next, these electrons will hit several dynodes with a decreasing negative potential in the EM, constructing a cascade effect that multiplies the signal drastically (up to 10^7) before reaching the anode (76, p. 67). To escalate the amplification even further, the operator can increase δEMV (delta electron multiplier voltage). This is sometimes necessary to generate strong enough signals, but it is important to keep in mind that the EM gets worn out with use (74, p. 177). By increasing the δEMV the lifespan of the EM will be decreased.

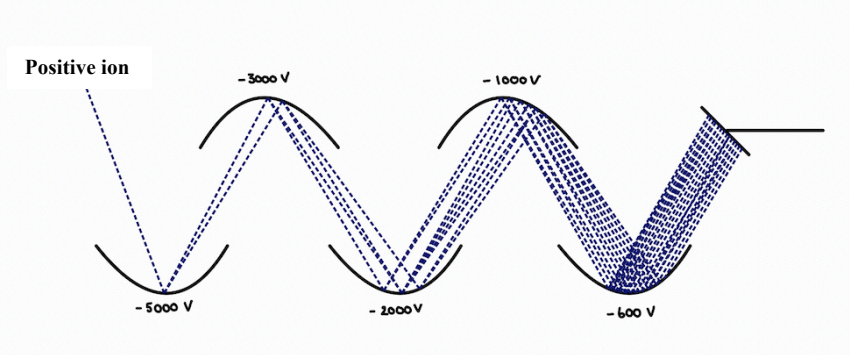

Figure 2.6: *Inner workings of an electron multiplier. Charged fragment ions (here illustrated as a positive ion) are converted to electrons (illustrated as blue, dashed lines) once hitting a high potential conversion dynode. By striking several dynodes in the EM, more and more electrons will be emitted, thus amplifying the signal. Adapted from (74, p. 178)*

2.3 LC-MS/MS

2.3.1 LC-MS/MS in drug development

LC-MS/MS an important and powerful analytical tool in all stages of drug discovery and development (77). Drug metabolism is especially important to investigate thoroughly during preclinical research to address any metabolic liabilities that can cause toxicity, or potential metabolites that contribute to the active pharmacological effects of the drug candidates (77). When it comes to ADME-TOX studies and Therapeutic Drug Monitoring (TDM), LC-MS/MS approaches are currently the most powerful analytical tool for drug analysis, where the precursor drug molecules and their metabolites can be quantified in different tissues and biofluids in regards of both biodistribution, biotransformation, and elimination (77). In addition, LC-MS/MS can contribute to structural characterization of metabolites, impurities, and degradation products, and have already been implemented in many studies for analysis of drugs in zebrafish and zebrafish larvae (1). As mentioned, LC-MS/MS have many favorable characteristics like high sensitivity and selectivity, as well as high throughput possibilities. Factors that contribute to the selectivity and sensitivity of LC-MS/MS analyses will be discussed in section 2.3.2.

2.3.2 Selectivity and sensitivity

Selectivity

The selectivity of a LC-MS/MS analysis can be increased by initial purification of the samples during sample preparation to eliminate noise and other interfering components. In addition, the mass spectrometer can be optimized by changing the ionization technique or by using more selective acquisition mode, like MRM (74, p. 262). Another consideration for increasing the selectivity the selectivity of an LC-MS/MS method, is to select quite large fragment ions for quantitation, > 200 Da if possible. The reason for this, is that larger fragment ions are more selective for the precursor ion than smaller fragments are (74, pp. 260-261). This is especially important when the samples are complex biological mixtures containing many similar molecules.

Sensitivity

There are many ways to increase the sensitivity of LC-MS/MS analyses. For one, the fragmentation ions chosen as quantifiers in MRM should be abundant, as with more ions available for detection, stronger signals will be generated. In addition, the MS/MS acquisition

can be optimized so that the ionization conditions suit the analytes in the best way possible. If the analytes of interest are small, or poorly ionizable, derivatization might be a useful approach as this can help obtain larger, and more easily ionizable analytes. Another approach is to test both positive and negative mode in the ESI (74, p. 262). Furthermore, different acquisition modes on the instrument will have different sensitivities, with MRM providing the most sensitive *and* selective mode when using a tandem MS (74, p. 193).

The lowest limit of detection is typically defined as the smallest sample quantity that yields a signal that can be distinguished from the background noise, typically by a 10-fold (74, p. 262). This is called "signal-to-noise ratio". Thus, a higher signal-to-noise ratio will decrease the limit of detection, making the method capable of quantitating even lower amounts of the analytes. Analyses performed with MRM mode have a higher sensitivity than those performed by SIM, because with the additional *m/z*-filtration in the second quadrupole, less noise-generating compounds will be able to pass the mass analyzer, and thus the signal-to-noise ratio will be increased (74, p. 264).

2.3.3 Internal standards and matrix effects

Internal standard

Quantitative analyses are especially vulnerable to be influenced by errors that might occur during sample preparation. The operator will contribute to errors during sample preparation, and the more steps in the preparation, the more accumulated these errors will become. In addition, variations in the conditions of the MS/MS may also contribute to inaccuracies. To reduce the influence of the accumulated errors to the results, and thereby increasing the confidence and reliability of the analysis, internal standards (ISTDs) can be included in the sample preparation. An ISTD is a compound with similar chemical properties to the analyte(s) that is chemically stable in the sample matrix and does not interact with the analytes. The same amount of ISTD is added to all the samples, as well as to the calibration curve. If conditions in the instrument varies, or steps in the sample preparation contribute to loss, the analytes and the ISTD will be affected in the same way, and thus the ratio between them will remain stable. Therefore, the ratio between these signals is used for quantitation when using an internal standard (74, pp. 266-268).

Matrix effects

Sample matrices are often complex, especially in biological analysis. Components from the matrix can in many cases co-elute with the analytes and may in such cases interfere with the ionization process of the analytes in the ion source (78). This influence can affect the signals wither by signal suppression or signal enhancement, and this effect is called the *matrix effect* (79, p. 114). For ionization methods under atmospheric pressure, such as ESI, matrix effects are a common problem. The ion source has a limit to its ionization capacity and with the introduction of several ionizable components from the sample matrix at once, the conflicting components may suppress or enhance the ionization of the analytes (79, p. 114). The droplet formation and evaporation in the ion source is critical to the ionization process. A change in viscosity or surface tension of the droplets may be a response to coeluting components, and this can influence the ability of the analyte to reach gas phase (78). In addition, non-volatile components in the matrix and mobile phases, such as a high grade of water, can also influence the droplets' ability to evaporate.

To increase the confidence in the analysis, matrix effects must be evaluated, and if possible, reduced or eliminated. One method for reducing matrix effects, is to dilute the samples, given that the sensitivity of the analysis remains adequate. Another approach is to simply reduce the injection volume of the sample (78). Sample clean-up is also useful in the effort of reducing matrix effects, but no matter how extensively this is done, it comes with limitations. The co-eluting components causing the matrix effects have very similar chemical properties to that of the analytes, and because of this the interfering components will not be adequately removed by even the most extensive clean-up regimens (80). The most efficient and secure method to compensate for potential matrix effects, is to add an ISTD that co-elutes with the analytes, ideally a stable isotope-labelled analog of the analyte (78, 80). When the ISTD does not co-elute with the analytes, the construction of matrix-matched calibration curves can help account for potential matrix effects (80).

One last remark that is to be mentioned when it comes to analysis considerations with LC-MS/MS, is that many sample matrices include components that will contaminate the instrument. Contamination in the ion source or on the cone and the heated capillary leading into the MS/MS may affect the signals negatively. Contamination happens more quickly when the samples are denser and less purified. When performing analysis on samples likely to cause contamination, maintenance and cleaning of the instrument is required more frequently.

2.4 Sample preparation

One advantage in using zebrafish larvae as a model system to study biotransformation, is that sample preparation can be made quite uncomplicated. Both the zebrafish larvae and their surrounding embryo water will be analyzed for the selected drugs and possible metabolites in this master project. In this section, different sample preparation techniques that have been implemented in this thesis will be presented.

2.4.1 Derivatization

Some analytes can be difficult to analyze using LC-MS/MS, such as molecules with a low molecular masses, or molecules that are highly hydrophilic (81). Derivatization can be a useful approach in these instances, as the analytes can be coupled with moieties that make them larger in size and less hydrophilic. For analytes that are poorly ionized in the ion source, chemical derivatization preliminary to analysis can also help generate larger and more easily ionizable analytes, in addition to possibly reducing the required amount of sample needed per injection (70, pp. 348-349, 82). Other uses for derivatization in quantitative bioanalysis using LC-MS/MS, is to stabilize analytes or to increase chromatographic separation (83).

In aqueous solutions, captopril will spontaneously form a disulfide-metabolite: disulfide captopril (84). Therefore, captopril is chemically derivatized with 2,4'-dibromoacetophenone (p-BPB) in the experiments performed in thesis, to stabilize it and stopping this spontaneous reaction prior to analysis. Ending this reaction is necessary to be able to accurately quantitate the amount of captopril left in the samples after a given amount of time. The reaction is shown in Figure 2.7. How samples are prepared, is explained in Methods.

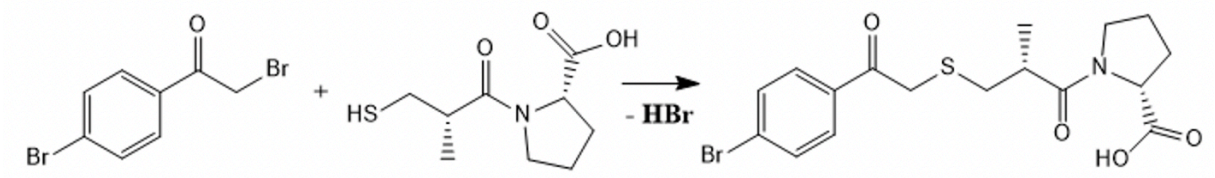

2,4-dibromoacetophenone Molecular Weight: 277,94 | **Captopril** Molecular Weight: 217,28 | **Captopril dervative** Molecular Weight: 414,31

***Figure 2.7**: Derivatization reaction with captopril and p-BPB.*

2.4.2 Protein precipitation

Protein precipitation is a commonly used method for drug extraction (85) and for cleaning up protein-rich samples (86), like plasma, and to disrupt protein-drug bindings prior to analysis

(86). Several parts of the LC-MS/MS system, such as the columns and tubing in the MS/MS can also easily be clogged if large particles, such as large proteins, enter the system. To reduce this risk, protein precipitation is an essential part sample preparation of protein-rich samples. In this thesis, homogenized zebrafish larvae dissolved in MeOH will be subject for analysis. To extract the drug molecules from the zebrafish larvae, as well as cleaning up the samples containing homogenized zebrafish larvae, protein precipitation is therefore implemented in the procedure (see Methods Section 3.4 for further details).

2.4.3 Sonication

To be able to analyze the presence of the drugs in zebrafish larvae following exposure, their cellular composition must be disrupted to release the drug compounds. One method for cellular disruption of biological tissues is sonication. Sonication is a mechanical disruption process in which ultrasonic frequencies are applied to a sample held in liquid to break up the cellular structure and to homogenize it (87). Microbubbles will be formed and implode in the liquid as a response to the ultrasonic vibrations, and the implosions generates shock waves with high enough energy to disrupt cell structures and shear nucleic acids (87). Sonication can be done using an ultrasonic bath, or with an ultrasonic probe.

2.4.4 Dilution of embryo water

In general, salts are incompatible with MS as they contaminate the ion source and cause signal and ion suppression (88). As the embryo water in which the zebrafish larvae live contain several types of salts (see p. 28 for details), the embryo water samples analyzed in this thesis will therefore be diluted with MQ or other organic solvents without salt contents to spare the MS for excessive salt-exposure.

2.5 Toxicity assays

In this master project, toxicity assays will be performed on zebrafish larvae to determine how much of the selected drugs they can be exposed to. Parameters that will be determined to evaluate the compounds' toxicity profiles on zebrafish larvae are "LC_{50}" and "MTC". LC_{50} stands for Lethal Concentration 50%, and it translates to the concentration of a compound that will kill 50% of the population upon exposure over a selected time frame. If for example the LC_{50} value after 24 hours is determined to be 600 nM, 50% of the population is expected to die after 24 hours exposure to 600 nM of the compound.

The Maximal Tolerated Concentration (MTC) translates to the highest concentration where no toxic effects are recognized upon exposure to the drug. When determining MTC, the exposed larvae should look and act identical to non-exposed larvae. In this thesis, oedema surrounding the heart of the zebrafish larvae and muscle impact were the key changes used to evaluate the compounds' MTCs. It is important to acknowledge these data for two reasons. First, if larvae are exposed to too high concentrations, their organ function may fail or be weakened, and this can impact the results of the biotransformation study that we want to perform. Next, it is beneficial to administer as much of the compounds possible, since more precursor molecules available for biotransformation possibly contributes to more metabolites formed. Even though LC-MS/MS is a very sensitive analysis method, the expected quantity of metabolites formed by the zebrafish larvae is very low, and so by giving as much of the drugs as possible will increase the chance – and confidence – of the peaks found.

3 Materials and methods

3.1 Chemicals and solutions

***Table 3.1**: List of chemicals used, their purity grades, and suppliers.*

Chemical	Purity	Supplier
Milli-Q water	–	–
Methanol	Hypergrade for LC-MS	Sigma-Aldrich
Acetonitrile	Hypergrade for LC-MS	Sigma-Aldrich
Ethanol	Rectified	Antibac AS
Simvastatin	Pharmaceutical Secondary Standard	Sigma-Aldrich
Fluvastatin sodium	Pharmaceutical Secondary Standard	Sigma-Aldrich
Captopril	Pharmaceutical Secondary Standard	Sigma-Aldrich
Captopril Disulfide	95 %	Toronto Research Chemicals
Enalapril maleate	99.9 ± 4 % (Reference material)	Sigma-Aldrich
2,4'-dibromoacetophenone	≥ 99 % (HPLC)	Sigma-Aldrich
Formic Acid	Concentrated	–
Ethyl-3-aminobenzoate methanesulfonate (Tricaine, MS222)	98%	Sigma-Aldrich
Dimethyl sulfoxide (DMSO)	≥ 99.5 %	Honeywell
Ammonium formate	≥ 99 % (HPLC)	Sigma-Aldrich

Embryo water blue (E3) was obtained from the Zebrafish Facility at the Department for Biological Sciences. It contained NaCl (4.5 mM), KCl (0.15 mM), $CaCl_2 * 2H_2O$ (0.3 mM), $MgSO_4 * 7H_2O$ (0.3 mM), and some drops of Methylene Blue (until it turned light blue) in water (personal communication with Ingeborg Nerbø Reiten, November 2022).

Table 3.2: *Stock-solutions kept at -80 ℃, aliquoted to Eppendorf-tubes (1.5 mL). The aliquots were maximum freeze-thawed a total of 3 times.*

Analyte	Solvent	Stock-concentration
Simvastatin (SMV)	DMSO	4,18 mg/ml (10 mM)
Fluvastatin (FLV)	DMSO	4,33 mg/ml (10 mM)
Captopril Disulfide (DICAPT)	Ethanol	0,19 mg/ml (439.2 μM)
Enalapril (ENA)	Ethanol	1 mg/ml (2.03 mM)
2,4'-dibromoacetophenone (p-BPB)	Methanol	1 mg/ml (3.6 mM)

3.2 Laboratory equipment

3.2.1 Equipment

Table 3.3: *Laboratory equipment used for sample preparation and incubation.*

Equipment	Specifications	Delivered by
HPLC vials	1.5 mL Screw Neck Vial (glass)	VWR, Cat. No: 548-0018A
HPLC inserts	Micro inserts 0.1 mL 30x5mm clear 15 mm top (glass)	VWR, Cat. No: 548-0020
HPLC septum	Septum 8 mm silicone/PTFE 0,9 mm slit	VWR, Cat. No: 548-0026
HPLC caps	Screw cap 8 mm black	VWR, Cat. No: 548-0025
LC-MS vials	Vial, screw, 2 mL, ambr, WrtOn, cert, 100 PK	Agilent Technologies Part No: 5182-0716
LC-MS inserts	250 μL insert, Polypropylene 100/PK	Agilent Technologies Part No: 5182-0549
LC-MS caps	Cap, 9mm blue screw cap, PTFE/RS, 100 PK	Agilent Technologies Part No: 5182-0717
Eppendorf-tube (1.5 mL)	Micro tube 1.5ml SafeSeal	SARSTEDT Ref: 72.706.400
Eppendorf-tube (2.0 mL)	Safe-Lock Tubes 2.0 mL	Eppendorf AG Order no: 0030 120.094
96-well plates	ThermoScientific Nunclon Delta Surface	ThermoScientific Cat. No: 167008
	TC-Plate 96 well, Suspension, Flat bottom	SARSTEDT Ref: 83.3924500

3.2.2 LC-MS/MS instrumentation and setup

The components of the LC-MS/MS instrumentation that was used for the analyses in this thesis are presented in Table 3.4.

Table 3.4: *LC-MS/MS instrument specifications.*

Module	Specifications	Delivered by
Binary pump (LC)	Agilent 1100 G1312A	Agilent Technologies
Autosampler (LC)	Agilent 1100 G1367A	Agilent Technologies
Column oven (LC)	Agilent 1100 G1316A	Agilent Technologies
Detector/Mass Spectrometer (MS)	Agilent Technologies 6420 Triple Quad LC/MS	Agilent Technologies
Software	Agilent MassHunter 10.0	Agilent Technologies
Columns	Fortis C18, 2,1 x 100 mm, A0181109-Z, 183-083-083 Kromasil 100-3.5-C18, 2,1 x 100 mm MHCLD10/P455524	–
Pre-filter (Guard kit for 2,1 mm)	Kromasil 100-3.5-C18 Batch: 170122-1 MHCLDSK	–

3.3 LC-MS/MS Methods and method development

For analyses of the selected drugs and their metabolites, LC-MS/MS methods run with both singe ion monitoring (SIM) and multiple reaction monitoring (MRM) were used. In this subchapter, LC-settings (Tables 3.5-3.6 and 3.7-3.9) and MS/MS acquisitions (Tables 3.10-3.13) applied for the LC-MS/MS methods of analyzing simvastatin (SMV), fluvastatin (FLV), and captopril (CAPT) and their selected metabolites, are presented. The MRM-method for SMV and its metabolite simvastatin-hydroxy-acid (SMVA) used in this thesis, had previously been established on the instrument, and the both MRM- and SIM-methods for FLV and FLV metabolites were based on this SMV method. A new method for CAPT and its metabolite disulfide captopril (DICAPT) was also developed, which will be described in detail in section 3.3.1.

3.3.1 LC-settings and mobile phase gradients

Simvastatin and fluvastatin

Table 3.5: *LC-conditions and mobile phase gradients for SMV and SMVA and all FLV methods. These LC-settings were the same for both methods.*

Mobile phase A	10 mM ammonium formate 0.1 % formic acid in MQ
Mobile phase B	ACN (100%, hypergrade for LC-MS)
Columns	C18 column, 2.1x100 mm (Fortis) C18 column, 2.1x100 mm (Kromasil)*
Run time	9 minutes
Injection volume	5 µL
Column temperature	40 °C
Temperature in the autosampler	5 °C

Time (minutes)	**0**	**1**	**2**	**5**	**5.1**	**8.8**	**8.9**	**9**
A (%)	70	40	5	5	70	70	70	70
B (%)	30	60	95	95	30	30	30	30
Flow (ml/min)	0.400	0.400	0.400	0.400	0.500	0.500	0.400	0.400

* Due to high pressure in the first column (Fortis), it was replaced by a C18-column with the same dimensions from Kromasil during the FLV experiments.

With these LC-gradient and flow settings, the retention time (RT) for the analytes were approximately 4,9 minutes for SMV, 4,5 minutes for SMVA and 4,2 minutes for FLV (see Figure 3.1).

With the LC-gradient described in Table 3.5, the hydroxylated metabolite of FLV (OH-FLV) eluted around the same time as FLV (around 4.2 minutes). In addition, the detected signals were quite weak. In an effort to optimize the chromatography when monitoring the metabolites of FLV with the FLV

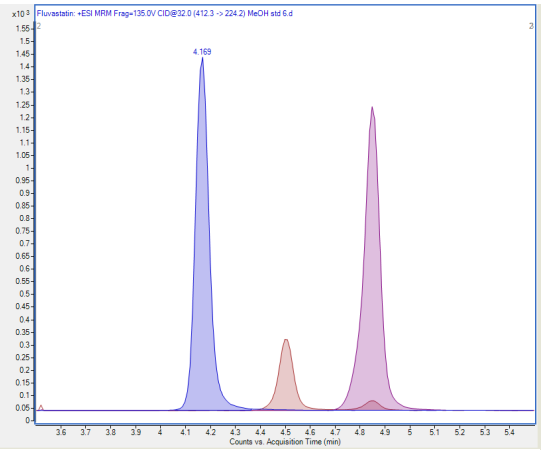

Figure 3.1: *Chromatogram of FLV (blue peak, RT: 4.2 minutes), SMV (purple peak, RT: 4.9 minutes) and SMVA (red peak, RT: 4.5 minutes). The concentrations of the analytes were 100 nM FLV, 100 nM SMV, and 50 nM SMVA, all diluted in MeOH (100%).*

SIM methods, a new gradient was therefore tested. This gradient is described in Table 3.6 below. With this gradient, the signal detection got weaker for both FLV and OH-FLV, and consequently the original gradient (Table 3.5) was used for all analyses of FLV after all.

***Table 3.6**. A new LC gradient tested for the FLV methods to see if separation of OH-FLV and FLV would be better than with the original gradient.*

Time (minutes)	**0**	**1**	**2**	**5**	**6**	**9**	**9.1**	**12.8**	**12.9**	**13**
A (%)	70	40	25	25	5	5	70	70	70	70
B (%)	30	60	75	75	95	95	30	30	30	30
Flow (ml/min)	0.40	0.40	0.40	0.40	0.40	0.40	0.50	0.50	0.40	0.40

The initial column (Fortis C18, 2.1 x 100 mm, A0181109-Z, 183-083-083) used for the FLV experiment had to be changed in February due to high pressure in the column and was replaced by a C18 column with the same dimensions from another supplier (Kromasil 100-3.5-C18, 2.1 x 100 mm, MHCLD10/P455524). The pre-column (C18) was also replaced by a pre-filter (Guard kit for 2.1 mm, Kromasil 100-3.5-C18, MH3CLDSK). The RT of FLV did not change drastically after this change (see Table 3.7), and no further modifications had to be made to the methods with the new column.

***Table 3.7**: Changes in the retention time (RT) for FLV using the MRM method after the column was changed.*

Analyte	**RT with original column**	**RT with new column**
FLV (MRM-method)	4,16	4,26

Captopril

How the CAPT method was optimized in terms of chromatographic conditions, is described in detail below in Section 3.2.2 (Figure 3.4). The following Tables (Tables 3.8-3.9) show the settings for column temperature, run time, injection volume and temperature in the autosampler, in addition to different mobile phase gradients and flow that were tested before the final gradient and flow conditions were established.

Table 3.8: *LC-conditions and for the CAPT method.*

Mobile phase A	0.1% formic acid in MQ
Mobile phase B	ACN (100%, hypergrade for LC-MS)
Column	C18 column, 2,1x100 mm (Kromasil)
Column temperature	40 °C
Run time	22.10 minutes
Injection volume	5 mL
Temperature in the autosampler	15 °C

Several LC-gradients and different eluent flow rates were tested for CAPT before the final gradient was established. The different gradients and flow rates that were tested, are presented in Table 3.9.

Table 3.9*: LC-gradients tested during method development for the Captopril method. Mobile phase A consisted of 0,1% formic acid in MQ, and mobile phase B was 100% ACN.* ***A****: gradient 1.* ***B****: Gradient 2.* ***C****: Gradient 3, final gradient, which was used for the experiments.*

A:

Time (minutes)	**0**	**10**	**10,1**	**15**	**15,1**	**18,1**	**18,2**	**22**	**22,1**
A (%)	80	80	50	50	5	5	80	80	80
B (%)	20	20	50	50	95	95	20	20	20
Flow (ml/min)	0.250	0.250	0.250	0.250	0.250	0.500	0.500	0.500	0.500

B:

Time (minutes)	**0**	**10**	**10.1**	**15**	**15.1**	**18.1**	**18.2**	**22**	**22.1**
A (%)	80	80	50	50	5	5	80	80	80
B (%)	20	20	50	50	95	95	20	20	20
Flow (ml/min)	0.400	0.400	0.400	0.400	0.500	0.500	0.500	0.500	0.400

C:

Time (minutes)	**0**	**2**	**2,10**	**10**	**10,1**	**15**	**15,1**	**18,1**	**18,2**	**22**	**22,1**
A (%)	80	80	70	70	50	50	5	5	80	80	80
B (%)	20	20	30	30	50	50	95	95	20	20	20
Flow (ml/min)	0.400	0.400	0.400	0.400	0.400	0.400	0.500	0.500	0.500	0.500	0.400

With the final LC-gradient and flow settings established for the CAPT method, the RT for ENA, DICAPT and CAPT-pBPB were 5,5 minutes, 5,8 minutes, and 13,8 minutes, respectively (Figure 3.2).

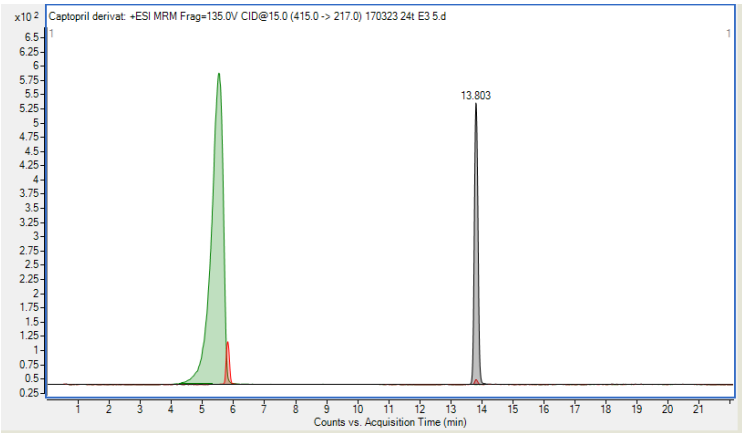

Figure 3.2: *Chromatogram of ENA (green peak, RT: 5.5 minutes, DICAPT (red peak, RT: 5.8 minutes, and CAPT-pBPB (black peak, RT: 13.8 minutes). This sample contained 100 nM ENA and 11.5 µM of CAPT. The DICAPT detected is a result of spontaneous formation of DICAPT from CAPT, and us therefore unknown. The sample was diluted in E3.*

3.3.2 MS/MS acquisitions

In this section, the applied MS/MS acquisition settings for all LC-MS/MS methods used in this study are presented (Tables 3.10-3.13). First, acquisition settings for the SMV, FLV, and CAPT MRM methods are presented, and below the MS/MS acquisitions for the FLV SIM methods are shown.

MRM-modes for quantitative analysis of SMV and SMVA, FLV, and CAPT and DICAPT

Table 3.10: *MS/MS acquisitions for the SMV and SMVA method. The ionization was run in positive mode for all analytes.*

Gas Temperature		325 °C				
Gas Flow		6 L/min				
Nebulizer		50 psi				
Capillary		4000 V (positive)				
Compound	**Precursor ion (*m/z*-value)**	**Product ion (*m/z*-value)**	**Dwell time**	**Fragmentor**	**Collision Energy**	**Cell Accelerator voltage**
SMV	436.3	285.2	200	120	11	4
SMVA	437.2	303.2	200	110	6	4
FLV (ISTD)	412.3	224.2	200	135	32	4

Table 3.11: *MS/MS acquisition settings for the FLV MRM method. The ionization was run in positive mode.*

Gas Temperature		325 °C				
Gas Flow		6 L/min				
Nebulizer		50 psi				
Capillary		4000 V (positive)				
Compound	**Precursor ion (*m/z*-value)**	**Product ion (*m/z*-value)**	**Dwell time**	**Fragmentor**	**Collision Energy**	**Cell Accelerator voltage**
FLV	412.3	224.2	150	135	32	4

Table 3.12: *MS/MS acquisition settings for the CAPT and DICAPT MRM method. The ionization was run in positive mode for all analytes.*

Gas Temperature		350 °C				
Gas Flow		12 L/min				
Nebulizer		60 psi				
Capillary		4500 V (positive)				
Compound	**Precursor ion (*m/z*-value)**	**Product ion (*m/z*-value)**	**Dwell time**	**Fragmentor**	**Collision Energy**	**Cell Accelerator voltage**
DICAPT	433.6	216	200	120	20	4
CAPT-pBPB	415	217	200	135	15	4
ENA (ISTD)	377.4	234.4	200	135	20	4

SIM modes for qualitative analysis of selected metabolites of FLV

The selected FLV metabolites to monitor were mono- and di-hydroxylated FLV (OH-FLV and 2OH-FLV, respectively), FLV with two added hydroxyl groups (2OH-FLV), FLV where the lactone ring is closed (Lactone FLV), FLV with a closed lactone ring *and* one hydroxy-group (Lactone OH-FLV) and FLV conjugated to glucuronic acid (GLU-FLV). To monitor these metabolites, SIM-methods with positive polarity were established. These selected analytes were monitored using three separate methods (Table 3.13). The main reason for doing this is that a low number of analytes to detect in a sample, makes it possible for the MS/MS to spend more time monitoring each analyte, providing a more sensitive analysis with less noise. Initially, only OH-FLV was monitored. Next, OH-FLV was included in a method with 2OH-FLV and GLU-FLV, and the Lactone FLV structures were monitored in another separate method. To analyze every sample for all these metabolites, it was determined that the samples needed to be injected to the LC-MS/MS a total of three times; one time for quantitation (FLV MRM method) in addition to two injections for monitoring metabolites. These SIM-methods for monitoring FLV metabolites were developed for qualitative analysis, and detected signals would consequently not be quantified.

The precursor ions were determined based on the molecular weights of the selected metabolites and adding 1 mass unit to their *m/z*: $[M+H]^+$. This accounts for ionization by protonation in the

ion source, which is common for ionization with ESI. As these methods were run with SIM, only selected precursor ions will pass through the MS/MS, and no collision energy will be applied. There were no reference compounds available for the metabolites monitored in these experiments, and the MS/MS conditions could therefore not be fully optimized. Nonetheless, acquisition settings determined for FLV in MRM mode were assumed suitable for monitoring of metabolites in SIM mode as well, based on the metabolites' high degree of structural similarity to FLV. Relevant acquisition settings from the MRM FLV method (Table 3.11) were therefore applied to these SIM FLV methods.

Table 3.13*: Established MS-acquisition settings for the qualitative SIM methods for FLV metabolites. The QQQ acquisition is the same as described in table 3.11, and the polarity is positive for all methods.* ***A****: Acquisition settings for the method monitoring for OH-FLV.* ***B****: Acquisition settings for the method monitoring for OH-FLV, 2OH-FLV, and GLU-FLV.* ***C****: Acquisition settings for the method monitoring for Lactone-FLV and OH-Lactone-FLV.*

A:

Compound	**Precursor ion (*m/z*-value)**	**Dwell time**	**Fragmentor**	**Cell Accelerator voltage**
OH-FLV	428.5	200	135	4
FLV	412.5	200	135	4

B:

Compound	**Precursor ion (*m/z*-value)**	**Dwell time**	**Fragmentor**	**Cell Accelerator voltage**
OH-FLV	428.5	150	135	4
2OH-FLV	444.5	150	135	4
GLU-FLV	604.5	150	135	4
FLV	412.5	150	135	4

C:

Compound	**Precursor ion (*m/z*-value)**	**Dwell time**	**Fragmentor**	**Cell Accelerator voltage**
Lactone FLV	394,5	150	135	4
OH-Lactone FLV	410,5	150	135	4
FLV	412,3	150	135	4

3.3.3 Captopril method development

With the intention of monitoring CAPT-pBPB (captopril derivative) and the metabolite DICAPT in embryo water samples and samples containing zebrafish larvae, a CAPT method (MRM) was developed based on a method published by Vancea et al. (84). Enalapril (ENA) was used as an internal standard. This development process will be described in detail below.

Determining precursor and product ions for the analytes

For the analyte CAPT-pBPB, MS1 (the first quadrupole) was set to static mode for 415 *m/z* and MS2 was set to scanning mode for product ions in the *m/z*-range from 200-420. Based on this scan, the fragmentation reaction selected for monitoring of this analyte was 415 *m/z* → 217 *m/z*. Previous publications were used to help identify precursor and product ion candidates for DISULF (433.6 *m/z* → 216 *m/z*, (89)) and ENA (377.4 *m/z* → 234.4 *m/z*, (90). Static modes run to test these product ions was done and confirmed that they were good fragmentation reactions for DICAPT and ENA. These reactions were therefore selected for the CAPT method in this study.

Tuning the MS/MS to the different analytes

The conditions in the MS/MS had to be optimized for the analytes in order to obtain as strong signals as possible. Separate samples containing CAPT-pBPB (11.9 μM), DICAPT (11.9 μM) and ENA (2 μM) were made for this purpose. Initially, the general acquisition settings (gas temperature, gas flow, nebulizer and capillary voltage and charge) for the ion source were tuned and optimized for CAPT-pBPB. The determined settings were assumed to be suitable for the other two analytes as well. Next, the collision energy and fragmentor voltage were optimized for all the analytes separately. These conditioned were adjusted based on what values produced the strongest response for the analytes, and the final settings are presented in Table 3.12 above.

Optimizing the chromatography

Once the instrument was tuned for the analytes, the chromatography had to be optimized. A mixture containing 1 μM of each of the three analytes (CAPT-pBPB, DICAPT and ENA) in EtOH was prepared for this purpose. This sample was injected several times, with the composition and flow of mobile phases altered from run to run to find optimal conditions with respect to separation, width, and shape of the peaks. The process of optimizing the chromatography for the analytes included in this method, is elaborated in Figure 3.4.

Isocratic conditions (starting with 60/40, 50/50, 70/30 and finally 80/20 mobile phase A/mobile phase B (v/v)) with a constant flow of 0.250 ml/min were initially introduced. With the 60/40-ratio, several issues occurred. First, both ENA and DICAPT eluted quite early, and possible interference with co-eluting salts from the matrix was considered problematic in terms of signal suppression. Next, ENA formed two peaks (see Figure 3.4.A) for the same fragmentation reaction (377.4 *m/z* → 234.4 *m/z*).

ENA has several chiral centers included in its molecular structure (Figure 3.3), and these two separate peaks may possibly represent two different stereoisomers. By altering the composition of the mobile phases to 50/50 (mobile phase A/B), the peaks got wider and still eluted undesirably early, so this was not a good solution (Figure 3.4.B). Next isocratic flow with 70/30 mobile phase A/B was applied. With these conditions, only one peak of ENA was observed, and the RTs were prolonged. However, an issue that occurred here, was that CAPT-pBPB did not elute within 15 minutes run time, and a gradient had to be applied in order to detect all three analytes in one run. Three different gradients were tested before the final gradient was selected (Table 3.9). At the end of the run, gradients for washing and equilibrating the column and the MS were applied. The equilibration conditions from the SMV and FLV methods were adapted to the CAPT method.

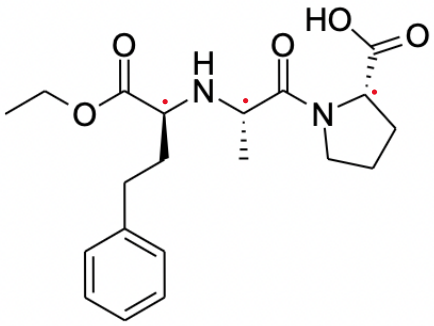

Figure 3.3: *Molecular structure of ENA. It has three chiral centers, marked with red dots in this figure.*

As seen in Figure 3.4, where the injected sample contained the same amount of each analyte (1 µM), the analytes produced signals with different intensities. The intensity of the signal is strongest for ENA, followed by DICAPT and finally for CAPT-pBPB. Based on this, it was determined that the concentration of ENA (the ISTD) added to the samples could be lower than the applied CAPT-exposure in the zebrafish larvae experiments.

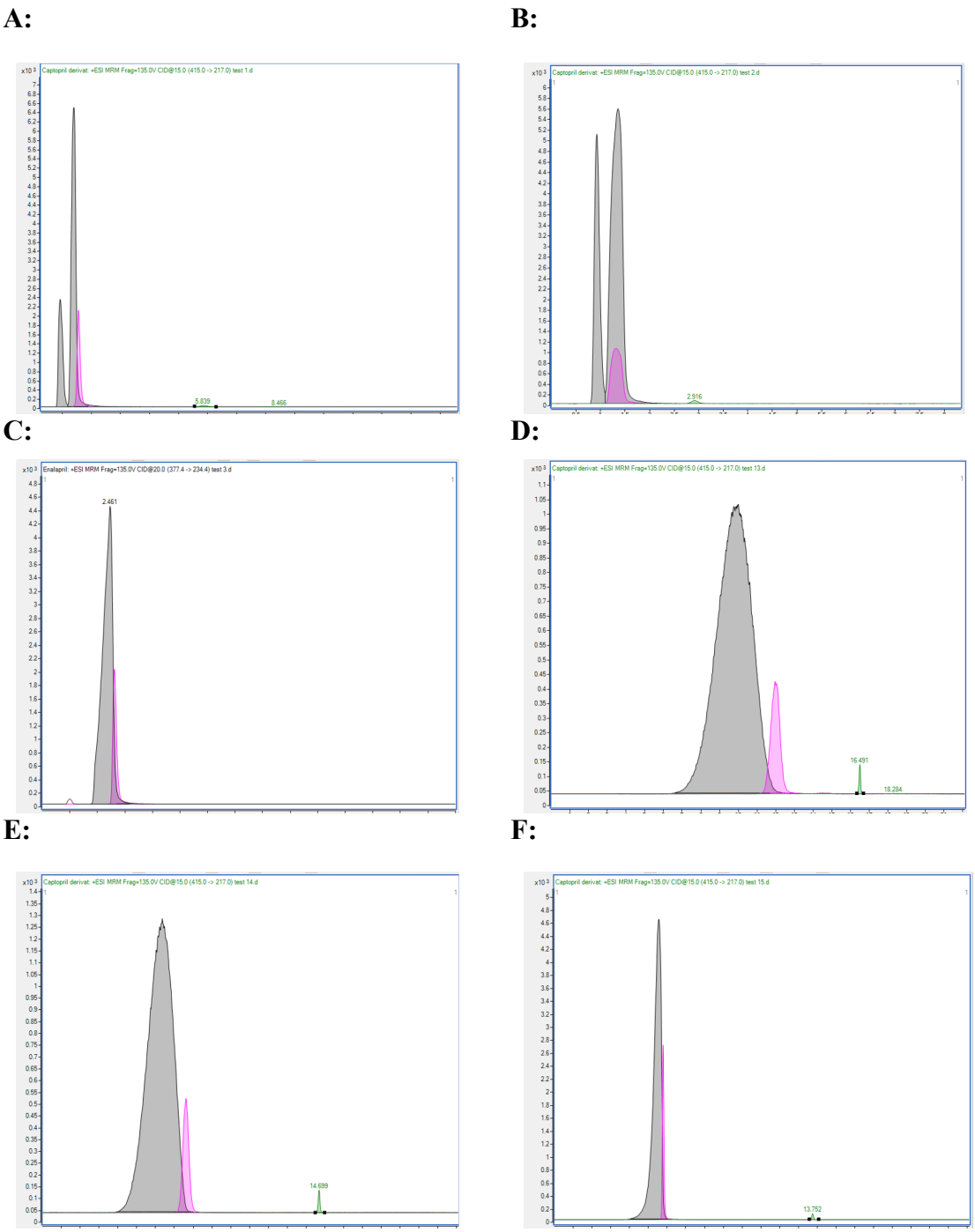

Figure 3.4: *Chromatographic optimization process for developing the LC-MS/MS method for CAPT-pBPB, DICAPT and ENA. The green peaks correlate to CAPT-pBPB, the pink peaks correlate to DICAPT, and the black peaks correlate to ENA.* ***A****: Isocratic conditions, 60/40 0.1% formic acid/ACN (v/v).* ***B****: Isocratic conditions, 50/50 0.1% formic acid/ACN (v/v).* ***C****: Isocratic conditions 70/30 0.1% formic acid/ACN (v/v).* ***D****: Application of LC-gradient 1 (Table 3.9.A).* ***E****: Application of LC-gradient 2 (Table 3.9.B).* ***F****: Application of LC-gradient 3, the final gradient that was used for the analyses (Table 3.9.C).*

3.4 Simvastatin and Fluvastatin: detection issues

Simvastatin

Calibration curves were prepared in both MQ and MeOH for SMV and SMVA, ranging from 6.25-100 nM and 5-50 nM, respectively. When MeOH was used as the solvent for the dilution series, linearity was seen within this range (Figure 3.5). However, when SMV was diluted in MQ, linearity was not seen (Figure 3.6). The data points included in the MQ-based calibration curve in Figure 3.6 correlates to noise from the basis line ($y = 4.54*10^{-5}\,x$). SMV is a lipophilic molecule (log P = 4.68 (91)), and the lack of responses were considered to possibly be related to either precipitation, or interactions with the surface of the laboratory equipment that had been used (plastic equipment).

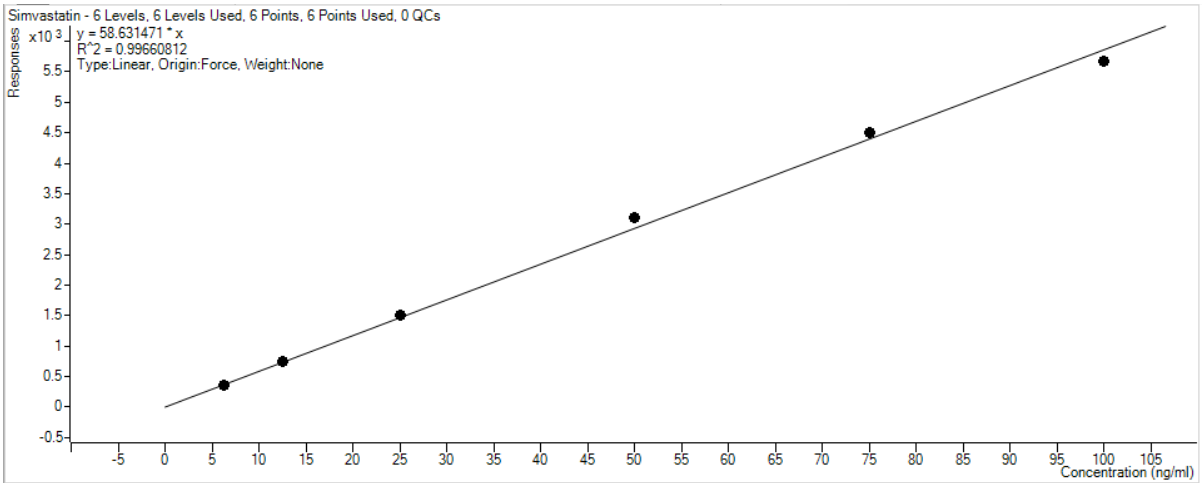

***Figure 3.5**: Calibration curve of SMV in MeOH, ranging from 6.25-100 nM.*

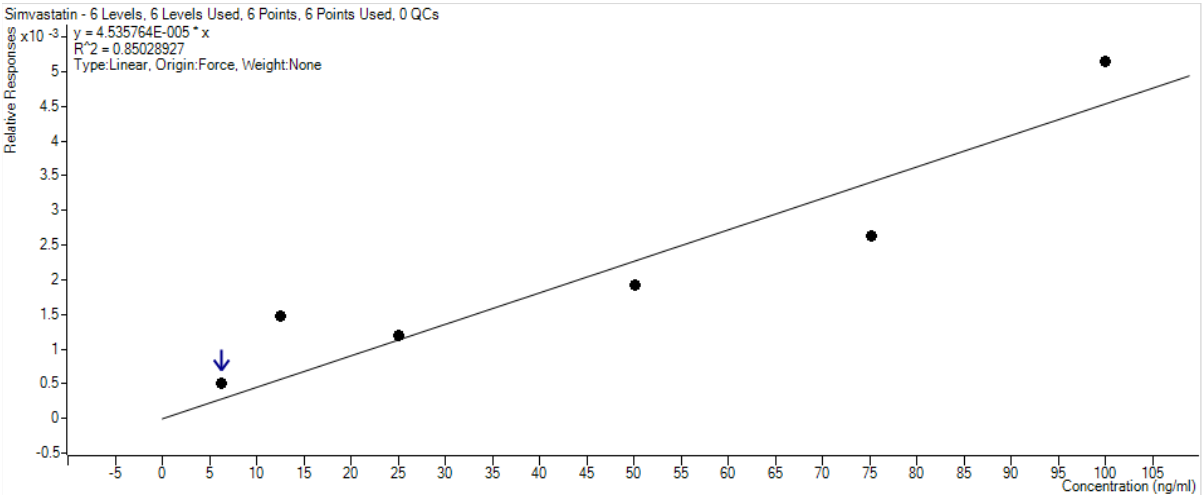

***Figure 3.6**: Calibration curve of SMV in MQ, ranging from 6.25-100 nM.*

In an effort to obtain responses for SMV in samples diluted in embryo water component, several approaches were tested:

1. The whole experimental pipeline was done exclusively in glass (except for the pipette tips). All samples contained 100 nM SMV in embryo water and were incubated at 28,5 °C for 24 hours prior to analysis.
2. The amount of DMSO was increased from 0.001% to 1%, and the dilution series was made with DMSO in all steps except for the last step of the dilution. This would ensure that SMV in embryo water would be held in plastic-based equipment for as short amount of time as possible. All samples contained 100 nM SMV in embryo water and were incubated at 28,5 °C for 24 hours prior to analysis.
3. The embryo water from the incubated samples was evaporated using a vacuum-centrifuge (Eppendorf Concentrator Plus), and the samples were resuspended in 100% MeOH. All samples contained 100 nM SMV in embryo water and were incubated at 28,5 °C for 24 hours prior to analysis.
4. The embryo water from the incubated samples was evaporated using a vacuum-centrifuge, and the samples were resuspended in 35/65 MQ/MeOH (v/v). In the latter scenario, MQ was added first to dissolve the salts from the E3, and MeOH was added last. Samples prepared like this was tested after 6 hours incubation and 24 hours incubation to see if the incubation time or temperature influenced signal detection.

All these samples were analyzed using the SMV and SMVA MRM-method on LC-MS/MS (Table 3.5 and 3.10). More details on these tests together with obtained results are presented in Section 4.2 in Results.

Fluvastatin

Similar experiments were conducted for FLV as for SMV, investigating the following variations:

1. The whole experimental pipeline in glass equipment vs. plastic equipment
2. The concentration of DMSO from increased from 0.001% to 1%.

All these samples contained 100 nM FLV diluted in embryo water and were incubated for 24 hours at 28,5 °C prior to analysis using the FLV MRM method on LC-MS/MS (Table 3.5 and 3.11). More details on these tests together with obtained results are presented in Section 4.2 in Results

3.5 Experimental workflow with zebrafish larvae experiments

The general experimental pipeline with experiments conducted in zebrafish larvae were as follows:

1. Expose zebrafish larvae to the selected drugs through aquatic exposure.
1. Incubate at 28.5 °C for 24 hours and 48 hours.
2. Prepare samples collected from embryo water and samples containing zebrafish larvae.
3. Prepare and run calibration curves within the same day and worklist as the samples.

More details regarding the conducted experiments and sample preparation procedures with FLV and CAPT in zebrafish, are presented below.

3.5.1 Fluvastatin and zebrafish larvae

Mobile phases

Mobile phase A consisted of 0.1% formic acid and 10 mM ammonium formate in MQ, and mobile phase B was 100% ACN. The mobile phases were refilled when needed, and mobile phase A was not used longer than 7 days after preparation, as both formic acid and ammonium formate are volatile components.

Preparing samples with FLV and zebrafish larvae

To a HPLC-vial, 3 zebrafish larvae (72 hpf), 100 µL embryo water and 50 µL FLV (600 nM) diluted in embryo water was added, giving a final exposure of 200 nM FLV and 0.002 % DMSO. The samples were next incubated at 28.5 °C for 24 hours and 48 hours. The HPLC-vials could not be covered during incubation since the zebrafish larvae need access to oxygen for gas-exchange. To decrease the risk of evaporation of samples during incubation, the HPLC-vials were therefore placed inside a closed pipette-box with damp tissue paper surrounding the vials in the incubation cabinet.

Embryo water samples

Embryo water samples were collected after 24 hours (from 96 hpf old zebrafish larvae) and 48 hours (from 120 hpf old zebrafish larvae) of incubation. To HPLC-inserts (glass), 120 µL of the samples were transferred. Next, the glass-inserts were wrapped in tissue paper, placed in Eppendorf-tubes (2.0 mL), and centrifuged for 5 minutes at 5000 rpm holding 19°C. To LC-MS vials, 320 µL MQ was added together with 80 µL of the centrifuged samples, diluting them 1:4. Finally, the samples were vortexed for 20 seconds prior to analysis.

Samples with zebrafish larvae

To extract FLV from the zebrafish larvae, the following procedure was established. The zebrafish larvae were transferred to clean HPLC-vials, and the remaining embryo water was pipetted of and tossed. Next, the larvae were washed twice with clean embryo water and transferred to a clean Eppendorf tube (1.5 mL). Next, 150 µL of ice-cold MeOH was added to dry zebrafish larvae in the Eppendorf-tubes, and the samples were sonicated to homogenize the larvae (see next paragraph for further details on this procedure). The samples were then centrifuged for 10 minutes at 14000 rpm and 4 °C. Finally, 50 µL of the supernatant was added to a LC-MS vial, making the samples ready for analysis.

Sonication

To extract the FLV and potential metabolites that may have been absorbed into the larvae, the zebrafish larvae had to be homogenized. Different sonication procedures were tested to achieve sufficient homogenization. Initially, Eppendorf-tubes with three zebrafish larvae (72 hpf) and 150 µL ice-cold MeOH were placed in a sonication bath, and after 5 minutes of treatment the larvae were completely homogenized. On this basis, 5 minutes in the sonication bath was incorporated as the homogenization step to the sample preparation. However, when the incubated samples (holding 96 hpf and 120 hpf old zebrafish larvae) were treated with this regimen, it was not sufficient for completely homogenizing all the samples. The different samples required varying times in the sonication bath, ranging from 5 to 25 minutes. This can possibly be explained by a less fragile cell structure as the zebrafish larvae are developing. Because of these variations, the zebrafish larvae were instead sonicated using a sonicator probe (Misonix sonicator ultrasonic liquid processor XL). The samples were sonicated for 20 seconds on the probe, prior to centrifugation. The probe was washed with MQ and dried using a tissue paper between each sample.

Cleaning of HPLC-vials

The experiments with FLV were conducted and incubated in HPLC-vials. The vials were reused throughout the experiment and were therefore thoroughly cleaned after each use. First, the vials were filled with MQ water and soap and soaked for 10 minutes. Next, the vials were washed with clean MQ three times to ensure that all the soap was rinsed completely off. Finally, the vials were filled with 40% ethanol, emptied, and air-dried overnight. Blank samples incubated

in cleaned HPLC-vials did not show any traces of FLV, showing that the washing procedure was sufficient.

Calibration curves and yield samples

Two types of calibration curves were constructed for these FLV experiments: one with the same matrix as the embryo water samples (1:4 dilution in MQ) and one in MeOH. For the matrix matched calibration curve for the embryo water samples, working standard solutions ranging from 12.5-250 nM were constructed, giving a calibration curve ranging from 2.5-50 nM FLV once diluted 1:4 with MQ. Linearity was seen within these ranges, as shown in Figures 3.8 and 3.9.

The calibration curve made in MeOH was intended for quantitation of FLV in the samples containing zebrafish larvae. In addition, matrix matched yield samples containing three homogenized zebrafish larvae were made to account for potential matrix effects caused by the sonicated zebrafish larvae. To obtain these yield samples, a dilution series was made of FLV in ice-cold MeOH, creating solutions of 5 nM, 10 nM, and 15 nM. Next, three zebrafish larvae were transferred to Eppendorf-tubes (1.5 mL), and their surrounding E3 was pipetted of, leaving them as dry as possible. To the dried zebrafish larvae, 150 µL of the FLV solutions were added. Next, the samples were sonicated and centrifuged as described above. There was no addition of internal standard to any of the samples in this experiment.

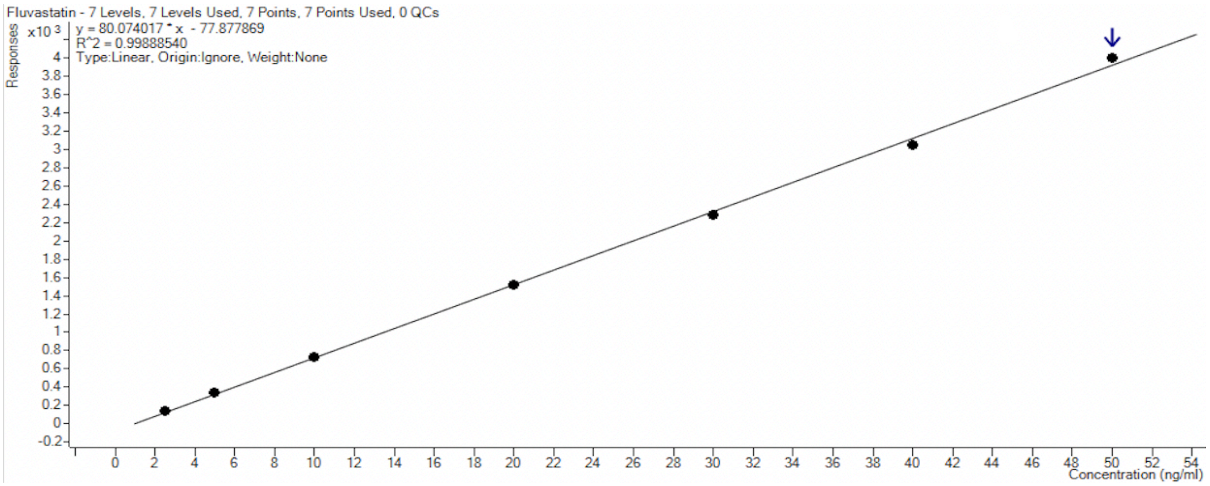

Figure 3.8*: Calibration curve with FLV in embryo water and MW (1:4, E3:MQ), ranging from 2.5-50 nM.*

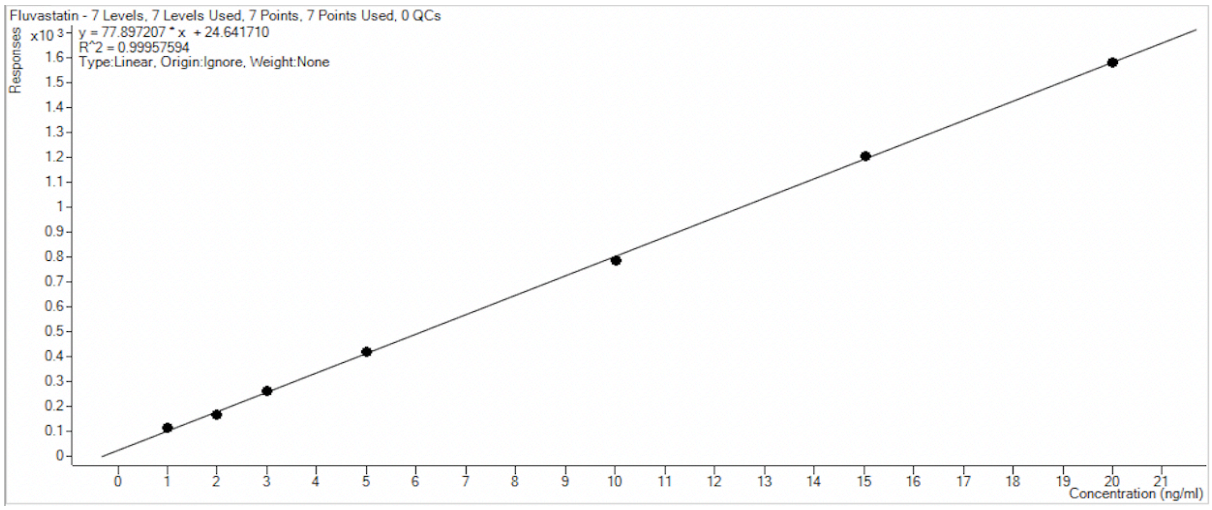

***Figure 3.9**: Calibration curve with FLV in MeOH, ranging from 1-20 nM.*

3.5.2 Captopril and zebrafish larvae

Mobile phases

Mobile phase A consisted of 0.1% formic acid in MQ and was prepared fresh for each experiment. Mobile phase B was 100% ACN and was refilled when needed.

Determining the reaction time for derivatizing CAPT to CAPT-pBPB

According to the article by Vancea S. et al. (84) in which the CAPT method in this thesis was based on, 30 minutes reaction time in room temperature was sufficient to fully derivatize free CAPT to CAPT-pBPB in human plasma. However, plasma is very different from embryo water. Therefore, the experimental conditions regarding this derivatization reaction were tested and established using the following procedure:

- To an Eppendorf-tube (1.5 mL), 160 µL embryo water was added, and spiked with 40 µL 18 µg/ml freshly diluted CAPT in embryo water, creating a sample with a final concentration of 13.8 µM CAPT.
- Next, 40 µL pBPB (1 mg/ml, 3.6 µM) diluted in MeOH was added to the sample, and the reaction ran in room temperature exposed to light (on the laboratory bench) for 30 minutes.
- Finally, the sample was vortexed with 300 µL MeOH and placed in the autosampler of the LC holding 15 °C. It was injected every 30 minutes for 5 hours, and in addition at 24 hours after the reaction was started.

Based on this monitoring, it was determined that the reaction for fully derivatizing free CAPT to CAPT-pBPB required 2 hours to be fully derivatized in E3.

Sample preparation

Fresh CAPT stock-solutions and dilution series in embryo water were prepared just before it was given to the zebrafish larvae. To wells of a 96-well plate, three zebrafish larvae (72 hpf) together with 200 µL of embryo water and 50 µL CAPT (50 µM) was added, ensuring a final exposure concentration of 10 µM CAPT to the zebrafish larvae in each well. The plate was then incubated at 28.5 °C (no light) before samples were collected. Samples were collected after 24 hours and 48 hours of incubation, with the age of the zebrafish larvae being 96 hpf and 120 hpf, respectively.

Embryo water samples

After incubation, 200 µL of embryo water from each well was transferred to Eppendorf tubes (1.5 mL). Next, 40 µL ice-cold p-BPB (1 mg/ml, 3.6 mM) was added to start the derivatization reaction. The reaction ran for 2 hours in room temperature with daylight exposure (on the laboratory bench). After 2 hours, 300 µL ice-cold MeOH was added to the samples, diluting them 1:2.7. They were first vortexed for 30 seconds, and then centrifuged for 10 minutes at 14000 rpm holding 19 °C. To new Eppendorf-tubes (1.5 mL), 100 µL of the supernatant together with 10 µL ENA (1100 nM, dilution series in MQ) as an IS was added. The mixture was vortexed once again for 30 seconds. Finally, the sample was pipetted over to LC-MS vials with inserts, making them ready for analysis.

Samples with zebrafish larvae

Zebrafish larvae (either three larvae from one well (a total of three larvae), or three larvae from three wells (a total of nine larvae)) were collected and transferred to new Eppendorf tubes (1.5 mL) using a transfer pipette. These Eppendorf tubes were placed on chilled for 5 minutes before further sample preparation to slow down the movements of the larvae. Next, the embryo water was removed from the larvae, and they were washed twice with 200 µL fresh embryo water, leaving them dry in the Eppendorf tubes. Then, 200 µL embryo water was added to the dry larvae, and they were once more placed on ice for 5 minutes before sonication. With the sonication probe, the sonication process was more sufficient when the larvae were gathered at the bottom of the tube, and not swimming around. Therefore, the larvae were chilled for 5

minutes prior to sonication, to reduce their movements. The larvae were sonicated for 60 seconds using a sonication probe (Misonix sonicator ultrasonic liquid processor XL). Following the sonication step, the samples containing zebrafish larvae were prepared in the same way as the embryo water samples as described above.

Calibration curves

On the day of analysis, fresh calibration curves for DICAPT and CAPT were constructed to match the matrix of both sample-types. The CAPT stock-solution was prepared fresh in embryo water for each calibration curve. For both CAPT and DICAPT, working calibration solutions (0.6-18 µg/ml) diluted in embryo water were used to spike 160 µL of clean embryo water or 160 µL of embryo water containing three sonicated zebrafish larvae. Next, the calibration standards were prepared just as the incubated samples, providing calibration curves ranging from 0.46-13.8 µM CAPT-pBPB and 0.23-6.9 µM DICAPT. Linearity was seen for both analytes within these ranges, as seen in Figures 3.10 and 3.11.

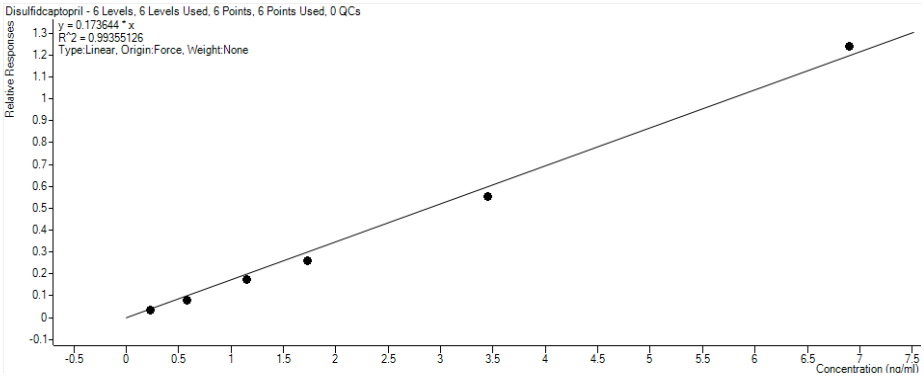

Figure 3.10: *Calibration curve for DICAPT, ranging from 0.23-6.9 µM.*

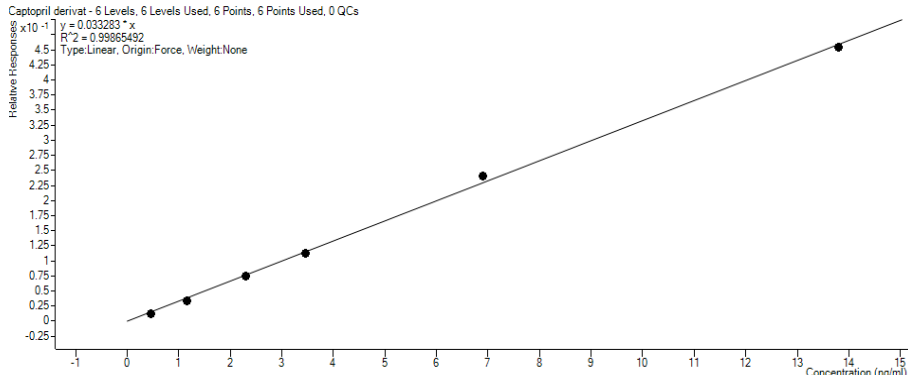

Figure 3.11: *Calibration curve for CAPT-pBPB, ranging from 0.46-13.8 µM.*

3.6 Zebrafish handling and care

Fertilized eggs from wild-type zebrafish were collected at the Zebrafish facility run by the Department for Biological Sciences at the University of Bergen. Adult fish were placed in a breeding container overnight, with mesh separating the adult fish from the eggs. The fertilized eggs were collected the following day and transported to Laboratoriebygget at Haukeland University Hospital. During transport, they were kept in a container ensuring a stable and suitable temperature. Next, approximately 50 embryos were transferred to each petri dish filled with 20 mL fresh E3 and the embryos were kept in a dark incubator at 28.5 °C. The embryos were monitored daily, and dead embryos and debris from their chorions after hatching were removed.

The embryos hatch spontaneously between 48-72 hpf (92, p. 298). If embryos were needed before spontaneous hatching, they were dechorionated under a microscope using forceps and a syringe to gently pull the chorion apart, releasing the embryo into the surrounding E3.

In order to study the larvae under the microscope, they were anesthetized using Tricaine (0,02% w/v). Immediately after microscopy, the E3 containing Tricaine was removed and replaced by fresh E3. By the age of 120 hpf, the petri dishes containing larvae were placed on ice for 20 minutes to sedate the larvae, before euthanizing them by freezing at -20 °C.

3.7 Statistics

Students t-tests were performed using Microsoft Excel for Mac (version 16.72), and f-tests were used to investigate is variances were assumed equal or not. All other statistical tests were performed using IBM SPSS for Mac (version 2.7). Details regarding the statistical analysis used are mentioned continuously throughout the Results chapter. The significance level for all analyses was defined as $p \leq 0.05$.

4 Results

4.1 Determining LC50 and MTC for the test compounds in zebrafish larvae

To evaluate the toxicity of each test compound, zebrafish embryos were exposed to SMV, FLV or CAPT from 2 dpf to 4 dpf in a 96-well plate with one zebrafish larva in each well. Zebrafish larvae that had not hatched spontaneously were dechorionated approximately 6 hours prior to drug exposure. The concentration ranges tested were 10 nM to 3000 nM for SMV, 50 nM to 4000 nM for FLV and 100 nM to 1 mM for CAPT. The concentration range tested for SMV was selected based on a previous toxicity assay with SMV on zebrafish larvae (93). Further, as FLV is less potent than SMV (4, pp. 190-191), the selected concentration-range for FLV was set slightly higher than that selected for SMV. A study performed by Margiotta-Casaluci et al. (94) found that zebrafish larvae tolerated up to 50 mM captopril if pH in the embryo water was adjusted to 7.4 with 1 M NaOH. However, since concentrations that high were not necessary with the developed LC-MS/MS method, we decided to use and test lower concentrations where pH-adjustment was not necessary. The larvae tolerated CAPT-concentrations up to 1 mM, and no mortality or signs of toxicity was observed within the tested concentration range for this drug.

Signs of toxicity and dead larvae were on the other hand seen for the statins. To define LC_{50} for SMV and FLV, the percentage of dead larvae from each exposure concentration was calculated (Figure 4.1). For SMV (n = 7), LC_{50} was between 1000-3000 nM after 24 hours, and between 200 and 300 nM after 48 hours exposure (see Figure 4.1). FLV was less toxic: LC_{50} was above

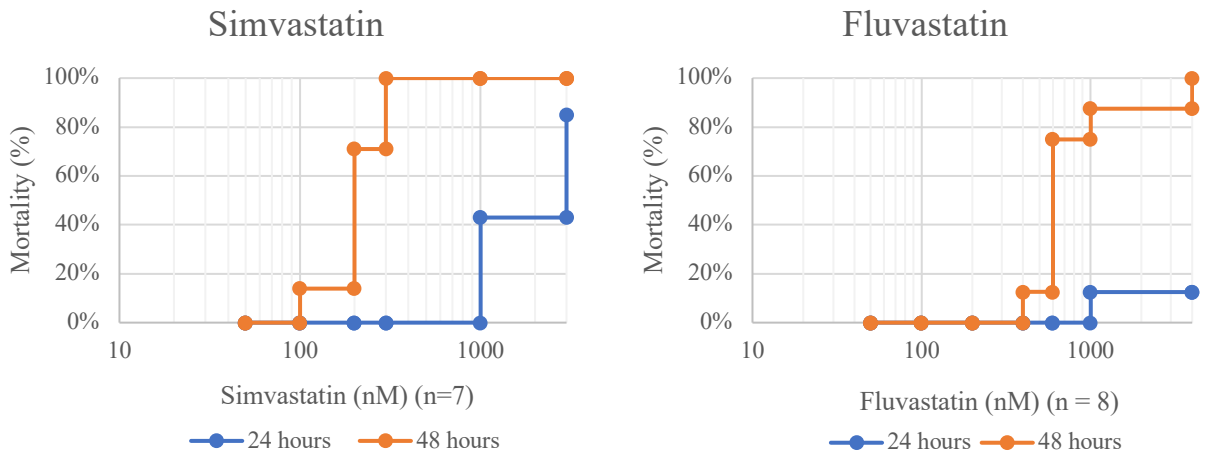

***Figure 4.1**: Mortality curves for estimating LC_{50}-values for SMV and FLV in zebrafish larvae after 24 and 48 hours of drug exposure.*

the tested range after 24 hours, and between 600 and 1000 nM after 48 hours exposure (Figure 4.1).

Statins are generally well tolerated by humans. However, they are known to cause side effects related to muscle symptoms, ranging from muscle weakness and pain to rhabdomyolysis (95). Based on this, signs of muscle affection in the tail region of the zebrafish larvae following drug exposure were used to evaluate toxicity. In addition, observations of pericardial edema were included in the toxicity assessment, since this is a commonly observed abnormality in zebrafish larvae following exposure to a wide range of chemicals (96). MTC was determined to be 100 nM for SMV, 200 nM for FLV and 1 mM for CAPT. Examples of oedema and muscle impact are shown in Figure 4.2. Dead zebrafish larvae were observed as clearly dissolved in the wells.

For all further experiments, the established MTC-values were used as a basis for determining what concentrations the zebrafish larvae would be exposed to. By administering the highest nonlethal concentration possible, more of the precursor molecules, i.e., SMV, FLV, and CAPT, would be available for metabolic degradation. In addition, by administering as high concentrations as possible, stronger signals were expected with all the LC-MS/MS analyses.

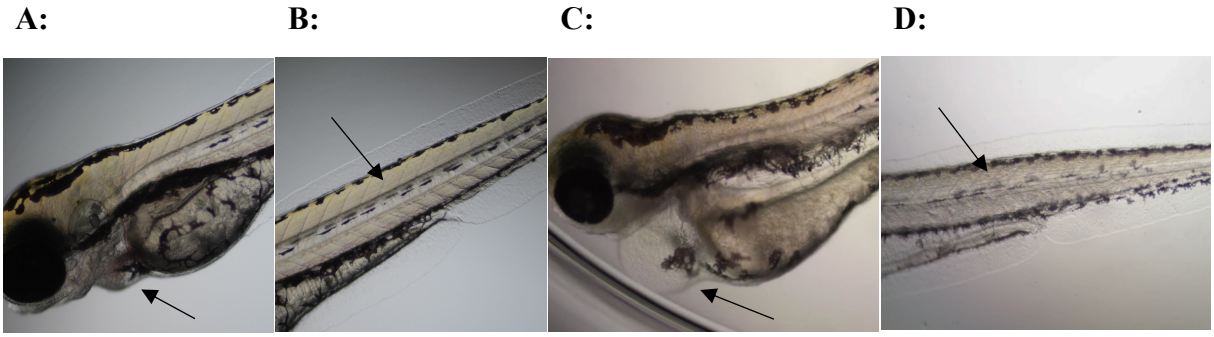

Figure 4.2: *Photographs of AB-strain zebrafish larvae aged 4 dpf under the microscope.* ***A:*** *Frontal part of a control zebrafish larva (not exposed to FLV).* ***B:*** *The same zebrafish larva as in picture A, showing healthy skeletal muscle along the body and tail.* ***C:*** *Zebrafish larva that has been exposed to 600 nM FLV for 48 hours. Severe oedema is seen surrounding the heart of the larva.* ***D:*** *The same zebrafish larva as in picture C with signs of muscle impact. The skeletal muscles appear rougher and less defined compared to the control.*

4.2 Simvastatin was excluded as a test compound because of detection issues

As mentioned in section 3.4, we had trouble detecting SMV and SMVA with the embryo water-based matrix, and several experimental variations were tested to see if signals could be obtained. The reason for doing these tests was not to quantitate the analytes, but rather to see if the

different experimental setups would lead to signal detection of SMV. Therefore, no calibration curves were run with these tests. An overview summarizing the results is presented in Table 4.1 below.

Table 4.1: *An overview of the different experimental conditions tested for SMV and SMVA in an effort to obtain signal responses. The results are listed with the mean values and standard deviations (n = 3 unless otherwise is stated). If no signals were detected, they are listed as n.d.*

Type of experiment	**Signal response SMV**	**Signal response SMVA**
Conducted exclusively in glass equipment (except pipette tips)	n.d.	1241 ± 26
Conducted exclusively in plastic material	n.d.	n.d.
Samples incubated in glass vials, evaporated, and resuspended in MeOH (100%)	n.d.	615 ± 98
Samples incubated in 96-well plate (plastic), evaporated, and resuspended in MeOH (100%)*	n.d.	729 ± 59

* n = 2, one of the samples were not run because of visible particles in the vial.

We could not exclude plastic materials entirely from the sample preparation, but we could ensure that SMV and embryo water together would not be in contact with plastic materials at the same time. Samples that ensured this, were prepared as follows: 2 µL of 10 µM SMV diluted in DMSO was added to 198 µL embryo water in a glass vial. The pipette tip was never in contact with the water, and the vial was vortexed for 20 seconds to blend. The final concentration of SMV and DMSO in these samples was then 100 nM and 1%, respectively. These samples were incubated for both 6 hours and 24 hours prior to sample preparation to see if the incubation time affected the results. After incubation, the samples were evaporated until dry using a vacuum-centrifuge. Next, they were resuspended by adding 70 µL MQ and 130 µL MeOH (100%), in that order, to dissolve the salts from the embryo water before adding MeOH. The results are shown in Table 4.2.

Table 4.2: *An overview of experiments performed where SMV diluted in water was not in contact with plastic materials during any stage of the sample preparation. Samples were incubated for 6 hours and 24 hours prior to analysis, and the obtained results are listed with the mean values and standard deviations (n = 3). If signals were not detected, they are listed as n.d.*

Type of experiment	Signal response SMV	Signal response SMVA
6 hours incubation	1892 ± 135	464 ± 164
24 hours incubation	n.d.	1886 ±169

As seen in Table 4.2, we did obtain signals for SMV when SMV diluted in embryo water never was in contact with plastic material. This suggests that interactions with plastic materials were the main issue causing the lack of detection for this analyte. However, this experiment also showed that SMV was rapidly converted to its metabolite SMVA over 24 hours of incubation at 28.5 °C. Based on the suggested issues with plastic materials, in addition to the instability of SMV and incubation time, we decided to not proceed further with SMV in experiments with zebrafish larvae.

4.3 Signal were stronger for fluvastatin when samples were incubated in glass vials

As mentioned, FLV and SMV belong to the same group of drugs and have similar molecular backbone and lipophilic profiles (log P = 4.85 (97) and log P = 4.68 (91), respectively). However, FLV contains a carboxylic group, while SMV has a closed lactone ring, making FLV more water soluble. Still, because of their structural similarities, initial tests to explore if the type of material and concentration of DMSO influenced the strength of the signal responses for FLV, were conducted. All samples in these experiments contained 100 nM FLV and were prepared in either glass vials or Eppendorf-tubes and 96-well plates, throughout the experiment. In the case of experiments conducted in glass vials, plastic pipette tips were still used for preparing dilution series. The final concentration of DMSO in the samples was either 0.001% or 1%. The results from these experiments showed that the signal responses were strongest with 0.001 % DMSO in glass equipment (Table 4.3), and thus all further experiments with FLV were prepared and incubated using glass vials.

***Table 4.3**: Tests to evaluate the most suitable laboratory equipment for sample preparation with FLV, percentage of DMSO in the samples, and the mean signal responses detected using the FLV MRM-method on LC-MS/MS.*

Type of sample	Signal response
Glass materials, 0.001% DMSO	9080 (n = 3)
Glass materials, 1% DMSO	8342 (n = 3)
Plastic materials, 0.001 % DMSO	3663 (n = 3)
Plastic materials, 1% DMSO	4099 (n = 2)

4.4 Experimental design

The next aim was to find experimental conditions for maximal biotransformation of the administered drugs into metabolites in the zebrafish larvae. It was hypothesized that the more zebrafish larvae available for performing metabolic reactions, the more metabolites were likely to be produced. To investigate this, samples containing 200 nM FLV in embryo water with no zebrafish larvae (n = 3), one zebrafish larva (n = 5) and three zebrafish larvae (n = 5) were incubated for 24 hours and 48 hours at 28.5 °C prior to analysis. The FLV-contents in the samples were then quantified using the MRM FLV-method on LC-MS/MS (see Table 3.5 and 3.11 in Methods). The remaining quantity of FLV in the embryo water after incubation was used as an indirect measure for metabolite production, providing an indication on how fluvastatin was affected in the presence of no zebrafish larvae, one zebrafish larva, and three zebrafish larvae. The obtained results are presented in Figure 4.3.

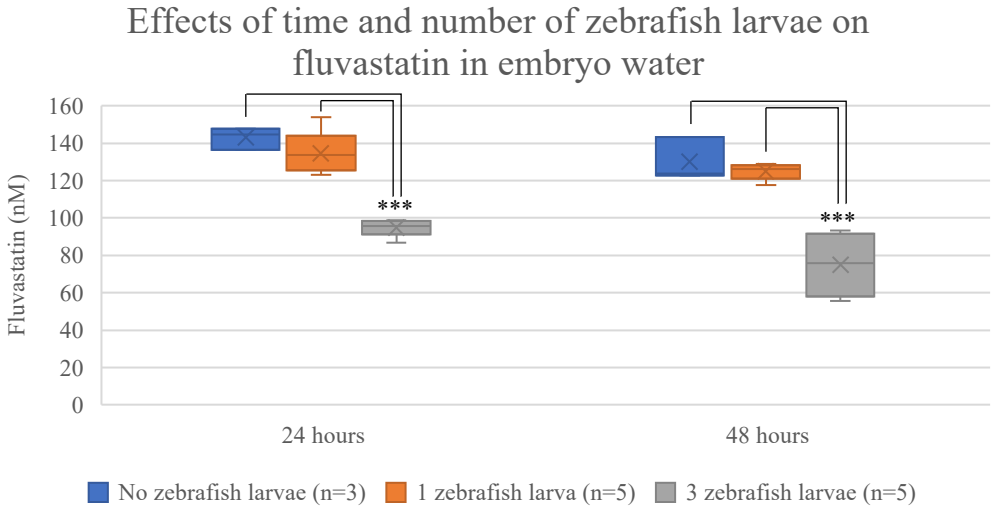

Figure 4.3:** Samples with no zebrafish larvae, one zebrafish larva, and three zebrafish larvae and 200 nM fluvastatin in embryo water were incubated at 28.5 ℃ for 24 hours and 48 hours prior to analysis. We found that there was a significant reduction of fluvastatin when three zebrafish larvae were present in the sample compared to no zebrafish larvae and one zebrafish larva (= $p < 0.005$) when incubated for both 24 hours and 48 hours.*

Several statistical tests were performed on these data to investigate differences between the groups. Initially, a univariate analysis of variance was performed for the two factors 'time' (24 hours or 48 hours) and 'number of zebrafish larva' (one or three zebrafish larvae). This showed that there was a significant reduction in the amount of FLV after 48 hours compared to 24 hours ($p < 0.01$), and when three zebrafish larvae were present compared to one zebrafish larva ($p < 0.005$). However, these two factors did not have a significant combined effect on the amount of FLV left in the embryo water.

By performing an ANOVA-analysis, we found that there was a significant difference between the groups of none, one, and three zebrafish larvae after both 24 hours and 48 hours incubation. The variance between the groups was determined unequal, and therefore the post-hoc test Dunnett's T3 was used for further analysis. Separate tests were run for the groups incubated for 24 hours and 48 hours. We found that after 24 hours, there was a significant difference in the reduction of FLV in the embryo water when three zebrafish larvae had been present during incubation compared to one zebrafish larva ($p < 0.005$) and no zebrafish larvae ($p < 0.005$). After 48 hours incubation, there was also a significant difference in samples with three zebrafish larvae compared to one zebrafish larva and no zebrafish larvae ($p = 0.005$[1] for both comparisons). There was no significant difference between the groups containing one and zero zebrafish larvae, neither after 24 hours nor 48 hours of incubation (Figure 4.3) For more details regarding these analyses, see Appendix 1.

Based on these results, we decided to use three zebrafish larvae per sample for all further experiments with both FLV and CAPT in zebrafish larvae.

[1] The significance level seen from this test was 0.005. However, we do not have more decimals to draw a conclusion to whether the p value was over or under 0.005. Therefore, it is written with an equal sign, and not a 'greater than'-sign ('<'). See Appendix 1 for further details.

4.5 Qualitative Analysis of fluvastatin: monitoring fluvastatin metabolites

For all further experiments with FLV, zebrafish larvae were exposed to 200 nM (the determined MTC) FLV at the age of 72 hpf. Samples were collected after 24 hours (larvae were aged 96 hpf) and 48 hours (larvae were aged 120 hpf) of incubation, and all zebrafish larvae were evaluated under a microscope for signs of toxicity or abnormalities prior to analysis.

Initially, only one metabolite of FLV was monitored: OH-FLV. As mentioned, two main metabolites of FLV are 5-OH-FLV and 6-OH-FLV (both with a molecular weight of 427.5 Da), making these metabolites good candidates for indications of FLV biotransformation in zebrafish larvae. With protonation as the main ionization method, OH-FLV would produce molecule ions with a *m/z*-value of 428.5 in the ion source. Using C18 chromatography, it was expected that OH-FLV would elute earlier than FLV since the OH-moiety would make the molecule slightly more hydrophilic. Samples with blank embryo water and samples with three zebrafish larvae exposed to 200 nM FLV were prepared. Peaks were detected for ions with a 428.5 *m/z*-ratio (RT was 4.2 minutes) in chromatograms from samples containing FLV and zebrafish larvae but not in blank embryo water, as shown in Figure 4.4. The blue lines in these chromatograms correlate to FLV (412.3 *m/z*-ratio) and the red lines correlate to 428.5 *m/z*-ratio, possibly representing OH-FLV. Both analytes elute around 4.2 minutes.

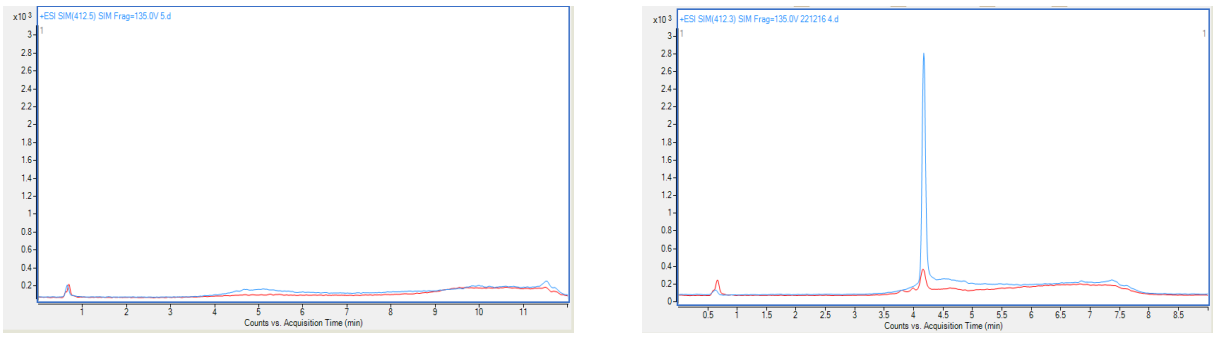

Figure 4.4*: Chromatograms of samples monitored for analytes with 428.5 m/z (OH-FLV) and 412.3 m/z (FLV). The blue lines correlate to FLV, and the red lines correlate to an analyte with OH-FLV. The chromatogram to the left is a sample with blank embryo water (no FLV contents), and to the right is chromatogram obtained is an embryo water sample that had contained three zebrafish larvae and 200 nM that had been incubated for 24 hours at 28.5 ℃.*

A: ***B:***

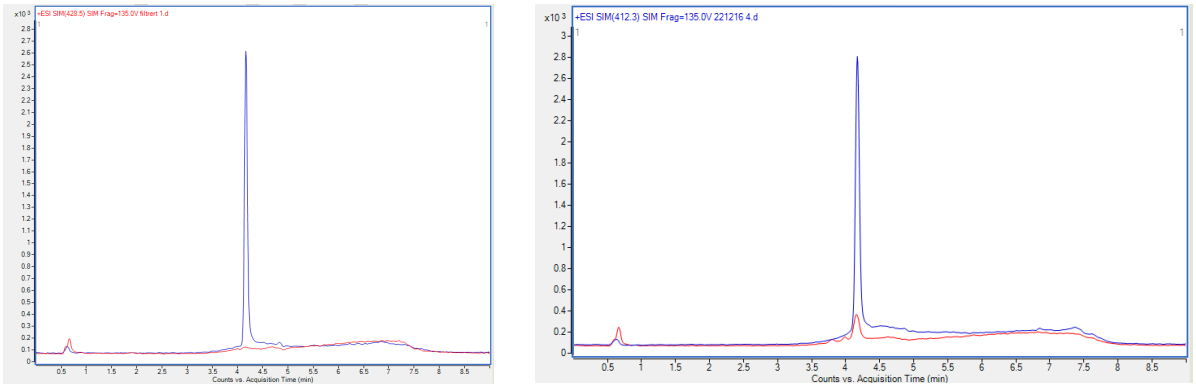

Figure 4.5: A*: Chromatograms monitoring FLV (412.3 m/z) and OH-FLV (428.5 m/z) obtained from samples with 200 nM FLV, incubated at 28.5 ℃ for 24 hours prior to analysis. The blue peaks correlates to FLV and the red lines correlate to ions with m/z-ratio 428.5.* ***A****: Sample where the embryo water had been sterile filtrated. B: Sample where the embryo water had <u>not</u> been sterile filtrated.*

However, the peak detected at 428.5 *m/z* was also present in FLV-samples without zebrafish larvae (Figure 4.5). The embryo water in which the zebrafish larvae are incubated is not sterile. Since bacteria have several metabolizing enzymes (98), it was of interest to find whether potential microbes in the embryo water could have contributed to the formation OH-FLV, or if this reaction had occurred spontaneously in the aqueous environment. To test this, embryo water was sterile filtrated using a 0.22 µm sterile syringe filter prior to dilution of FLV. The samples (n = 5) were then incubated at 28.5 °C for 24 hours. Qualitative analysis did not show any traces of peaks correlating to an analyte with *m/z*-ratio of 428.5 (see Figure 4.5), supporting the theory that microbes from the embryo water contributed to the formation of this analyte.

4.5.1 Interpretation of results obtained for the monitored fluvastatin metabolites

As mentioned in Methods, selected metabolites of FLV were monitored using separate methods. One method included the FLV-metabolites OH-FLV (428.5 *m/z*-ratio), 2OH-FLV (444.5 *m/z*-ratio) and GLU-FLV (604.5 *m/z*-ratio). The other method included the metabolites LACTONE-FLV (394.5 *m/z*) and LACTONE-OH-FLV (410.5 *m/z*). All these precursor ions were selected based on protonation as the main ionization technique, creating ions with $[M+H]^+$ *m/z*-ratios. The embryo water from zebrafish larvae exposed to 200 nM FLV (n = 10) was collected after 24 hours and 48 hours of incubation. In addition, the zebrafish larvae from these wells were homogenized and analyzed (n = 10). To evaluate whether the detected peaks correlated to analytes produced by the zebrafish larvae or if they had been produced spontaneously, embryo water with FLV and no zebrafish larvae was also analyzed (n = 5). Blank samples were blank

embryo water (n = 3), and non-exposed, homogenized zebrafish larvae aged 96 hpf (n = 3) and 120 hpf (n = 3). The results from these analyses were obtained by comparing the chromatograms from the different samples to their representative blanks. An example of how this comparison was done will be shown for ion with 444.5 *m/z*-ratio, which is the same as the expected *m/z* for 2OH-FLV. The remaining results are presented in Tables 4.2-4.8.

A: ***B:***

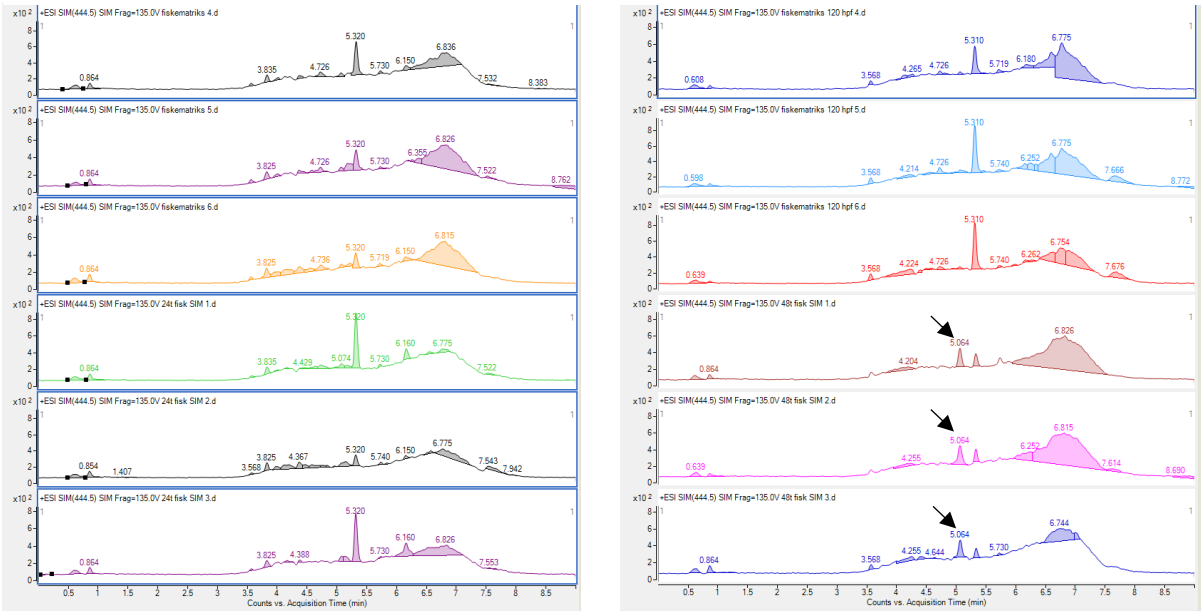

Figure 4.6: *Chromatograms correlating to ions with a m/z-value of 444.5.* ***A****: The larvae in these samples were aged 96 hpf and had been exposed to FLV for 24 hours prior to analysis.* ***B****: The larvae in these samples were aged 120 hpf and had been exposed to FLV for 48 hours prior to analysis. For both* ***A*** *and* ***B****, the top three chromatograms represent blank samples without any FLV contents, and the bottom three are homogenized zebrafish larvae that have been exposed to FLV. The arrows point to a difference observed in samples with exposed zebrafish larvae, that was not seen in the representative blanks.*

When the chromatograms from these analyses were interpreted, the presence of peaks in samples containing FLV and representative blanks, the RT of these peaks, and their signal strengths were the main differences that were investigated. An example of how this was done will now be described. When comparing zebrafish larvae and their embryo water that had been exposed to FLV to non-exposed zebrafish larvae (representative blank) analyzed after 24 hours incubation (aged 96 hpf), none of the detected peaks were present only in samples containing FLV (Figure 4.6). Therefore, we concluded that no metabolite of FLV correlating to ions with a *m/z*-value of 444.5 was present in these samples. However, when looking at the chromatograms obtained from larvae after 48 hours incubation (larvae aged 120 hpf), there was

a difference between larvae exposed to FLV and the matrix-matched blanks (Figure 4.6). There was a peak eluting at 5.064 minutes correlating to *m/*z-value 444.5 that was distinctive for all samples with FLV exposure that was not present in the blanks. Yet, the ion of interest (2OH-FLV) should be more hydrophilic than FLV, as two OH-moieties would have been added to the FLV backbone, and thus have a shorter retention time than FLV. Since FLV has a RT of 4.2 minutes, this peak could therefore not correlate to 2OH-FLV, but it could potentially represent another metabolite from FLV with the same molecular mass as 2OH-FLV. After investigating the chromatograms for the remaining samples, peaks at 5.064-5.074 were also present in blank embryo water, meaning that these peaks likely originate from another molecule than FLV.

4.5.1.1 Monitoring OH-FLV, 2OH-FLV and GLU-FLV

Since the RT for FLV with the applied LC-conditions is known (around 4.2 minutes), peaks detected at 4.269-4.276 minutes for the ion 412.3 *m/z*-ratio can with a high degree of certainty be correlated to FLV (see Tables 4.4 and 4.8). For the other analytes, detected peaks present in samples containing FLV and absent in blanks, do correlate to ions with the selected *m/z*-ratio, but their correlation to the selected FLV-metabolites is much less certain.

Table 4.4: *Results obtained from qualitative chromatographic analysis of analytes correlating to* ***412.3 m/z-ratio*** *(FLV) in E3 and zebrafish larvae (ZFL), and their representative blanks. Cells marked with 'X' indicate that a peak was detected, and cells marked with '–' indicate that no peak was detected.*

RT (minutes)	E3 with FLV (96 hpf)	E3 with FLV (120 hpf)	E3 with FLV, no ZFL	Blank E3	ZFL (96 hpf) exposed to FLV	Blank (96 hpf) ZFL	ZFL (120 hpf) exposed to FLV	Blank (120 hpf) ZFL
4,255-4,265	X	X	X	–	X	–	X	–

Table 4.5: *Results obtained from qualitative chromatographic analysis of analytes correlating to* ***428.5 m/z-ratio*** *(possibly OH-FLV) in E3 and zebrafish larvae (ZFL), and their representative blanks. Cells marked with 'X' indicate that a peak was detected, and cells marked with '–' indicate that no peak was detected.*

RT (minutes)	E3 with FLV (96 hpf)	E3 with FLV (120 hpf)	E3 with FLV, no ZFL	Blank E3	ZFL (96 hpf) exposed to FLV	Blank (96 hpf) ZFL	ZFL (120 hpf) exposed to FLV	Blank (120 hpf) ZFL
4.173	–	–	–	–	X	X	X	–
4.306-4.326*	X	X	X	–	–	–	–	–
6.017-6.037	X	X	X	X	–	–	–	–

* Appears as two unseparated peaks (see Figure 4.7)

For the 428.5 *m/z* ion (likely OH-FLV), weak signals are detected around 4.306-4.326 minutes. These peaks are only present in embryo water samples containing FLV, and not in blanks (see Table 4.5). By examining these signals, they appear as if two peaks are overlapping (see Figure 4.9). If these peaks are OH-FLV, the unseparated peaks may represent both 5-OH-FLV and 6-OH-FLV, since these two analytes are very similar in structure and would produce precursor ions with the same *m/z*-ratio.

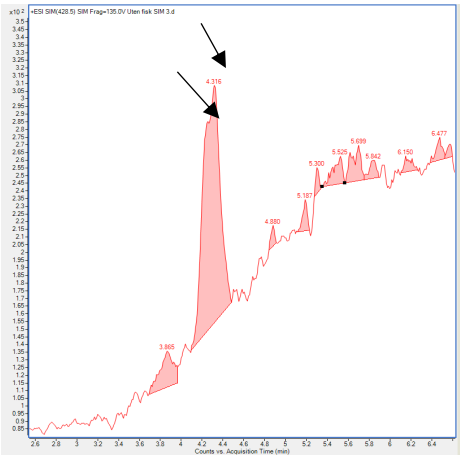

Figure 4.7: *Chromatogram ions with* m/z*-ratio of 428.5. The two peaks are not fully separated (pointed at with arrows) and may correlate to two different compounds with the same* m/z*-ratio (likely 5-OH-FLV and 6-OH-FLV)*

For the ion with *m/z*-ratio 444.5, some weak signals were detected in embryo water samples eluting around 3.599-3.609 minutes. As 2OH-FLV is more hydrophilic than FLV, it should elute earlier than FLV with the C18-column. Therefore, it is likely that the peaks detected with RT 3.599-3.609 represent 2OH-FLV. Peaks with this RT for the 444.5 *m/z*-ion were present in all embryo water samples containing FLV but were not present in any of the homogenized zebrafish larvae samples (see Table 4.6). This suggests that these signals likely correlate to 2OH-FLV, and that this metabolite only is detected in embryo water samples and not in zebrafish larva samples.

Table 4.6: *Results obtained from qualitative chromatographic analysis of analytes correlating to* ***444.5 m/z-ratio*** *(possibly 2OH-FLV) in E3 and zebrafish larvae (ZFL), and their representative blanks. Cells marked with 'X' indicate that a peak was detected, and cells marked with '–' indicate that no peak was detected.*

RT (minutes)	**E3 with FLV (96 hpf)**	**E3 with FLV (120 hpf)**	**E3 with FLV, no ZFL**	**Blank E3**	**ZFL (96 hpf) exposed to FLV**	**Blank (96 hpf) ZFL**	**ZFL (120 hpf) exposed to FLV**	**Blank (120 hpf) ZFL**
3,568	–	–	–	–	X	X	X	X
3,599-3,609*	X	X	X	–	–	–	–	–
3,825	–	–	–	–	X	X	X	–
5,064-5,074	X	X	X	X	–	–	X	–
5,310-5,320	–	–	–	–	X	X	–	X
5,330	–	–	–	–	–	–	X	–
5,604	–	–	–	–	–	–	X	–

*Weak signals.

For GLU-FLV, strong peaks eluting at 5.187 minutes were present in all analyzed samples, both embryo water, zebrafish larvae, and blanks (see Table 4.7). The peaks are much stronger in E3 samples after 48 hours incubation and homogenized zebrafish larvae aged 120 hpf (incubated 48 hours). What this peak may correlate to is unknown, but it is not a metabolite of FLV because of its presence in blank embryo water and blank zebrafish larvae.

Table 4.7: *Results obtained from qualitative chromatographic analysis of analytes correlating to* ***604.5 m/z-ratio*** *(possibly GLU-FLV) in E3 and zebrafish larvae (ZFL), and their representative blanks. Cells marked with 'X' indicate that a peak was detected, and cells marked with '–' indicate that no peak was detected.*

RT (minutes)	**E3 with FLV (96 hpf)**	**E3 with FLV (120 hpf)**	**E3 with FLV, no ZFL**	**Blank E3**	**ZFL (96 hpf) exposed to FLV**	**Blank (96 hpf) ZFL**	**ZFL (120 hpf) exposed to FLV**	**Blank (120 hpf) ZFL**
4.225	–	–	–	–	X	X	–	–
5.187	X (11.5 k)*	X (155 k)*	X (37 k)*	X (31 k)*	X (12 k)*	X (13 k)*	X (215 k)*	X (10 k)*

*The numbers noted peaks detected at 5.187 minutes show the mean values in kilo units of the signal responses for the detected peaks.

4.5.1.2 Monitoring Lactone-FLV and OH-Lactone-FLV

Table 4.8: *Results obtained from qualitative chromatographic analysis of analytes correlating to* ***412.3 m/z-ratio*** *(possibly GLU-FLV) in E3 and zebrafish larvae (ZFL), and their representative blanks. Cells marked with 'X' indicate that a peak was detected, and cells marked with '–' indicate that no peak was detected.*

RT (minutes)	E3 with FLV (96 hpf)	E3 with FLV (120 hpf)	E3 with FLV, no ZFL	Blank E3	ZFL (96 hpf) exposed to FLV	Blank (96 hpf) ZFL	ZFL (120 hpf) exposed to FLV	Blank (120 hpf) ZFL
4,269-4,276	X	X	X	–	X	–	X	–

For ions with 394.5 *m/z*-ratio (possibly Lactone-FLV), peaks eluting at 4.269-4.276 minutes were detected in all E3 samples containing FLV (see Table 4.9). As mentioned in the Introduction chapter, FLV has an open lactone ring that reversibly can be closed, forming Lactone-FLV. These signals are not detected in samples from untreated zebrafish larvae or blank embryo water, supporting the possibility that these signals may correlate to a molecule that originates from FLV.

No signals that could be interpreted as the analyte OH-Lactone-FLV (410.5 *m/z*-ratio) were detected of interest were detected (see Table 4.10).

Table 4.9: *Results obtained from qualitative chromatographic analysis of analytes correlating to* ***394.5 m/z-ratio*** *(possibly LACTONE-FLV) in E3 and zebrafish larvae (ZFL), and their representative blanks. Cells marked with 'X' indicate that a peak was detected, and cells marked with '–' indicate that no peak was detected.*

RT (minutes)	E3 with FLV (96 hpf)	E3 with FLV (120 hpf)	E3 with FLV, no ZFL	Blank E3	ZFL (96 hpf) exposed to FLV	Blank (96 hpf) ZFL	ZFL (120 hpf) exposed to FLV	Blank (120 hpf) ZFL
4,207	–	–	–	–	X	X	X	X
4,223	–	–	–	–	–	–	–	X
4,269-4,276	X	X	X	–	–	–	–	–
5,375-5,383	X	X	–	X	X	X	X	X
5,398	–	–	X	–	–	–	–	–

Table 4.10: *Results obtained from qualitative chromatographic analysis of analytes correlating to* ***410.5 m/z-ratio*** *(possibly OH-Lactone-FLV) in E3 and zebrafish larvae (ZFL), and their representative blanks. Cells marked with 'X' indicate that a peak was detected, and cells marked with '–' indicate that no peak was detected.*

RT (minutes)	E3 with FLV (96 hpf)	E3 with FLV (120 hpf)	E3 with FLV, no ZFL	Blank E3	ZFL (96 hpf) exposed to FLV	Blank (96 hpf) ZFL	ZFL (120 hpf) exposed to FLV	Blank (120 hpf) ZFL
3,869-3,877	–	–	–	–	X	X	X	X
4,276-4,292	X	X	X	X	X	X	X	X
4,737-4,745	–	X	X	X	X	–	X	X

4.6 Quantitative Analysis of Fluvastatin

In addition to monitoring selected metabolites of FLV with SIM-methods, samples were also analyzed quantitatively with the FLV MRM-method on LC-MS/MS. As described in the Methods section, calibration curves were freshly prepared for each experiment, and no internal standard was used. To calculate the total amount of FLV in each sample, the detected quantities from the E3 and zebrafish larvae from the same incubated samples were combined. The dilution factor from preparation of the embryo water samples (1:4) was accounted for in this calculation (see Equation 4.1).

$$\text{Total amount of FLV} = (5 * \text{FLV in E3}) + \text{FLV in ZFL} \qquad \text{(Equation 4.1)}$$

4.6.1 Would it be sufficient to quantitate using only the SIM method?

To perform both qualitative and quantitative analysis, the samples were injected a total of three times into the MS/MS for analysis; two for monitoring FLV metabolites and one for quantitation of FLV. Running all samples three times was time consuming. Even though the LC-MS/MS did not need continuous monitoring by the operator while the samples were being analyzed, it would save both time and mobile phases if the SIM-data were sufficient for quantitation purposes. To test if the SIM-method (Tables 3.5 and 3.13) provided similar results as the MRM-method (Tables 3.5 and 3.11), a calibration curve was therefore run with the SIM-mode, and the two sets of data were compared. The calibration curves had quite different slopes when plotting with linear regression: $y = 77.8\ x$ ($r^2 = 0.997$) for the MRM-method and $y = 220.8\ x$ ($r^2 = 0.994$) for the SIM-method. In addition, samples without zebrafish larvae containing 200 nM FLV that had been incubated for 24 hours at 28.5 °C, were run with MRM and SIM, and were quantitated using the respective calibration curves. The concentrations calculated with the

SIM-method were significantly higher than with the MRM-method (student t-test, assumed unlike variances, $p < 0.005$, see Table 4.11). As MRM is a more sensitive and selective method than SIM, FLV was therefore quantitated using the MRM-method.

Table 4.11: *Calculated quantities using both SIM- and the MRM-methods for FLV on LC-MS/MS to see if it would be sufficient to quantitate FLV using the SIM-method only. All samples contained one zebrafish larva, embryo water with 200 nM FLV, and they were incubated for 24 hours at 28.5 ℃.*

Sample	SIM-method (nM)	MRM-method (nM)
1	166.35	117.75
2	160.80	127.20
3	153.45	124.55
4	139.05	126.25
5	170.80	129.05
Mean ± standard deviation	158.1 ± 12.5	124.9 ± 4.3

4.6.2 Matrix effects were observed for FLV when homogenized zebrafish larvae were present in the matrix

As described in section 3.5.1 in Methods, matrix-matched calibration samples with known quantities of FLV (referred to as 'yield samples' in this study) were prepared to be able to account for potential matrix effects when homogenized zebrafish larvae were present in the matrix compared to only MeOH. As seen in Figures 4.8 and 4.9, yield samples containing zebrafish larvae and known concentrations of FLV in MeOH gave quite different slopes compared to the calibration standards. For lower concentrations (5 nM) the yield samples provided stronger signals compared to the calibration standards, but at higher concentrations (15 nM), the yield samples provided weaker signals compared to the calibration standards. This was interpreted as a matrix effect caused by the presence of homogenized zebrafish larvae in the sample matrix.

In addition, the calibration standards from these two dates (26.01.23 and 03.02.23) also gave different slopes; $y = 79.673\ x$ and $y = 44.522\ x$, respectively (Figures 4.8 and 4.9). The calibration curve from 26.01.2023 (experiment 1, see Figure 4.8) was run with the originally used column (C18, 2.1x100mm from Fortis), and the calibration curve from 03.02.2023 (experiment 2, see Figure 4.9) was run the same day as the column change (the original column was replaced with a C18 column from Kromasil with the same dimensions). The calibration

curves and signal responses from 13.02.2023 (experiment 3, y = 79,04 x, r^2 = 0,998)) were very similar to that from 26.01.2023.

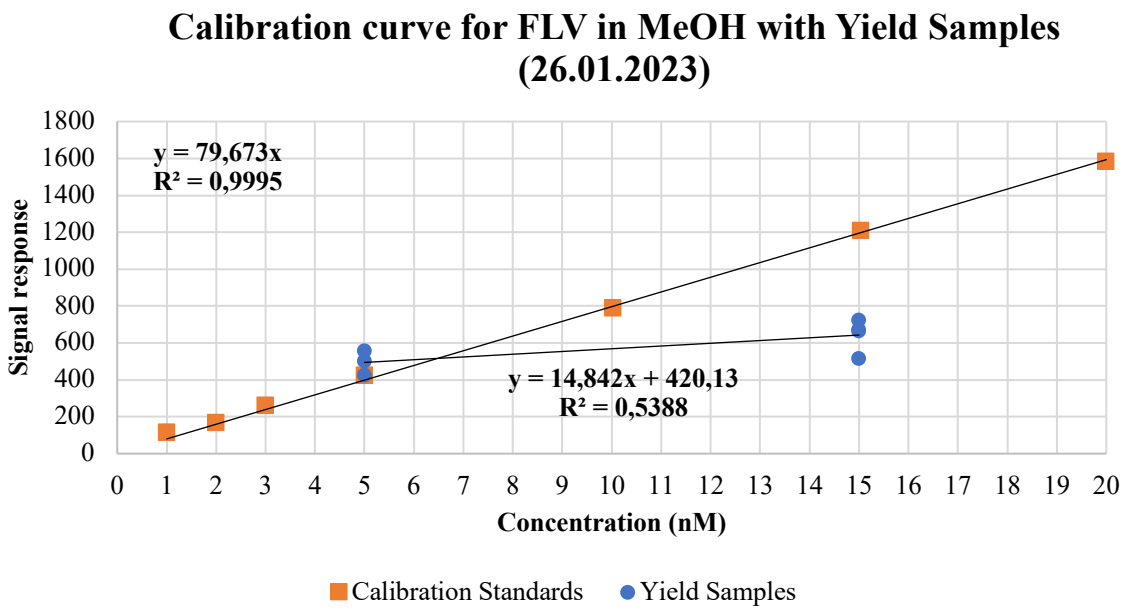

***Figure 4.8**: Calibration curve for FLV in MRM mode and yield samples containing three sonicated zebrafish larvae and FLV with concentrations of 5 and 15 nM of FLV in MeOH.*

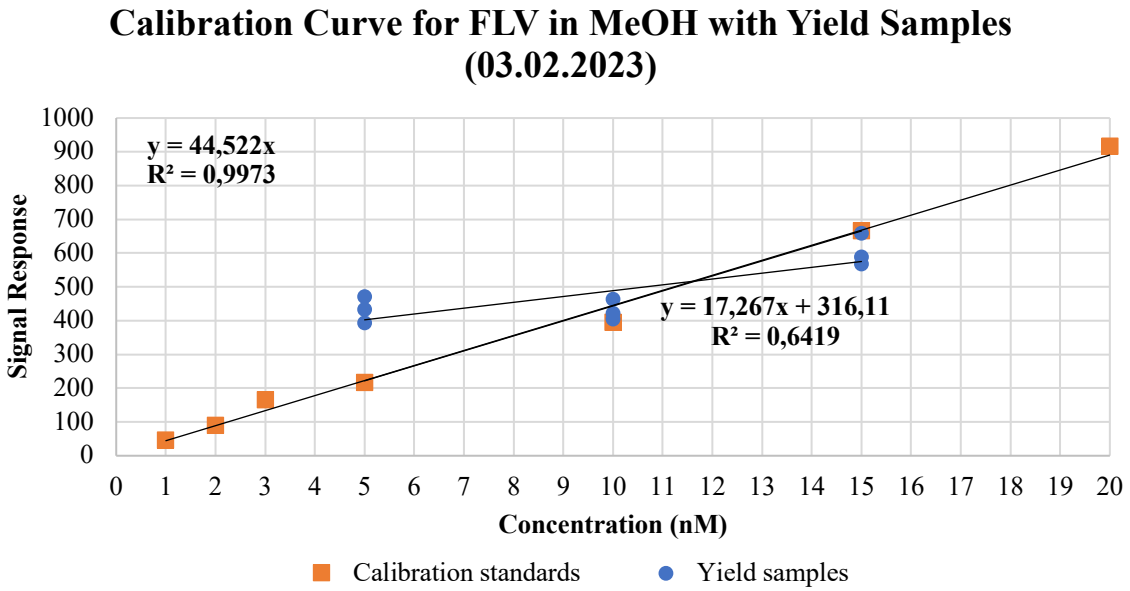

***Figure 4.9**: Calibration curve for FLV in MRM mode with yield samples containing three sonicated zebrafish larvae and FLV with concentrations of 5, 10 and 15 nM in MeOH.*

4.6.3 Calculating the total amount of FLV in the samples with zebrafish larvae

Experiments for FLV in zebrafish larvae were performed three times. However, due to difficulties with sonication procedures, in addition to differences in calibration curve slopes, it was difficult to compare these results. In experiment 1, the zebrafish larvae were homogenized in a sonication bath in glass vials, and the time required to fully dissociate the zebrafish larvae varied from 10-24 minutes. For two of the parallels in this experiment (sample 5 and vial 6), a zebrafish larva got stuck to the wall of the glass vials during sonication. These parallels did therefore not contain three fully sonicated larvae, but only two at the end of the sonication time. In experiment 2, the zebrafish larvae were sonicated in the sonication bath, this time in Eppendorf-tubes (plastic) instead of glass vials. These tubes had a narrower bottom and seemed to homogenize the zebrafish larvae quicker than in glass vials. In addition, with the Eppendorf-tubes, zebrafish larvae sticking to the wall of the vials was no longer a problem. In experiment 2, 10 parallel samples for both 24 hours (96 hpf) and 48 hours (120 hpf) were prepared. However, during this experiment the column had to be changed due to high pressure, and all samples that had been analyzed, had to be run once more. With the new column, only parallels that had been sonicated for 15 minutes were run, so that they could more readily be compared (five parallels for 24 hours incubation and four parallels for 48 hours incubation). The remaining six samples of the 48 hour-parallels were sonicated for 15 minutes in the bath, and then 20 seconds using the sonication probe. In experiment three, there were not many zebrafish larvae available, so gaining more samples for the 24-hour parallels was prioritized. These zebrafish larvae (24-hour parallels) were all sonicated by the probe for 20 seconds.

Because of all these variations, the obtained results are presented individually, with their respective mean values and calculated standard deviations. Outliers are not accounted for in the FLV in E3 and FLV in zebrafish larvae results, which can be seen from the relatively large standard deviations in some of the results (see Tables 4.12 and 4.13). The reason for doing this, is that the quantitative results from the E3 had to be considered together with the amount detected in the zebrafish larvae. The quantities of FLV presented in these tables, are obtained using a calibration curve prepared in MeOH. As seen from the yield samples, the zebrafish larvae matrix interferes with the FLV-responses. Therefore, these results are not representative for the quantities of FLV that was actually present in the zebrafish larvae.

***Table 4.12**: Results obtained from the 24-hour parallels of the different experiments performed with FLV in zebrafish larvae. The values shown in the table are the calculated mean values and standard deviations.*

Experiment 1	**FLV in E3 (24 hours) (nM)**	**FLV in ZFL (96 hpf) (nM)***	**Total FLV (nM)**
1 (n = 6)	88.48 ± 10.31	6.70 ± 1.91	95.18 ± 10.6
2 (n = 5)	67.61 ± 6.01	22.83 ± 6.56	90.44 ± 4.60
3 (n = 6)	36.73 ± 14.81	19.27 ± 4.36	55.99* ± 11.16

*Low compared to the other experiments. This is commented in section 4.4.4.

***Table 4.13**: Results obtained from the 48-hour parallels of the different experiments performed with FLV in zebrafish larvae. The values shown in the table are the calculated mean values and standard deviations.*

Experiment number	**FLV in E3 (48 hours) (nM)**	**FLV in ZFL (120 hpf) (nM)**	**Total FLV (nM)**
1 (n = 6)	82,39 ± 16,57	4,82 ± 1,21	87,22 ± 17,64
2 (n = 4) Sonicated in bath	80, 53 ± 22,66	4,83 ± 0,59	85, 37 ± 22,94
2 (n = 6) Sonicated with probe	87,35 ± 17,33	6,41 ± 3,06	93,76 ± 15,70

4.6.4 "0"-samples and samples without zebrafish larvae

To test how much FLV that was present in samples with zebrafish larvae just after administration of FLV, "0"-samples were prepared. These samples were made by adding three zebrafish larvae and 150 µL 200 nM FLV in embryo water to a glass vial. The vial stood in room temperature for one minute, and then the embryo water was collected for sample preparation (see Methods, section 3.5.1) and analysis. In this experiment, the zebrafish larvae were not analyzed. The obtained results are presented in Table 4.14:

***Table 4.14:** "0"-samples collected from zebrafish larvae (96 hpf) exposed to 200 nM FLV for one minute prior to analysis, analyzed using the FLV MRM-method.*

Sample	**Calculated concentration (nM)**
1	64,6
2	81,0
3	86,4

These results are lower than expected, as the amount of FLV added to the samples was 200 nM. Other embryo water samples (prepared with a different dilution series of FLV) run within the same worklist also gave unexpectedly low results (experiment 3, see Table 4.12). It might be that changes in the LC-MS/MS conditions contributed to these low results, but this is not certain.

4.6.5 Sterile filtrated samples obtained stronger signal responses than non-filtrated samples

The samples with sterile filtrated embryo water were also analyzed quantitatively with the FLV MRM-method. The amount of FLV added at the start of incubation was 200 nM. However, the quantified amounts of FLV in these samples were on average higher than what was added (see Table 4.9). The calibration curve from which these results were obtained, was not sterile filtrated, and the matrix was therefore not completely matched. However, this suggests that something in the embryo water prior to filtration might be causing signal suppression of FLV.

Table 4.15: *Quantities of FLV detected in samples after 24 hours incubation. The E3 in the samples was sterile filtrated prior to dilution of FLV, and 200 nM of FLV was added at the start of incubation.*

Sample	**1**	**2**	**3**	**4**	**5**
Calculated Concentration (nM)	241,6	249,9	240,7	244,1	254,1
Mean (nM)					246,1

4.7 Quantitative Analysis of Captopril and its Metabolite Disulfide Captopril

For analysis of CAPT and DICAPT, samples were prepared as described in section 3.5.2 in Methods. Samples with three zebrafish larvae, samples without zebrafish larvae and blank samples (blank E3 and non-exposed zebrafish larvae) were analyzed after 24 hours and 48 hours of incubation, and the experiment was carried out three times in total. ENA (100 nM) was used as an internal standard. The amount of CAPT (in the derivatized form CAPT-pBPB) and the metabolite DICAPT was quantified using the CAPT MRM-method on LC-MS/MS, and the ratio between these two analytes was calculated. For every DICAPT-molecule formed, two CAPT-molecules are required (see Equation 4.2). This stoichiometry was accounted for when the total amount of CAPT in the samples was calculated, using Equation 4.3.

$$2\ \text{Captopril} \rightleftharpoons 1\ \text{Disulfide Captopril} \qquad \text{(Equation 4.2)}$$

$$\text{Total amount of CAPT } (\mu\text{M}) = \text{CAPT } (\mu\text{M}) + (2 * \text{DICAPT } (\mu\text{M})) \qquad \text{(Equation 4.3)}$$

4.7.1 Analysis of Embryo Water Samples

Even though the three experiments were done following the same procedure, the obtained results were a bit conflicting. These differences will be presented in this chapter, but they will be further discussed in section 5.2.2 in Discussion.

Figure 4.10 illustrates the quantities of CAPT and DICAPT detected and the calculated total amount of CAPT in the E3 samples of each experiment, including samples with and without zebrafish larvae. The same results are also presented numericly in Table 4.16. Generally, the amount of DICAPT was relatively low compared to the starting concentration of CAPT in all samples and experiments. In addition, the DICAPT concentration was lower in samples when zebrafish larvae had been present during incubation, compared to samples without zebrafish larvae (t-test (assumed same variances, excel) $P < 0{,}001$ for all three experiments).

An observed difference between the experiments, is that the amount of CAPT in the embryo water from zebrafish larvae exposed to CAPT for 24 hours, is considerably higher in experiment 3 than in experiments 1 and 2. In the first two experiments (experiment 1 and 2), the amount of CAPT was significantly lower in the 24-hour samples than in the 48-hour samples (t-test (assumed similar variances, excel) $P < 0{,}001$). However, in the third experiment there was no difference in the detected CAPT concentration between the 24 hours and 48 hours samples ($P = 0{,}504$). The detected quantities of DICAPT also varied from between all three experiments. This is more demonstrated when looking at the ratios between CAPT and DICAPT (Figure 4.11).

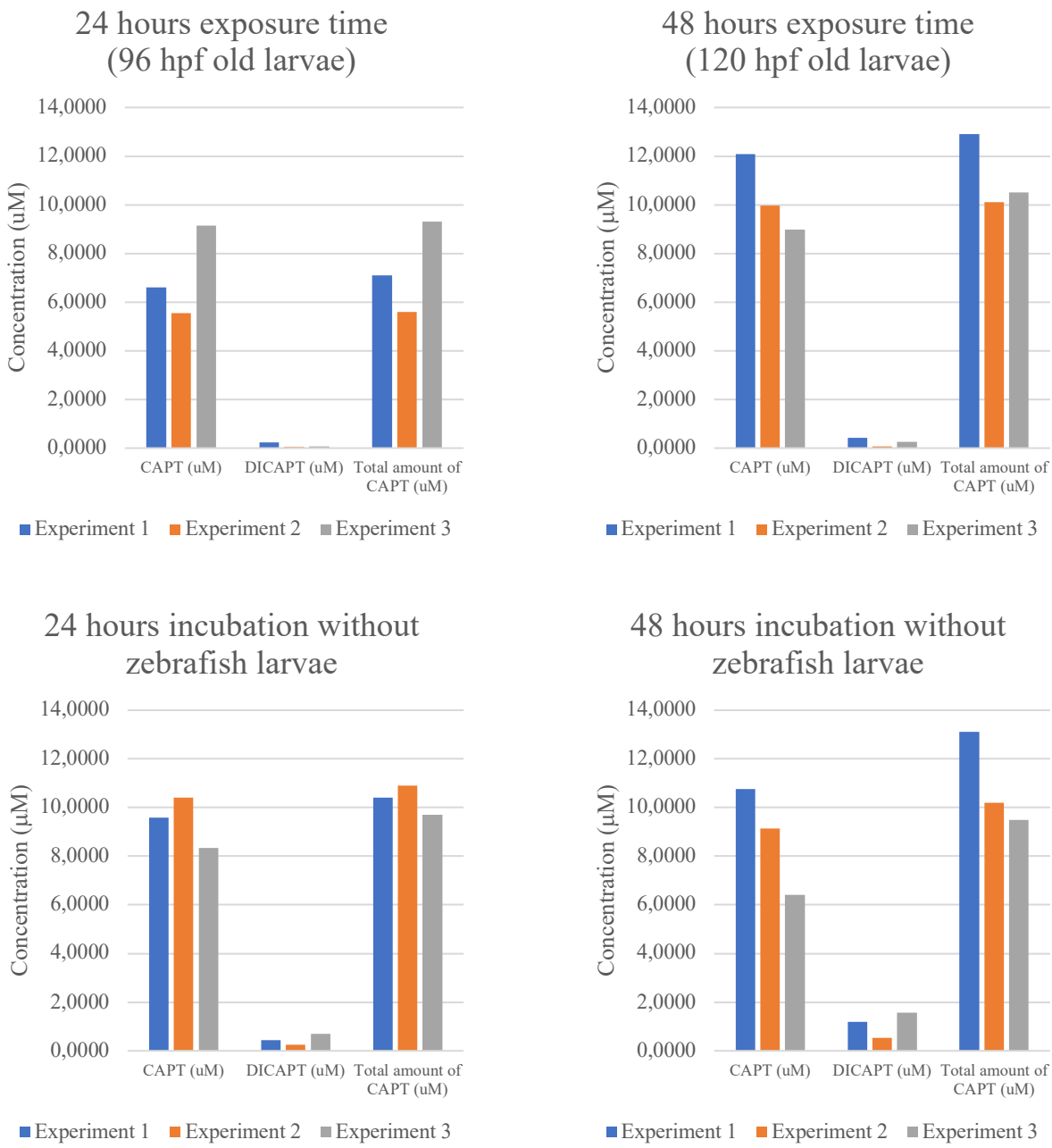

Figure 4.10: *Obtained results from the three experiments performed for CAPT in zebrafish larvae.The diagrams show the amount of CAPT, DICAPT, and the calculated total amount of CAPT detected in samples collected from embryo water from zebrafish larvae (96 hpf and 120 hpf) and from embryo water without zebrafish larvae(24 hours and 48 hours incubation)*

Table 4.16: *Results obtained from zebrafish experiments with CAPT. The results are presented with mean values and their standard deviations.* ***A****: Data from experiment 1.* ***B****: Data from experiment 2.* ***C****: Data from experiment 3.*

A:

Experiment 1	**24 hours incubation without zebrafish larvae (n = 3)**	**48 hours incubation without zebrafish larvae (n = 5)**	**24 hours exposure time/incubation with zebrafish larvae (n = 3)**	**48 hours exposure time/incubation with zebrafish larvae (n = 5)**
CAPT (μM)	9.5759 ± 0.4655	10.7565 ± 0.2794	5.9111 ± 0.8486	12.0807 ± 0.1198
DICAPT (μM)	0.4288 ± 0.0295	1.1959 ± 0.1104	0.2323 ± 0.0234	0.4232 ± 0.0480
Ratio CAPT/DICAPT	22	9	29	29

B:

Experiment 2	**24 hours incubation without zebrafish larvae (n = 5)**	**48 hours incubation without zebrafish larvae (n = 5)**	**24 hours exposure time/incubation with zebrafish larvae (n = 9)**	**48 hours exposure time/incubation with zebrafish larvae (n = 9)**
CAPT (μM)	10.3972 ± 0.2723	9.1388 ± 0.5993	5.5363 ± 0.4055	9.9623 ± 1.6055
DICAPT (μM)	0.2518 ± 0.0065	0.5344 ± 0.0216	0.0490 ± 0.0062	0.0752 ± 0.0053
Ratio CAPT/DICAPT	41	17	114	133

C:

Experiment 3	**24 hours incubation without zebrafish larvae (n = 4)**	**48 hours incubation without zebrafish larvae (n = 5)**	**24 hours exposure time/incubation with zebrafish larvae (n = 6)**	**48 hours exposure time/incubation with zebrafish larvae**
CAPT (μM)	8.3044 ± 0.1961	6.4186 ± 0.1115	9.1486 ± 0.4818	8.9879 ± 0.2996
DICAPT (μM)	0.7401 ± 0.0260	1.5632 ± 0.0185	0.0723 ± 0.0204	0.1917 ± 0.0175
Ratio CAPT/DICAPT	12	4	136	48

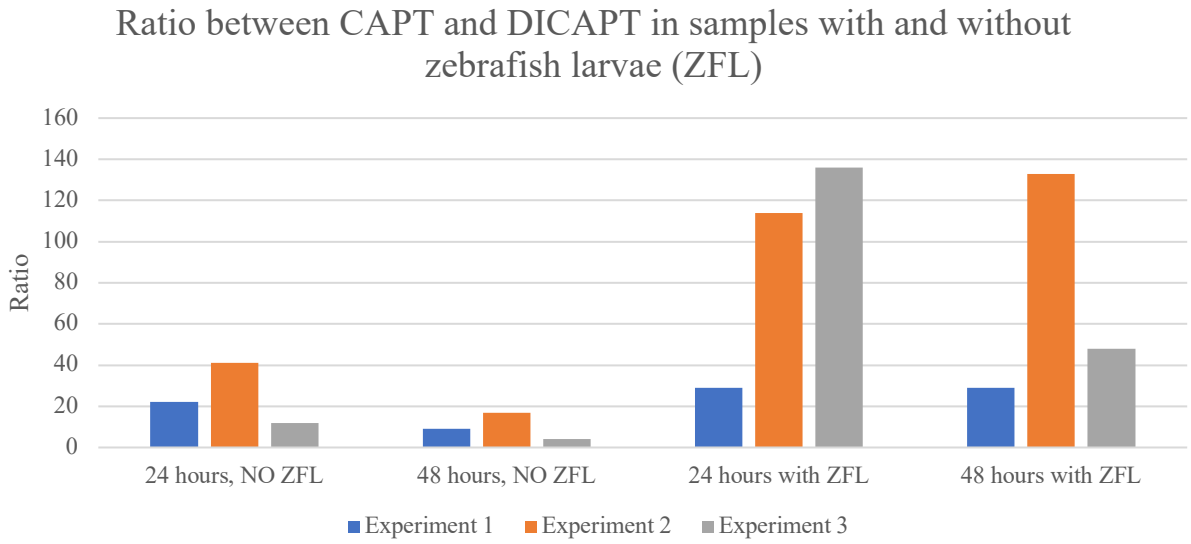

Figure 4.11: *Calculated ratios between CAPT and DICAPT in samples with and without zebrafish larvae. Results from all three experiments shown.*

As shown in Figure 4.11 and Table 4.16, the ratios between CAPT and DICAPT varied considerably among the three experiments. In samples without zebrafish larvae, the difference in ratios between the three separate experiments were similar; the ratio was highest for experiment 2, followed by experiment 1 and finally experiment 3.

In samples without zebrafish larvae (Figure 4.11), the results look different. In the first experiment, the ratio between 24-hour and 48-hour parallels without zebrafish larvae remained the same (ratio was 29 for both sample-types). In experiment 2, the amount of DICAPT formed after 24 hours with zebrafish larvae was considerably lower than in experiment 1 (Table 4.16), leaving the ratio between the analytes much higher for this experiment. In experiment 3, the amount of CAPT was considerably higher after 24 hours than in the other two experiments This difference contributed to a much higher ratio between the analytes in this experiment.

4.7.2 Analysis of Zebrafish Larvae Samples

Initially, the three zebrafish larvae that had been incubated together in a well were homogenized and prepared as one sample. However, no samples prepared this way gave any responses with the developed method for CAPT on LC-MS/MS. Next, three larvae from three wells (a total of nine zebrafish larvae) were prepared as one sample, but this also did not generate detectable signals for the analytes. A final test to see if signals could be detected using the developed method, was to increase δEMV from to 500. One of the samples containing 9 homogenized zebrafish larvae which had been exposed to CAPT, was run with this acquisition change, but

still no signals were detected for neither CAPT-pBPB nor DICAPT. Therefore, no CAPT was detected within the zebrafish larvae in these experiments.

4.7.3 A new batch of embryo water was introduced

In the third experiment, a new batch of E3 had to be used, as there was not enough E3 left from the original batch. To test if the different batches of E3 impacted the results significantly, two separate stock solutions and dilution series were prepared with the old and the new batch, and the samples were not incubated over time. The samples (n = 3) were prepared and run on the same day, and the results are presented in Table 4.10. There was an unexpected difference between the two batches. It appeared as though the old batch gave lower signals for CAPT than the new batch, and the formation of DICAPT seemed lower in the new batch compared to the old one (P = 0,045). This can possibly suggest that the batch and age of the E3 might have had an impact on the conflicting results seen in the experiments, and this will be discussed further in the next chapter (Discussion).

Table 4.17: *Results obtained from quantitative analysis of freshly prepared samples containing 10 µM CAPT. One set of samples was prepared with the same batch of embryo water as used in experiments 1 and 2 ("old batch"). The other set of samples was prepared with a new batch of E3, the same as used in experiment 3 ("new batch").*

Sample	CAPT (µM)	DICAPT (µM)	ENA (Areal)	Total amount of CAPT	Ratio CAPT/DICAPT
New batch	8,57	0,0716	17612	8,7	120
New batch	8,84	0,0772	17341	9,0	115
New batch	8,88	0,0790	17156	9,0	112
Mean	*8,76*	*0,0759*	*17370*	*8,9*	*116*
Old batch	3,96	0,0931	17159	4,1	43
Old batch	4,41	0,1104	16252	4,6	40
Old batch*	8,32	0,0873	14391	8,5	95
Mean	*4.05*	*0.1018*	*16706*	*4.4*	*42*

* Not included in the calculation of the means because this parallel was an outlier. The signal response for ENA was quite low, likely a human error from pipetting. The concentrations for CAPT and DICAPT might therefore have been calculated wrongly.

5 Discussion

In this thesis, experiments were performed with the aim of monitoring metabolites of simvastatin, fluvastatin, and captopril in zebrafish larvae and their surrounding embryo water with qualitative and quantitative analysis on LC-MS/MS. Several challenges and concerns were addressed throughout the experiments, mainly related to biological, physicochemical, and analytical conditions. These conditions and their influence on the obtained results and developed LC-MS/MS methods in this master project, will be further discussed in this chapter. Despite several tests to optimize the experimental conditions for simvastatin, issues concerning the chemical stability of simvastatin and lack of detection were recurring. Therefore, biotransformation studies of simvastatin in zebrafish larvae were not carried out in this study. These observed issues and what might have caused them will be further elaborated in section 5.3.

5.1 Experimental design

As described in section 4.4, the design of these experiments was based on tests investigating the remaining quantities of fluvastatin left in wells with one and three zebrafish larvae that had been incubated for 24 hours and 48 hours at 28.5 °C. The remaining amount of fluvastatin in each sample was used as an indirect measure for biotransformation, and the loss of fluvastatin compared to the administered drug, was interpreted as metabolic degradation. We found that the number of larvae contained in each well during incubation, as well as the incubation time, both had a significantly reducing effect on the quantity of fluvastatin in samples when considered separately ($p < 0.01$ for 'time' and $p < 0.005$ for 'number of larvae'). Yet, these two factors combined did not contribute significantly to the reduction of fluvastatin in the samples. Moreover, these experiments showed that zebrafish larvae had a significant influence on fluvastatin when administered aquatically, which points in a positive direction in terms of using this model system for investigating biotransformation of drugs.

5.2 Zebrafish larvae as model organisms for biotransformation

As mentioned in the Introduction (Section 1.4.3), the maturation of the zebrafish larvae needs to be considered when interpreting results from biotransformation studies (54). The activity of CYP-enzymes increases in zebrafish larvae post-hatching (from 72 hpf), underlining why it can be of interest to investigate metabolite production from this age rather than in earlier larvae and embryos. Alderton et al. (58) did an extensive study on biotransformation in zebrafish larvae

where they investigated the presence of metabolites of CYP-prone drugs. They found that the amounts of any specific metabolite were low compared to the administered parent compound, and this was interpreted a limitation with zebrafish larvae as model systems for biotransformation studies and safety pharmacology tests. In this master project, we also found relatively small amounts of the monitored metabolites of both FLV and CAPT in the embryo water from incubated zebrafish larvae compared to the administered concentration of these drugs, as presented in Section 4.6 for FLV-metabolites and Section 4.7 for DICAPT. This pattern, however, differs from what is seen in humans, where FLV is eliminated primarily as metabolites (99) and CAPT also to a great extent is eliminated in the form of disulfide-metabolites (100). The relationship between the amounts of metabolites and unchanged FLV and CAPT observed in humans, is therefore not accurately reflected by the zebrafish larva model system. That being said, it is important to consider that the zebrafish larvae are continuously exposed to the drugs from their aquatic environment, and the administration of the drug is constant. In addition, the metabolites which are eliminated from the larvae, will appear very little, because it is diluted in the relatively large sample volume surrounding embryo water. Thus, it was expected that the metabolite formation in this zebrafish larva model would be low, and different to the ratios of parent drug compared to metabolites known from human metabolism.

5.2.1 Traces of CYP2C-activity

FLV is undergoes enzymatic conversion to 5-OH-FLV and 6-OH-FLV mainly by CYP2C9 in humans, but a small part of this biotransformation is also accounted for by CYP2C8, CYP2D6, CYP3A4 (Figure 1.3). However, zebrafish do not express an ortholog to any CYP2C genes (Table 1.1). In this study, the presence of OH-FLV was investigated with qualitative analysis using a developed SIM-method for selected molecular ions with LC-MS/MS (see Tables 3.5 and 3.13 in Methods). OH-FLV could likely be correlated to molecular ions with a *m/z* value of 428.5, and peaks eluting around 4,269 minutes for this ion were interpreted as this metabolite (Table 4.5 in Results). Jones et al. (62) did a similar study where they investigated the biotransformation of ibuprofen in zebrafish larvae (72 hpf to 96 hpf). They found traces of hydroxy-ibuprofen in the zebrafish larvae; a metabolite that, similarly to 5- and 6-OH-FLV, also is catalyzed by the CYP2C9 in humans. This suggests that zebrafish larvae might have a CYP2C9-like mediated metabolism, despite the lack of an ortholog gene to that seen in humans (58). This underlines that differences in biotransformation between humans and zebrafish larvae

are present, and further investigations to better understand the relationship between the species is necessary.

5.2.2 Differences in developmental stages likely affected the results

In this study, experiments investigating the metabolism of FLV and CAPT were conducted several times, but the results from the performed experiments varied a lot. With the conflicting data obtained from experiment to experiment with zebrafish larvae for both FLV and CAPT, the developmental biology of the zebrafish larvae must be considered as an influencing factor. The timeframe in which the experiments in this thesis are conducted (from the age of 3 dpf to 5 dpf (72 hpf to 120 hpf)) and a lot happens with the biological development of the zebrafish larvae. The kidneys of zebrafish larvae are fully size-selective and mature by 4 dpf (66), and at the same age, a continuous passage through the digestive tract is also opened (67). This means, that from 96 hpf, the zebrafish larvae have more developed and readily available elimination routes for xenobiotics than at younger ages. Several functions of the zebrafish liver, including the ability to perform xenobiotic metabolism, is found to be fully functional at 120 hpf (56, 101), and metabolites formed by several groups of metabolizing enzymes like CYPs, UGTs, and SULTs in zebrafish larvae have all been observed in zebrafish larvae from the age of 52 hpf (60). Hence, research has demonstrated the metabolic activity of the zebrafish larvae. In humans, FLV is eliminated through feces predominantly as metabolites (99). CAPT and its disulfide-metabolites are primarily eliminated renally, but a small part is also eliminated through feces (100).

In the first two experiments conducted with CAPT, there was much less CAPT in the embryo water from samples with zebrafish larvae when collected after 24 hours incubation (larvae aged 96 hpf) than 48 hours incubation (larvae aged 120 hpf). It should be considered that the development and opening of the intestinal tract, in addition to more mature kidneys, probably had an influence on these results, since more elimination routes would be available in older larvae. Therefore, an increased quantity of CAPT and DICAPT in embryo water samples collected from 120 hpf old larvae compared to 96 hpf old larvae, as observed in this study, are not unexpected.

When evaluating the differences between the detected quantity of CAPT in the embryo water collected from zebrafish larvae aged 96 hpf and 120 hpf, the influence of the yolk sac on the

obtained results must also be considered. The yolk sac is providing nutrients to the developing zebrafish larva until it reaches the age of 120 hpf (92). A study by Halbach et al. (102), found that a selection of test compounds administered through embryo water exposure to zebrafish larvae were more abundant in the yolk sac compared to the embryonic body of the larva. Samples were collected 24-, 48- and 72-hours post administration, and this distribution pattern was seen in all samples. Thus, if CAPT is accumulated in the yolk sac, the consumption of the yolk sac as the larvae grew older might also have contributed to the increasing quantities of CAPT in the embryo water that was observed in samples collected from larvae aged 120 hpf compared to 96 hpf. In addition, if the administered drugs (FLV and CAPT) are accumulated in the yolk sacs during incubation and not reaching the metabolizing enzymes of the larvae. The yolk sac consists mainly of fats and proteins. The distribution of hydrophobic drugs to this organ, would therefore be expected. For CAPT, one can also expect a degree of accumulation in this organ, because of potential disulfide-bindings to the proteins in the yolk sac.

Neither CAPT nor DICAPT were detected in the dissociated zebrafish larva samples. In addition to forming the metabolite DICAPT, CAPT can reversibly form several disulfide-metabolites with cysteine or cysteine-containing compounds, such as glutathione (45). The zebrafish plasma proteome shares significant similarities with the plasma proteome of humans (103). Binding of CAPT to plasma proteins in zebrafish larvae is therefore a possibility and might have influenced the low concentrations quantitated for CAPT in this study. Since the CAPT MRM-method (Tables 3.8 and 3.12) only monitor CAPT and DICAPT, other disulfide-metabolites present in the samples would not have been detected. However, these samples are also quite diluted 1:2.7 during sample preparations, which could also be an explaining factor for the lack of detection of CAPT in the larvae.

The metabolites of FLV that were detected in these experiments, were only present in embryo water samples, and not in zebrafish larva samples when analyzed with the SIM-methods on LC-MS/MS (Table 4.5 (OH-FLV), Table 4.6 (2OH-FLV), and Table 4.9 (Lactone-FLV)). As already discussed, the metabolite-production was expected to be low. The fact that metabolites were detected in the embryo water and not in samples with dissociated zebrafish larvae can have several explanations. One reason can be explained biologically: the produced metabolites might have already been eliminated to the embryo water, and thus detectable quantities of FLV might not have been present inside the zebrafish larvae at the time of the analysis. Another explanation is more related to the sensitivity of the SIM FLV-methods. If the methods were not

sensitive enough to detect remaining metabolites in the zebrafish larvae, or that matrix effects caused signal suppression. With dissociated zebrafish larvae present in the samples, the matrix becomes more complex, and matrix-compounds might have had a suppressing influence on the signals.

5.3 Chemical considerations and detection issues with SMV and FLV

Several different experimental setups were tested for SMV in this study, but the lack of detected signal was a recurrent issue (see Section 4.2 in Results). It seemed like SMV was easily converted to its metabolite SMVA when incubated at 28.5 °C for 24 hours. As the lactone ring of SMV is quite unstable, the high incubation temperature might have contributed to loss of SMV to SMVA (which has an opened ring structure, see Figure 1.2 in Introduction). The unstable lactone ring would likely be stabilized by keeping samples chilled, diluted in other non-aquatic matrices or by the addition of EDTA to keep the lactone ring from opening and becoming a carboxylic acid group (personal communication with Nils Tore Vethe). All these conditions can however not be met with the aquatic matrix and incubation temperature required for the experiments in this master project.

Even though several experimental conditions were tested, different MS/MS acquisitions and LC settings were not further explored for SMV. The column used in this thesis was a C18-column, which is suitable for separation of pharmaceutical formulations (70, p. 319). However, as SMV's backbone contains two aromatic rings (Figure 1.2) a phenyl-hexyl column would have been interesting to test. This type of column allows for greater retention of aromatic compounds because of pi-pi-interactions with the packing of the column, and thus facilitating for separation. Nevertheless, several published and validated LC-MS/MS methods for determination of SMV and SMVA have used C18-columns for separation of these compounds (104-107), underpinning why it was chosen for these experiments in the first place.

5.3.1 Simvastatin, fluvastatin and interactions with plastic materials

It is well known that some drugs cannot be kept in plastic-based containers because of sorption issues leading to loss of the drugs (108). A study investigating how the combination of SMV and nanoplastics (polystyrene) affected toxicity in zebrafish larvae, found that the combination of these given by aquatic exposure gave a higher EC_{50}-value (effective concentration of the drug on 50% of the population) than for SMV alone (109). They proposed that adsorption of

SMV to the nanoplastics might have led to lower bioavailability of SMV, and thus a higher EC_{50}-value when administered aquatically (109).

Most plastic-based laboratory equipment (pipette-tips, vials, tubes, and well-plates) have hydrophobic characters (110). Hydrophobic interactions between these types of laboratory equipment and hydrophobic drugs are a common reason for low and variable recovery of such analytes in LC-MS/MS bioanalysis (110). In this thesis, lack of detection of SMV and weaker signals detected of FLV when held in plastic equipment compared to glass equipment, was observed (Section 4.3 in Results). Both SMV and FLV have hydrophobic characters (log P = 4.68 and log P = 4.85, respectively). However, FLV is more water soluble than SMV because it contains a carboxylic acid group, while SMV has a closed lactone ring (Figure 1.2). These characteristics might help explain the lack of SMV-detection when diluted in embryo water, and in addition contribute to answer why the FLV signals were stronger when incubated in glass vials than plastic vials.

5.4 Analytical reservations

5.4.1 No reference compounds available for optimization of FLV methods

An important part of developing methods for LC-MS/MS, is to optimize the LC and MS/MS conditions for the analytes as best as possible to obtain strong signals and a suitable separation. This optimization is normally done with the use of reference standards, as was done when developing the LC-MS/MS method for CAPT and DICAPT. However, for the selected metabolites of FLV, no reference compounds were available, and without reference standards, the analytical conditions for these metabolites could not be fully optimized.

To determine what ions to monitor, we assumed ionization by protonation, creating ions with $[M+H]^+$ *m/z* values. This presumption was made since protonation is a common ionization process when using positive mode ESI (73). However, it should be noted that not all analytes are prone to be ionized this way, especially when buffers are added to the mobile phases. For all methods used for analyzing FLV, mobile phase A contained 10 mM ammonium formate and 0.1% formic acid. With these buffers in the mobile phase, other adducts than $[M+H]^+$, such as $[M+NH_4]^+$ could also have been produced. However, other precursor ions than $[M+H]^+$ were not further monitored for the selected metabolites. With SIM (Single Ion Monitoring) on MS/MS, we only monitor specific *m/z* values, and all ions that do not match this, will be excluded from detection. Therefore, if some of the metabolites selected for monitoring were

readily ionized by other adducts than H^+, we would not be able to detect them with the developed methods.

Assumptions were also made on the selected metabolites' retention times (RTs); Metabolites that were more hydrophilic than FLV were expected to elute earlier than FLV, and metabolites that were less hydrophilic than FLV were expected to elute later than FLV. As seen from the obtained chromatograms in Figure 4.6 the basis lines from the SIM-method chromatograms were very noisy, and a lot of signals that did not correlate to FLV-metabolites were present for each tested *m/z*-value. In addition, the detected signals most likely to be correlating to FLV-metabolites were generally weak. Without knowledge of the monitored analytes actual RTs, taken together with the weak signals, these analyses were not as selective and sensitive as they could have been if reference standards were available for optimization. The obtained results from this experiment therefore have a high degree of uncertainty.

5.4.2 Running quantitative analyses of fluvastatin without an internal standard

An important criterion for accurate and sensitive quantitative analysis with MS/MS-instruments, is to be able to ensure that variations in the performance of the instrument over time are accurately accounted for. Therefore, internal standards are important factors to include in sample preparation, especially when the analyses are to be run over a long period of time (79, p. 104). However, the MRM method developed for quantitating FLV is run without an internal standard. The only reference standard available to be considered as an internal standard at time of the experiments was SMV. Yet, because of stability and detection issues with SMV, the inclusion of this compound as an internal standard could potentially add more uncertainty than confidence to the quantitative results. SMV was therefore concluded to be unfit as an internal standard in the experiments conducted for FLV in this master project. By choosing not to use an internal standard, the LC-MS/MS analyses are less accurate, and we have to "trust" that the conditions and performance of the MS/MS are in order both within the same worklist, and from day to day.

5.4.3 Embryo water as a matrix

Embryo water is a relatively uncomplex matrix compared to other matrices typically analyzed with LC-MS/MS-instruments, such as plasma, blood, or urine. These matrices contain a complex mixture of endogenous and exogenous compounds (called matrix components) from

the test subjects. With the qualitative analyses done in this thesis, the uncomplex nature of embryo water as a matrix was expected to increase the certainty of the results, as the detected peaks correlating to the selected ions are less likely to represent other components in the matrix than metabolites of the added drugs.

However, the analyses performed in this thesis showed several issues that could be related to the embryo water matrix after all. There are mainly two issues to be addressed here: microbial presence in the embryo water and its salt-contents. When the embryo water was sterile filtrated though a 0.22 μm syringe filter, the quantified amounts of FLV were higher than in non-filtered samples (Table 4.15). This might suggest that something in the embryo water prior to filtration contributes to signal suppression, loss, or possibly degradation of the administered FLV. The embryo water contains different salts and methylene blue (Methods p. 28), and these compounds are expected to pass the syringe filter based on their molecular sizes. The filter will however stop bacteria from passing (111). We interpreted the results as though the bacteria present in the embryo water prior to filtration had affected the drugs, possibly by metabolic degradation. It should however be noted that these samples were not prepared aseptically: the preparation was done on the laboratory bench, and the vials for incubation were not sterile. However, the growth and presence of bacteria would be much lower in samples containing filtered embryo water than non-filtered embryo water. Nevertheless, since OH-FLV was present in both unfiltered embryo water samples with and without zebrafish larvae, we do not know how much of this formation can be associated with the zebrafish larvae compared to bacteria present in the embryo water. Consequently, the influence from bacteria on drug degradation and -transformation when collecting samples from embryo water in biotransformation experiments conducted on zebrafish larvae, should be considered.

The embryo water contains salts that is optimized for incubating and nursing zebrafish larvae (see Methods, p. 28). However, salts are not really welcomed in MS/MS-instruments, as they can contaminate the ion source and might contribute to signal suppression (88). Salts from the embryo water might therefore have had an impact on the ionization process of the analytes in the ion source. In addition, the salts did contribute to contamination of the cone leading into the MS and despite regular maintenance, this might also have had an impact on the results. Even though only 5 μL of each sample was injected, multiple injections over time would cause a build-up of salts in the ion source. To reduce the salt-exposure when using this matrix, all embryo water samples were therefore diluted in the sample preparation.

5.4.4 Calibration curves, matrix matched yield samples and evaluation of linearity

With FLV, we did neither have an internal standard available, nor a fully matrix-matched calibration curve. The calibration curves used to estimate the quantities of FLV in zebrafish larvae was prepared in MeOH, and to account for matrix effects on FLV in the presence of dissociated zebrafish larvae, matrix matched yield samples were prepared. However, with these yield samples, the estimated slopes via linear regression were quite different to that of the calibration curve in MeOH (Figures 4.8 and 4.9 in Results). This suggested that dissociated zebrafish larvae did affect the ionization process of FLV, and therefore caused a matrix effect.

The observed trend was not the same for both high and low concentrations of the yield-samples. With the lowest yield sample concentration (5 nM), signal responses were stronger than the calibration standards, and for the highest yield sample concentration (15 nM), signal responses were weaker compared to the calibration standards. All the matrix matched yield samples prepared (5 nM, 10 nM, and 15 nM) contained three dissociated zebrafish larvae in MeOH and the selected concentration of FLV. Therefore, it was only the FLV-concentration that varied, and not the concentration of other matrix components. As described in Section (section 2.3.3), matrix effects are a result of interference with the ionization process when matrix components are co-eluting with the analytes. It might be that with only 5 nM of the analyte, the matrix effects were not as pronounced because less components (both matrix-components *and* analytes) from the sample were present in the ion source at once. This could explain how the matrix effects first became significant at higher concentrations. Nonetheless, it would be expected that both low and higher concentrations of FLV would be affected in the same way: either with signal enhancement or signal suppression.

The concentration range tested was quite narrow (ranging from 5 nM to 15 nM) as this range included values a bit under and a bit over the middle value of the MeOH-calibration curve (which ranged from 1 nM to 20 nM). To fully understand what might have happened here, it would be interesting to construct a full calibration curve over a larger concentration-range than what was done with the yield samples. However, at the time of these experiments, there were not enough zebrafish larvae available to carry this out. Because of these unclear effects observed with the yield samples, the quantities of FLV in zebrafish larvae were estimated using the MeOH calibration curve, despite not being able to account for the matrix effects. Therefore,

the obtained results from these analyses are not representative for the actual amount of FLV that was present in the zebrafish larvae.

In the case of DICAPT, calibration curves were prepared ranging from 0.23-6.9 μM, and linearity was observed within this range (Figure 3.10). However, the responses detected for DICAPT in most of the embryo water samples in these experiments were outside of the calibrated range (lower than the lowest calibration standard). When creating calibration curves for quantitative analyses, a representative range of calibration samples should be included to test and ensure that linearity is a fact for all the included samples. If not, we cannot guarantee that the calculated concentrations are accurate. This adds an uncertainty to the detected quantities of DICAPT (presented in Figure 4.10/Table 4.16) that were outside of the calibrated concentration range of the calibration-curve.

Another uncertainty to be addressed with the CAPT-experiments, is that for each experiment, fresh stock-solutions were prepared prior to dilution. CAPT was weighed using an analytical weight and dissolved in embryo water to create the stock-solutions, and separate stock-solutions had to be prepared for the incubated samples and the calibration curves. This was necessary, since spontaneous conversion from CAPT to DICAPT is expected with storage, meaning that the concentration of the stock-solution is most accurate just after dissolving CAPT in embryo water. With quantitative analysis, slight differences in the stock-solutions can influence the results, as this will affect the whole dilution series and thereby also all the samples. As seen in Figure 4.10 (Results), the different experiments with CAPT obtained quite different results. In addition to the biological factors discussed earlier in this chapter, faults due to different stock-solutions should also be taken into consideration as an influencing factor on the results from the CAPT-experiments. The DICAPT and the FLV stocks, however, were aliquoted and kept at -80 °C (see Table 3.2 in Methods for details) and were therefore the same for each experiment.

6 Concluding remarks

The aim of this master project was to explore zebrafish larvae as a model system to study biotransformation of drugs. SMV and FLV were selected as test compounds since they are known substrates for CYP-mediated metabolism, and CAPT was selected based on its known metabolic profile and protein binding abilities. The metabolism of these drugs in zebrafish larvae was investigated by administration through aquatic exposure and by analyzing both embryo water and zebrafish larvae for drug and metabolite contents. The selected method for analysis was LC-MS/MS – a suitable instrument due to its high sensitivity and selectivity this instrument offers.

Both the number of zebrafish larvae present in each well and the exposure time had a significant effect on the administered drug in the embryo water, indicating that the larvae did influence the administered drugs (see Section 4.4 in Results). Therefore, the experiments were conducted with three zebrafish larvae in each well, with samples being collected after 24 hours and 48 hours exposure. Sample preparation procedures including dilution of embryo water, sonication of zebrafish larvae, and a derivatization reaction stabilizing captopril with pBPB were explored and optimized.

This study highlights the importance of considering the different developmental stages of the zebrafish larvae when setting up and interpreting data from biotransformation studies. During the first 120 hpf, zebrafish larvae develop and mature several biological structures, such as kidneys, liver, and intestinal tract. With the development of these organs, the elimination rates of xenobiotics might increase as the larvae ages and matures. In addition, the yolk sac represents an important structure where drugs might accumulate during the time of drug exposure. This was apparent with experiments conducted with CAPT, since the detected quantities were lower in embryo water samples collected from 96 hpf old larvae compared to the embryo water from 120 hpf old larvae.

We also encountered issues relating to the physicochemical properties of the selected drugs. In this these experiments, we were not able to detect SMV. With non-charged hydrophobic drugs, like SMV, interactions with plastic materials such as pipette tips, Eppendorf-tubes, and 96-well plates can cause issues regarding lack of detection due to adsorption of the drug to the plastic materials. Moreover, it appeared as though SMV was converted to its metabolite SMVA to a

great extent when incubated in embryo water at 28.5 °C for 24 hours. Thus, the hydrophilic properties of administered drugs and their stability in aquatic environments, must be considered when conducting similar experiments in the future.

The LC-MS/MS methods for fluvastatin developed in this thesis could have been further optimized if an internal standard and reference compounds to the selected metabolites had been available. Furthermore, dilution of the embryo water samples (1:2.7 for CAPT and 1:4 for FLV) probably increased the limit of detection for these LC-MS/MS methods, making them less sensitive. With the CAPT analyses, most of the detected signals for the metabolite DICAPT were outside the calibrated range of the standard curve, making the results less reliable. They were however above the lowest limit of detection.

Using embryo water as a sample matrix was at first considered as a strength to these analyses, because of its assumed uncomplex nature. However, this was not the case. Embryo water as a sample matrix presented several issues with analysis on LC-MS/MS. Its salt contents might have influenced the ionization process of the analytes, and the presence of bacteria could provide false positive results as they were shown to contribute to metabolite production. Moreover, with sonicated zebrafish larvae present in the sample matrix (MeOH), matrix effects were observed for FLV. Thus, the presence of endogenous compounds from zebrafish larvae, even in small amounts, holds the possibility of interfering with LC-MS/MS analyses, and for FLV there is probably need for better sample preparation.

FLV and selected metabolites were monitored with a qualitative approach. We did detect traces of molecular ions likely correlating to OH-FLV (428.5 m/z), 2OH-FLV (444.5 m/z) and Lactone-FLV (410.5 m/z) in embryo water samples. However, these metabolites were present in samples where zebrafish larvae had been present *and* in samples without zebrafish larvae, and thus bacteria might have affected these results. We did not detect any metabolites within the zebrafish larvae. This could be a result of signal interference caused by matrix components in these samples, or because the metabolites were already eliminated from the larvae.

Taken together, we did observe metabolites in embryo water samples from zebrafish larvae that are also seen in humans for both CAPT and FLV in this study. However, we encountered some issues related to the chemical properties of the selected drugs, in addition to analytical considerations regarding the matrices used and the sample preparation. These complications

need to be resolved before one can conclude that zebrafish larvae are a reliable model for biotransformation of drugs. However, since FLV metabolites were detected with this analytical method and approach, this model could potentially be valuable for investigating biotransformation in lead compounds where metabolic profiles are not known. Further experiments and method optimizations are still needed to adequately evaluate and understand biotransformation in zebrafish larvae.

7 References

1. de Souza Anselmo C, Sardela VF, de Sousa VP, Pereira HMG. Zebrafish (Danio rerio): A valuable tool for predicting the metabolism of xenobiotics in humans? Comparative Biochemistry and Physiology Part C: Toxicology & Pharmacology. 2018;212:34-46.

2. Hughes JP, Rees S, Kalindjian SB, Philpott KL. Principles of early drug discovery. Br J Pharmacol. 2011;162(6):1239-49.

3. Wouters OJ, McKee M, Luyten J. Estimated Research and Development Investment Needed to Bring a New Medicine to Market, 2009-2018. Jama. 2020;323(9):844-53.

4. Patrick GL. An introduction to medicinal chemistry. 6th ed. Oxford: Oxford University Press; 2017.

5. Chi LH, Burrows AD, Anderson RL. Can preclinical drug development help to predict adverse events in clinical trials? Drug Discov Today. 2022;27(1):257-68.

6. U.S. Food and Drug Admninistration. The Drug Development Process [Internet]. U.S. Food and Drug Administration [updated 04.01.2018; cited 08.02. 2023]. Available from: https://www.fda.gov/patients/learn-about-drug-and-device-approvals/drug-development-process.

7. Global Antibiotic Research & Development Partnership. New chemical entity (NCE), new molecular entity (NME) [Internet]. REVIVE Advancing Antimicrobial R&D [cited 19.05. 2023]. Available from: https://revive.gardp.org/resource/new-chemical-entity-nce-new-molecular-entity-nme/?cf=encyclopaedia.

8. Sun D, Gao W, Hu H, Zhou S. Why 90% of clinical drug development fails and how to improve it? Acta Pharm Sin B. 2022;12(7):3049-62.

9. Liu T, Altman RB. Identifying druggable targets by protein microenvironments matching: application to transcription factors. CPT Pharmacometrics Syst Pharmacol. 2014;3(1):e93.

10. National Institute on Aging. What are Clinical Trials and Studies? [Internet]. National Institute of Health (NIH), National Institute on Aging (NIA)2023 [updated 22.03.2023; cited 18.04. 2023]. Available from: https://www.nia.nih.gov/health/what-are-clinical-trials-and-studies.

11. U.S. Food and Drug Admninistration. Step 4: FDA Drug Review [Internet]. Food and Drug Administration (FDA) [updated 01.04.2018; cited 06.05. 2023]. Available from: https://www.fda.gov/patients/drug-development-process/step-4-fda-drug-review.

12. Beninger P. Pharmacovigilance: An Overview. Clin Ther. 2018;40(12):1991-2004.

13. Institute of Medicine (US) Forum on Drug Discovery, Development, and Translation. 2009. In: Breakthrough Business Models: Drug Development for Rare and Neglected Diseases and Individualized Therapies: Workshop Summary [Internet]. Washington (DC): National Academies Press (US). Available from: https://www.ncbi.nlm.nih.gov/books/NBK50972/.

14. Paul SM, Mytelka DS, Dunwiddie CT, Persinger CC, Munos BH, Lindborg SR, et al. How to improve R&D productivity: the pharmaceutical industry's grand challenge. Nat Rev Drug Discov. 2010;9(3):203-14.

15. Ward KW. Recent advances in pharmacokinetic extrapolation from preclinical data to humans. Expert Opin Drug Metab Toxicol. 2005;1(4):583-94.

16. Ritter JM, Flower RJ, Henderson G, Loke YK, MacEwan DJ, Rang HP. Rang and Dale's pharmacology. 9th ed. Edinburgh: Elsevier; 2019. 789 p.

17. Cheng F, Ma Y, Uzzi B, Loscalzo J. Importance of scientific collaboration in contemporary drug discovery and development: a detailed network analysis. BMC Biol. 2020;18(1):138.

18. Ekins S, Mestres J, Testa B. In silico pharmacology for drug discovery: methods for virtual ligand screening and profiling. Br J Pharmacol. 2007;152(1):9-20.

19. Bruno A, Costantino G, Sartori L, Radi M. The In Silico Drug Discovery Toolbox: Applications in Lead Discovery and Optimization. Curr Med Chem. 2019;26(21):3838-73.

20. Lombardo F, Desai PV, Arimoto R, Desino KE, Fischer H, Keefer CE, et al. In Silico Absorption, Distribution, Metabolism, Excretion, and Pharmacokinetics (ADME-PK): Utility and Best Practices. An Industry Perspective from the International Consortium for Innovation through Quality in Pharmaceutical Development. J Med Chem. 2017;60(22):9097-113.

21. Kåss E. *in vitro* [Internet]. Store medisinske leksikon: Store norske leksikon; 2021 [updated 07.11.2021; cited 18.04. 2023]. Available from: https://sml.snl.no/in_vitro.

22. Tonholo DR, Maltarollo VG, Kronenberger T, Silva IR, Azevedo PO, Oliveira RB, et al. Preclinical toxicity of innovative molecules: In vitro, in vivo and metabolism prediction. Chem Biol Interact. 2020;315:108896.

23. Hickman DL, Johnson J, Vemulapalli TH, Crisler JR, Shepherd R. Chapter 7 - Commonly Used Animal Models. In: Suckow MA, Stewart KL, editors. Principles of Animal Research for Graduate and Undergraduate Students. Boston: Academic Press; 2017. p. 117-75.

24. Pellegatti M. Dogs and monkeys in preclinical drug development: the challenge of reducing and replacing. Expert Opin Drug Metab Toxicol. 2013;9(9):1171-80.

25. Hubrecht RC, Carter E. The 3Rs and Humane Experimental Technique: Implementing Change. Animals (Basel). 2019;9(10).

26. European Medicines Agency. Ethical use of animals in medicine testing [Internet]. European Medicines Agency [cited 24.01. 2023]. Available from: https://www.ema.europa.eu/en/human-regulatory/research-development/ethical-use-animals-medicine-testing.

27. Strähle U, Scholz S, Geisler R, Greiner P, Hollert H, Rastegar S, et al. Zebrafish embryos as an alternative to animal experiments—A commentary on the definition of the onset of protected life stages in animal welfare regulations. Reproductive Toxicology. 2012;33(2):128-32.

28. Directive 2010/63/EU of the European Parliment and the Council of 22. september 2010 on the protection of animals used for scientific purposes, (2010).

29. Grogan S, Preuss CV. Pharmacokinetics. StatPearls. Treasure Island (FL)2023.

30. Fan J, de Lannoy IA. Pharmacokinetics. Biochem Pharmacol. 2014;87(1):93-120.

31. Øye I. Biotransformasjon [Internet]. Store norske leksikon: Store medisinske leksikon; 2020 [updated 24.04.2020; cited 19.04. 2023]. Available from: https://sml.snl.no/biotransformasjon.

32. Phang-Lyn S, Llerena V. Biochemistry, Biotransformation [Internet]. Treasure Island (FL): Stat Pearls Publishing; 2022 [updated 22.08.2022; cited 11.02. 2023]. Available from: https://www.ncbi.nlm.nih.gov/books/NBK544353/.

33. Fosskaug K, Ali AM. cytokrom P450 [Internet]. Store medisinske leksikon: Store norske leksikon; 2023 [updated 27.01.2023; cited 19.05. 2023]. Available from: https://sml.snl.no/cytokrom_P450.

34. Jancova P, Anzenbacher P, Anzenbacherova E. Phase II drug metabolizing enzymes. Biomed Pap Med Fac Univ Palacky Olomouc Czech Repub. 2010;154(2):103-16.

35. Walther R, Rautio J, Zelikin AN. Prodrugs in medicinal chemistry and enzyme prodrug therapies. Adv Drug Deliv Rev. 2017;118:65-77.

36. Moyer AM, Fridley BL, Jenkins GD, Batzler AJ, Pelleymounter LL, Kalari KR, et al. Acetaminophen-NAPQI hepatotoxicity: a cell line model system genome-wide association study. Toxicol Sci. 2011;120(1):33-41.

37. Rosenson R. Statins: Actions, side effects and administration [Internet]. UpToDate [updated 07.10.2022; cited 12.02. 2023]. Available from: https://www.uptodate.com/contents/statins-actions-side-effects-and-administration?search=statins&source=search_result&selectedTitle=2~142&usage_type=default#H2.

38. Legemiddelhåndboka. L8.15.1 Statiner [Internet]. Oslo: Foreningen for utgivelse av Norsk Legemiddehåndbok; [updated 25.01.2017; cited 12.02. 2023]. Available from: https://www.legemiddelhandboka.no/L8.15.1/Statiner.

39. Legemiddelhåndboka. L8.15.1.6 Simvastatin [Internet]. Norsk legemiddelhåndbok: Foreningen for utgivelse av norsk legemiddelhåndbok; [updated 05.04.2018; cited 12.02. 2023]. Available from: https://www.legemiddelhandboka.no/L8.15.1.6/Legemidler_ved_hjerte-_og_karsykdommer.

40. Drugbank. Simvastatin [Internet]. Drugbank Online [updated 12.02.2023; cited 12.02. 2023]. Available from: https://go.drugbank.com/drugs/DB00641.

41. Scripture CD, Pieper JA. Clinical pharmacokinetics of fluvastatin. Clin Pharmacokinet. 2001;40(4):263-81.

42. Mitani H, Kimura M. Fluvastatin, HMG-CoA Reductase Inhibitor: Antiatherogenic Profiles Through Its Lipid-Lowering–Dependent and -Independent Actions. Cardiovascular Drug Reviews. 2000;18(4):284-303.

43. Norsk Legemiddelhåndbok. L8.6.1 Angiotensinkonverterende enzymhemmere [Internet]. Norsk Legemiddelhåndbok,: Foreningen for utgivelse av Norsk legemiddehåndbok; 2017 [updated 25.01.2017; cited 15.03. 2023]. Available from: https://www.legemiddelhandboka.no/L8.6.1/Angiotensinkonverterende_enzymhemmere.

44. Drugbank. Captopril [Internet]. Drugbank Online [updated 19.05.2023; cited 15.03. 2023]. Available from: https://go.drugbank.com/drugs/DB01197.

45. Duchin KL, McKinstry DN, Cohen AI, Migdalof BH. Pharmacokinetics of captopril in healthy subjects and in patients with cardiovascular diseases. Clin Pharmacokinet. 1988;14(4):241-59.

46. Barros TP, Alderton WK, Reynolds HM, Roach AG, Berghmans S. Zebrafish: an emerging technology for in vivo pharmacological assessment to identify potential safety liabilities in early drug discovery. Br J Pharmacol. 2008;154(7):1400-13.

47. Letrado P, de Miguel I, Lamberto I, Diez-Martinez R, Oyarzabal J. Zebrafish: Speeding Up the Cancer Drug Discovery Process. Cancer Res. 2018;78(21):6048-58.

48. Langenau DM, red. Cancer and Zebrafish : Mechanisms, Techniques, and Models. 1st ed. Cham: Springer International Publishing : Imprint: Springer; 2016. 552 p.

49. Gore AV, Monzo K, Cha YR, Pan W, Weinstein BM. Vascular development in the zebrafish. Cold Spring Harb Perspect Med. 2012;2(5):a006684.

50. Yaniv K, Isogai S, Castranova D, Dye L, Hitomi J, Weinstein BM. Live imaging of lymphatic development in the zebrafish. Nat Med. 2006;12(6):711-6.

51. David RM, Jones HS, Panter GH, Winter MJ, Hutchinson TH, Chipman JK. Interference with xenobiotic metabolic activity by the commonly used vehicle solvents dimethylsulfoxide and methanol in zebrafish (Danio rerio) larvae but not Daphnia magna. Chemosphere. 2012;88(8):912-7.

52. Cleal M, Gibbon A, Fontana BD, Parker MO. The importance of pH: How aquarium water is affecting behavioural responses to drug exposure in larval zebrafish. Pharmacol Biochem Behav. 2020;199:173066.

53. Peterson RT, Macrae CA. Systematic approaches to toxicology in the zebrafish. Annu Rev Pharmacol Toxicol. 2012;52:433-53.

54. Van Wijk RC, Krekels EHJ, Kantae V, Ordas A, Kreling T, Harms AC, et al. Mechanistic and Quantitative Understanding of Pharmacokinetics in Zebrafish Larvae through Nanoscale Blood Sampling and Metabolite Modeling of Paracetamol. Journal of Pharmacology and Experimental Therapeutics. 2019;371(1):15-24.

55. Park YM, Meyer MR, Muller R, Herrmann J. Drug Administration Routes Impact the Metabolism of a Synthetic Cannabinoid in the Zebrafish Larvae Model. Molecules. 2020;25(19).

56. Cassar S, Adatto I, Freeman JL, Gamse JT, Iturria I, Lawrence C, et al. Use of Zebrafish in Drug Discovery Toxicology. Chem Res Toxicol. 2020;33(1):95-118.

57. Goldstone JV, McArthur AG, Kubota A, Zanette J, Parente T, Jonsson ME, et al. Identification and developmental expression of the full complement of Cytochrome P450 genes in Zebrafish. BMC Genomics. 2010;11:643.

58. Alderton W, Berghmans S, Butler P, Chassaing H, Fleming A, Golder Z, et al. Accumulation and metabolism of drugs and CYP probe substrates in zebrafish larvae. Xenobiotica. 2010;40(8):547-57.

59. Saad M, Matheeussen A, Bijttebier S, Verbueken E, Pype C, Casteleyn C, et al. In vitro CYP-mediated drug metabolism in the zebrafish (embryo) using human reference compounds. Toxicol In Vitro. 2017;42:329-36.

60. Brox S, Seiwert B, Haase N, Kuster E, Reemtsma T. Metabolism of clofibric acid in zebrafish embryos (Danio rerio) as determined by liquid chromatography-high resolution-mass spectrometry. Comp Biochem Physiol C Toxicol Pharmacol. 2016;185-186:20-8.

61. Drugbank. Ibuprofen [Internet]. Drugbank Online2023 [updated 19.04.2023; cited 19.04. 2023]. Available from: https://go.drugbank.com/drugs/DB01050.

62. Jones HS, Trollope HT, Hutchinson TH, Panter GH, Chipman JK. Metabolism of ibuprofen in zebrafish larvae. Xenobiotica. 2012;42(11):1069-75.

63. Drugbank. Midazolam [Internet]. Drugbank Online2023 [updated 19.04.2023; cited 19.04. 2023]. Available from: https://go.drugbank.com/drugs/DB01050.

64. de Souza Anselmo C, Sardela VF, Matias BF, de Carvalho AR, de Sousa VP, Pereira HMG, et al. Is zebrafish (Danio rerio) a tool for human-like metabolism study? Drug Test Anal. 2017;9(11-12):1685-94.

65. Rombough P. Gills are needed for ionoregulation before they are needed for O(2) uptake in developing zebrafish, Danio rerio. J Exp Biol. 2002;205(Pt 12):1787-94.

66. Drummond IA, Davidson AJ. Chapter 9 - Zebrafish Kidney Development. In: Detrich HW, Westerfield M, Zon LI, editors. Methods in Cell Biology. 100: Academic Press; 2010. p. 233-60.

67. Bates JM, Mittge E, Kuhlman J, Baden KN, Cheesman SE, Guillemin K. Distinct signals from the microbiota promote different aspects of zebrafish gut differentiation. Dev Biol. 2006;297(2):374-86.

68. Coskun O. Separation techniques: Chromatography. North Clin Istanb. 2016;3(2):156-60.

69. Pedersen-Bjergaard S, Rasmussen KE. Legemiddelanalyse. 2 ed. Bergen: Fagbokforlaget; 2010. 505 p.

70. Watson DG. Pharmaceutical Analysis: A Textbook for Pharmacy Students and Pharmaceutical Chemists. 3rd ed: Churchill Livingstone Elsevier; 2012. 427 p.

71. Wibetoe G, Egeland ES. HPLC – Høypressisjonsvæskekromatografi [Internet]. Store norske leksikon2022 [updated 08.07.2022; cited 20.04. 2023]. Available from: https://snl.no/HPLC_-_høypresisjonsvæskekromatografi.

72. Hsieh Y. HPLC-MS/MS in drug metabolism and pharmacokinetic screening. Expert Opin Drug Metab Toxicol. 2008;4(1):93-101.

73. Banerjee S, Mazumdar S. Electrospray ionization mass spectrometry: a technique to access the information beyond the molecular weight of the analyte. Int J Anal Chem. 2012;2012:282574.

74. de Hoffmann E, Stroobant V, De Hoffmann E. Mass Spectrometry : Principles and Applications. 3rd ed. New York: John Wiley & Sons, Incorporated; 2007. 489 p.

75. Agilent Technologies. Agilent 6400 Series Triple Quad LC/MS System: Concepts guide. Agilent Technologies; 2010.

76. Kraj A, Desiderio DM, Ekman R, Nibbering NM, Silberring J, Westma AM. Mass Spectrometry: Instrumentation, Interpretation, and Applications. 1. Aufl. ed. Hoboken: Hoboken: Wiley; 2008.

77. Beccaria M, Cabooter D. Current developments in LC-MS for pharmaceutical analysis. Analyst. 2020;145(4):1129-57.

78. Van Eeckhaut A, Lanckmans K, Sarre S, Smolders I, Michotte Y. Validation of bioanalytical LC-MS/MS assays: evaluation of matrix effects. J Chromatogr B Analyt Technol Biomed Life Sci. 2009;877(23):2198-207.

79. Mallet AI. Quantitative biological and clinical mass spectrometry : an introduction. 1st ed. Pondicherry: Wiley Blackwell; 2018. 213 p.

80. Hewavitharana AK. Matrix matching in liquid chromatography-mass spectrometry with stable isotope labelled internal standards--is it necessary? J Chromatogr A. 2011;1218(2):359-61.

81. Toyo'oka T. Derivatization-based High-throughput Bioanalysis by LC-MS. Anal Sci. 2017;33(5):555-64.

82. Chen CJ, Lee DY, Yu J, Lin YN, Lin TM. Recent advances in LC-MS-based metabolomics for clinical biomarker discovery. Mass Spectrom Rev. 2022:e21785.

83. Deng P, Zhan Y, Chen X, Zhong D. Derivatization methods for quantitative bioanalysis by LC-MS/MS. Bioanalysis. 2012;4(1):49-69.

84. Vancea S, Imre S, Donath-Nagy G, Bela T, Nyulas M, Muntean T, et al. Determination of free captopril in human plasma by liquid chromatography with mass spectrometry detection. Talanta. 2009;79(2):436-41.

85. Fu Y, Li W, Picard F. Non-regulated LC-MS/MS bioanalysis in support of early drug development: a Novartis perspective. Bioanalysis. 2023;15(3):109-25.

86. Polson C, Sarkar P, Incledon B, Raguvaran V, Grant R. Optimization of protein precipitation based upon effectiveness of protein removal and ionization effect in liquid chromatography-tandem mass spectrometry. J Chromatogr B Analyt Technol Biomed Life Sci. 2003;785(2):263-75.

87. Grabski AC. Chapter 18 Advances in Preparation of Biological Extracts for Protein Purification. In: Burgess RR, Deutscher MP, editors. Methods in Enzymology. 463: Academic Press; 2009. p. 285-303.

88. Ohta Y, Iwamoto S, Kawabata S, Tanimura R, Tanaka K. Salt Tolerance Enhancement of Liquid Chromatography-Matrix-Assisted Laser Desorption/Ionization-Mass Spectrometry Using Matrix Additive Methylenediphosphonic Acid. Mass Spectrom (Tokyo). 2014;3(1):A0031.

89. Mahmoud WM, Kummerer K. Captopril and its dimer captopril disulfide: photodegradation, aerobic biodegradation and identification of transformation products by HPLC-UV and LC-ion trap-MS(n). Chemosphere. 2012;88(10):1170-7.

90. Halder D, Dan S, Pal MM, Biswas E, Chatterjee N, Sarkar P, et al. LC-MS/MS assay for quantitation of enalapril and enalaprilat in plasma for bioequivalence study in Indian subjects. Future Sci OA. 2017;3(1):FSO165.

91. National Center for Biotechnology Information. PubChem Compound Summary for CID 54454, Simvastatin [Internet]. 2023 [cited 19.05. 2023]. Available from: https://pubchem.ncbi.nlm.nih.gov/compound/54454.

92. Kimmel CB, Ballard WW, Kimmel SR, Ullmann B, Schilling TF. Stages of embryonic development of the zebrafish. Dev Dyn. 1995;203(3):253-310.

93. Bjornstad R, Reiten IN, Knudsen KS, Schjott J, Herfindal L. A liposomal formulation of simvastatin and doxorubicin for improved cardioprotective and anti-cancer effect. Int J Pharm. 2022;629:122379.

94. Margiotta-Casaluci L, Owen SF, Rand-Weaver M, Winter MJ. Testing the Translational Power of the Zebrafish: An Interspecies Analysis of Responses to Cardiovascular Drugs. Front Pharmacol. 2019;10:893.

95. Attardo S, Musumeci O, Velardo D, Toscano A. Statins Neuromuscular Adverse Effects. Int J Mol Sci. 2022;23(15).

96. Wiegand J, Avila-Barnard S, Nemarugommula C, Lyons D, Zhang S, Stapleton HM, et al. Triphenyl phosphate-induced pericardial edema in zebrafish embryos is dependent on the ionic strength of exposure media. Environ Int. 2023;172:107757.

97. National Center for Biotechnology Information. PubChem Compound Summary for CID 446155, Fluvastatin [Internet]. PubChem2023 [cited 19.05. 2023]. Available from: https://pubchem.ncbi.nlm.nih.gov/compound/446155.

98. Jutshurk PJ. Chapter 4 Bacterial Metabolism. In: S. B, editor. Medical Microbiology. 4th ed1996.

99. Drugbank. Fluvastatin [Internet]. Drugbank Online2023 [updated 15.05.2023; cited 15.05. 2023]. Available from: https://go.drugbank.com/drugs/DB01095.

100. Raia JJ, Jr., Barone JA, Byerly WG, Lacy CR. Angiotensin-converting enzyme inhibitors: a comparative review. DICP. 1990;24(5):506-25.

101. Chu J, Sadler KC. New school in liver development: lessons from zebrafish. Hepatology. 2009;50(5):1656-63.

102. Halbach K, Ulrich N, Goss KU, Seiwert B, Wagner S, Scholz S, et al. Yolk Sac of Zebrafish Embryos as Backpack for Chemicals? Environ Sci Technol. 2020;54(16):10159-69.

103. Li C, Tan XF, Lim TK, Lin Q, Gong Z. Comprehensive and quantitative proteomic analyses of zebrafish plasma reveals conserved protein profiles between genders and between zebrafish and human. Sci Rep. 2016;6:24329.

104. Patel BN, Sharma N, Sanyal M, Shrivastav PS. Simultaneous determination of simvastatin and simvastatin acid in human plasma by LC-MS/MS without polarity switch: application to a bioequivalence study. J Sep Sci. 2008;31(2):301-13.

105. Apostolou C, Kousoulos C, Dotsikas Y, Soumelas GS, Kolocouri F, Ziaka A, et al. An improved and fully validated LC-MS/MS method for the simultaneous quantification of simvastatin and simvastatin acid in human plasma. J Pharm Biomed Anal. 2008;46(4):771-9.

106. Pilli NR, Mullangi R, Inamadugu JK, Nallapati IK, Rao JV. Simultaneous determination of simvastatin, lovastatin and niacin in human plasma by LC-MS/MS and its application to a human pharmacokinetic study. Biomed Chromatogr. 2012;26(4):476-84.

107. Zhang Y, He J, Tang X, Zhang Z, Tian Y. A validated LC-MS/MS method for simultaneous quantification of simvastatin and simvastatin acid in beagle plasma: Application to an absolute bioavailability study. Biomed Chromatogr. 2022;36(3):e5290.

108. Sahnoune M, Tokhadzé N, El Kettani SEC, Devémy J, Goujon F, Chennell P, et al. Drug Interactions with Plasticized PVCs. Washington, DC :2022. p. 4538-50.

109. Barreto A, Santos J, Amorim MJB, Maria VL. Polystyrene Nanoplastics Can Alter the Toxicological Effects of Simvastatin on Danio rerio. Toxics. 2021;9(3).

110. Kumar D, Gautam N, Alnouti Y. Analyte recovery in LC-MS/MS bioanalysis: An old issue revisited. Anal Chim Acta. 2022;1198:339512.

111. Sigma Aldrich. Syringe Filters [Internet]. Sigma Aldrich [cited 19.05. 2023]. Available from: https://www.sigmaaldrich.com/NO/en/technical-documents/technical-article/analytical-chemistry/filtration/syringe-filters.

Appendix 1

Statistical analysis performed in IBM SPSS for determining the experimental design

Data from 24-hour group tests:

ANOVA

Data_24t

	Sum of Squares	df	Mean Square	F	Sig.
Between Groups	5778.766	2	2889.383	41.126	<.001
Within Groups	702.568	10	70.257		
Total	6481.335	12			

Multiple Comparisons

Dependent Variable: Data_24t
Dunnett T3

(I) Grupper_24t	(J) Grupper_24t	Mean Difference (I-J)	Std. Error	Sig.	95% Confidence Interval	
					Lower Bound	Upper Bound
1 fisk	3 fisk	39.63610*	5.63798	.002	20.8062	58.4660
	0 fisk	-8.50497	6.20928	.486	-28.3833	11.3734
3 fisk	1 fisk	-39.63610*	5.63798	.002	-58.4660	-20.8062
	0 fisk	-48.14107*	3.93815	.001	-63.7225	-32.5596
0 fisk	1 fisk	8.50497	6.20928	.486	-11.3734	28.3833
	3 fisk	48.14107*	3.93815	.001	32.5596	63.7225

*. The mean difference is significant at the 0.05 level.

Data from 48-hour group tests:

Multiple Comparisons

Dependent Variable: Data_48t
Dunnett T3

(I) Grupper_48t	(J) Grupper_48t	Mean Difference (I-J)	Std. Error	Sig.	95% Confidence Interval	
					Lower Bound	Upper Bound
1 fisk	3 fisk	49.95840*	7.77089	.005	22.4747	77.4421
	0 fisk	-5.10817	6.97265	.845	-42.7506	32.5343
3 fisk	1 fisk	-49.95840*	7.77089	.005	-77.4421	-22.4747
	0 fisk	-55.06657*	10.07239	.005	-87.7592	-22.3739
0 fisk	1 fisk	5.10817	6.97265	.845	-32.5343	42.7506
	3 fisk	55.06657*	10.07239	.005	22.3739	87.7592

*. The mean difference is significant at the 0.05 level.

Univariate analysis of variance:

Between-Subjects Factors

		Value Label	N
Tid	1.00	24t	10
	2.00	48t	10
Tal_fisk	1.00	1 fisk	10
	2.00	3 fisk	10

Tests of Between-Subjects Effects

Dependent Variable: VAR00002

Source	Type III Sum of Squares	df	Mean Square	F	Sig.
Corrected Model	11251.556[a]	3	3750.519	32.552	<.001
Intercept	230492.151	1	230492.151	2000.507	<.001
Tid	1084.401	1	1084.401	9.412	.007
Tal_fisk	10033.968	1	10033.968	87.088	<.001
Tid * Tal_fisk	133.187	1	133.187	1.156	.298
Error	1843.470	16	115.217		
Total	243587.177	20			
Corrected Total	13095.026	19			

a. R Squared = ,859 (Adjusted R Squared = ,833)